Norwegian University of Life Sciences
Faculty of Biosciences
Department of Plant Sciences

Philosophiae Doctor (PhD)
Thesis 2021:72

Identification of photoreceptors with functional characterization of photolyase in *Pseudoidium neolycopersici*

Identifikasjon av fotoreseptorer med funksjonell karakterisering av fotolyase i *Pseudoidium neolycopersici*

Ranjana Pathak

Identification of photoreceptors with functional characterization of photolyase in *Pseudoidium neolycopersici*

Identifikasjon av fotoreseptorer med funksjonell karakterisering av fotolyase i *Pseudoidium neolycopersici*

Philosophiae Doctor (PhD) Thesis

Ranjana Pathak

Department of Plant Sciences
Faculty of Biosciences
Norwegian University of Life Sciences

Ås 2021

Thesis number 2021:72
ISSN 1894-6402
ISBN 978-82-575-1848-6

PhD supervisors:

Dr. Aruppillai Suthaparan
Researcher
Department of Plant Sciences
Faculty of Biosciences
Norwegian University of Life Sciences
P. O. Box 5003, 1432 Ås, Norway
Email: aruppillai.suthapran@nmbu.no

Dr. Arne Stensvand
Senior Researcher
Division of Biotechnology and Plant Health
Norwegian Institute of Bioeconomy Research
P. O. Box 115, 1431 Ås, Norway
Email: arne.stensvand@nibio.no

Dr. Åshild Ergon
Associate Professor
Department of Plant Sciences
Faculty of Biosciences
Norwegian University of Life Sciences
P. O. Box 5003, 1432 Ås, Norway
Email: ashild.ergon@nmbu.no

Dr. Knut Asbjørn Solhaug
Professor
Faculty of Environmental Science and Nature Management
Norwegian University of Life Sciences
P. O. Box 5003, 1432 Ås, Norway
Email: knut.solhaug@nmbu.no

Dr. Lance E Cadle-Davidson
Research Plant Pathologist
Grape Genetics Research Unit, USDA-ARS
630 W. North St., Geneva, NY 14456, USA
Email: Lance.CadleDavidson@ARS.USDA.GOV

Evaluation committee:

Prof. Dr. Monica Höfte
Head of the Laboratory of Phytopathology
Department of Plants and Crops
Faculty of Bioscience Engineering
Ghent University, Belgium
Coupure Links 653, Geb. A, 9000 Gent
Email: monica.hofte@ugent.be

Dr. Johanna Riikonen
Senior Scientist
Nursery Production and Plant Physiology
Natural Resources Institute Finland, Luke
Latokartanonkaari 9, 00790 Helsinki, Finland
Email: johanna.riikonen@luke.fi

PhD coordinator:

Prof. Odd Arne Rognli
Pro-Dean for Research/Head of Department
Department of Plant Sciences
Faculty of Biosciences
Norwegian University of Life Sciences
P.O. Box 5003, 1432, Ås, Norway
Email: odd-arne.rognli@nmbu.no

Table of Contents

ACKNOWLEDGEMENTS

Firstly, I would like to express my deepest gratitude to my PhD supervisor, Dr. Aruppillai Suthaparan for giving me an opportunity to carry out my PhD thesis in his group, and for his valuable guidance and support during the entire PhD duration. I am very thankful for his motivation, timely advices, and his patience towards me. I highly appreciate Sutha for keeping his faith in me, especially during last two years, when I needed his support. I owe him all my PhD achievements. Thank you Sutha!!

My sincere thanks to Prof. Hans Ragnar Gislerød, and my co-supervisors- Prof. Arne Stensvand, Assoc. Prof. Åshild Ergon, Prof. Knut Asbjørn Solhaug, and Assoc. Prof. Lance-Cadle Davidson. I highly appreciate them for their scientific and friendly advices throughout PhD tenure.

A very special thanks to Karin for her wonderful support with fungal isolates maintenance. She was always ready to help whenever I needed an extra hand for my work. I would like to thank SKP scientific and technical staff, who contributed to different levels in making this thesis possible. Thanks to Gry, Ida, Marit, Astrid, Linda, Silje, and Tone.

I extend my appreciation to my fellow colleagues for sharing their knowledge and discussing scientific problems anytime, and maintaining a friendly environment in the lab. Special thanks to Anders, Dajana, Mani, Nicolas, Payel, and Sheona. I want to thank all my friends for making life much easier and creating wonderful memories during our time together in Ås. I appreciate my friend, Abhilash, Niveditha and Puneeth.

A million thanks to my family for their love and support. My parents, brothers (Vipin, Nitin), Bhabhi (Kriti), sisters (Rachna, Deepika, Priyanka), and whole family. Lots of thanks to my niece (Prisha) and nephews (Manomay, Shivin) who always brought smile on my face. Special thanks to my husband, Ankur without his support this thesis was not possible. He always motivated me to be optimistic. I express my deepest gratitude to my mother- Mrs. Shashi Pathak, and father- Mr. Babu Ram Pathak for their endless support, security and love. I dedicate my thesis work to them. Thanks, Mumma-Papa!!

Ranjana Pathak

ABSTRACT

Powdery mildew caused by *Pseudoidium neolycopersici* is one of the most destructive diseases, occurring predominantly on greenhouse grown tomatoes, and has gained importance worldwide due to severe economic losses in terms of quality and yield. Because of long winter months, the Norwegian tomato production is dependent on protected cultivation systems with controlled environment facilities. Microclimate inside greenhouses provide ideal conditions for development of powdery mildew. The use of resistant cultivars is the first priority for efficient and environmentally friendly management of this disease. However, most of the greenhouse tomato varieties have attained susceptibility to powdery mildew. Therefore, powdery mildew is essentially managed by the use of chemical fungicides.

Previous research demonstrated that short wavelength (< 290 nm) ultraviolet radiation (UV) alone or in combination with red light has a practical potential in combating powdery mildew through inhibition of its development. The efficacy of short wavelength UV on germination inhibition of conidia was significantly reduced by UV of longer wavelengths or blue light. This suggested the possible involvement of a light-mediated repair of UV induced DNA damage in powdery mildew.

This thesis is based on four articles. In the first article, the effect of short wavelength UV, and subsequent exposure to different incubation wavelengths on conidial germination was assessed to determine the germination recovery spectra of *P. neolycopersici*. The second article was centered on genome-wide investigation of the presence of photoreceptor genes in three powdery mildew fungi; *P. neolycopersici*, *Podosphaera xanthii*, and *Podosphaera aphanis*. The third article is focused on the identification of the photolyase gene in *P. neolycopersici*, and its functional characterization. Variation in inhibition and recovery of conidial germination among five isolates of *P. neolycopersici* treated with similar optical conditions, and a possible explanation for this variation are reported in the fourth article.

Petri dish level experiments with conidia of *P. neolycopersici* were conducted in controlled environment chambers to examine i) the wavelength and dose dependent efficacy of UV (254 nm to 313 nm) on inhibition of conidial germination, ii) the recovery action potential of optical radiation (310 nm to 730 nm) applied subsequently to

inhibitory UV treatment, and iii) the lapse time between inhibitory UV treatment, and subsequent exposure to recovery wavelength (peak at 454 nm). After treatments with UV at 254 nm or 283 nm for 30 s followed by dark incubation, less than 10% of the conidia germinated compared to 100% in non-UV controls. Conidial germination was almost negligible if the exposure duration increased to 4 min. With broad spectrum UV (peak 313 nm) conidial germination was about 60% after 1 min of exposure, and about 35% after 2 to 4 min of exposure followed by subsequent dark incubation. UV of 310 nm was ineffective in conidial germination inhibition when applied for ≤ 4 min. Germination of conidia treated with inhibitory UV (254 nm, 283 nm, or broad spectrum UV with peak at 313 nm) was significantly higher (above 73%) if incubated subsequently in optical radiation within the 350 nm to 500 nm range (germination recovery) than if incubated in darkness (control). Furthermore, germination recovery depended on the characteristics of the inhibitory UV treatment (wavelength, and duration of exposure) and the lapse time between inhibitory UV treatment, and subsequent exposure to optical radiation in the recovery range. These findings indicated the presence of photoreceptors in powdery mildew fungi with light mediated UV damage recovery function.

Draft genomes of *P. neolycopersici*, *P. xanthii*, and *P. aphanis*, causal agents of powdery mildews of tomato, cucumber and strawberry respectively, were assembled from next generation high throughput sequence data and annotated. An in-depth sequence analysis of these draft genomes revealed the presence of genes similar to all major classes of photoreceptor genes including photolyase, cryptochrome, white collar, phototropin, phytochrome, and UVR8. Three genes were identified as similar to blue light photoreceptors of the cryptochrome/photolyase family (CPF).

Photolyase mutant *Escherichia coli* cells were transformed separately with each of the three CPF-like genes identified in *P. neolycopersici*, and exposed to brief UV with peak at 254 nm followed by blue light or by darkness (control). One of the three putative CPF-like genes showed photoreactivation activity with cell survival rate of > 98% under blue light compared to the control, and was therefore confirmed as a functional photolyase. Phylogenetic analysis showed that it belonged to class I cyclobutane pyrimidine dimer (CPD) photolyases. The *in vitro* action spectra of this photolyase was between 365 nm and 454 nm. This perfectly coincides with the conidia germination recovery spectra of *P. neolycopersici*. Quantitative RT-PCR suggested that the expression

of the photolyase gene in *P. neolycopersici* conidia was significantly induced by brief UV treatment (peak at 254 nm). The expression level was maximum at 4 h after UV treatment (peak at 254 nm) under dark incubation. Photolyase gene expression was significantly reduced in UV (peak at 254 nm) treated conidia when subsequently incubated in red light.

The effect of similar doses of UV treatment (peak at 254 nm) followed by incubation with dark or blue light on conidial germination was studied in five isolates of *P. neolycopersici* collected from different regions in Norway and the Netherlands. Conidia were assessed for germination 24 h after incubation. The results showed variation in the effect of UV on germination and germination recovery under blue light incubation after UV treatment. Two isolates showed more germination recovery compared to the other three isolates. Genomic DNA from these five isolates were extracted, and the photolyase gene was PCR amplified by primer walking. Amplified PCR fragments were sequenced by Sanger sequencing and reads were analyzed for variation. The photolyase gene showed no variation among the five isolates.

The findings of this study provide application strategies for designing optical based management programs against powdery mildews by appropriate selection and combination of wavelengths with application time and duration.

Keywords: *Pseudoidium neolycopersici*, tomato, ultraviolet, photolyase, action spectra, photoreactivation, DNA damage repair, germination recovery, disease management

SAMMENDRAG

Meldugg forårsaket av *Pseudoidium neolycopersici* av er en av de alvorligste sykdommene på tomater og gir store skader i mange land. På grunn av den lange vinteren foregår norsk tomatproduksjon i veksthus, og mikroklimaet i veksthus gir ideelle forhold for meldugg. Bruk av resistente sorter er den mest effektive og miljøvennlige måten å kontrollere sykdommen på. De fleste tomatsortene brukt i veksthus er mottakelige for meldugg, og derfor blir det brukt kjemiske midler til bekjempelse.

Det er tidligere vist at kortbølget (< 290 nm) ultrafiolett lys (UV) brukt alene eller i kombinasjon med rødt lys er effektivt som tiltak mot meldugg. Effekten av slik UV-behandling på spiring av konidiesporer av melduggsoppen ble signifikant redusert av UV av høyere bølgelengder og blått lys. Dette indikerer at det skjer en lys-påvirket reparasjon av skaden som UV ved lavere bølgelengder har påført soppen.

Denne avhandlingen er basert på fire artikler. I den første ble effekten av kortbølge-UV med påfølgende eksponering for andre bølgelengder undersøkt for å finne lysspekteret som gjenoppretter sporespiring hos *P. neolycopersici*. Den andre artikkelen er et studium av forekomst av fotoreseptor-gener i genomene til tre melduggsopper; *P. neolycopersici*, *P. xanthii* og *P. aphanis*. Den tredje artikkelen er fokusert på identifisering av fotolyase-genet hos *P. neolycopersici* og karakterisering av genets funksjon. Variasjon i inhibering og reparasjon av sporespiring blant fem isolat av *P. neolycopersici* behandlet under de samme optiske forholdene og mulig forklaring på denne variasjonen er rapportert i den fjerde artikkelen.

Forsøk i Petri-skåler ble gjennomført under kontrollerte forhold i vekstrom for å undersøke i) bølgelengde- og doseavhengig effekt av behandling med kortbølge-UV (254 – 313 nm) på spiring av konidiesporer, ii) aksjonspotensialet for gjenoppretting av spiring ved hjelp av optisk stråling (310 – 730 nm) tilført etter kortbølge-UV, iii) effekt av lengde på tidsrom mellom behandling med kortbølge-UV og behandling med bølgelengder som gjenoppretter spiring (topp ved 454 nm). Mindre enn 10% av sporene spirte etter 30 sekunders eksponering ved 254 eller 283 nm og påfølgende inkubering i mørket, sammenlignet med 100% for kontrollen. Det var ingen spiring hvis eksponeringstiden økte til 4 minutter. Ved bruk av en bredspektret UV-lampe (topp på

313 nm) var sporespiringen respektive 60 og 35% sammenlignet med ubehandlet kontroll ved eksponering i 1 og 2 – 4 minutt. UV på 310 nm hadde ingen spirehemmende effekt når det ble påført i ≤ 4 min. Hos konidiesporer som var behandlet med kortbølge-UV (254, 283 eller bredt spekter med topp på 313 nm) etterfulgt av eksponering ved bølgelengder mellom 350 og 500 nm (gjenoppretting), var spireprosenten signifikant høyere (73%) enn hos de som ble inkubert i mørke etter behandlingen med kortbølge-UV (kontroll). Videre var gjenoppretting av sporespiring etter behandling med kortbølge-UV avhengig av bølgelengde og lengde av UV-behandlingen og hvor langt tidsrommet er mellom UV-behandling og påfølgende lyseksponering var. Disse funnene indikerer tilstedeværelse av fotoreseptorer hos melduggsopper med lysregulert reparasjon av UV-skade.

Utkast til genomsekvenser for *P. neolycopersici*, *P. xanthii* og *P. aphanis* (patogener på respektive tomat, agurk og jordbær) basert på neste-generasjons-sekvensering ble satt sammen og annotert. En grundig analyse av genomene påviste gener i alle hovedklassene av fotoreseptor-gener, inkludert fotolyase, kryptokrom, white collar, fototropin, fytokrom og UVR8. Tre gener ble identifisert som fotoreseptorer for blått lys i kryptokrom/fotolyase superfamilien (CPF).

Hvert av de tre CPF-lignende genene hos *P. neolycopersici* ble enkeltvis klonet i en fotolyase-mutant av *Escherichia coli*. Mutantene ble eksponert for kortvarig UV med topp på 254 nm etterfulgt av blått lys eller inkubering i mørke (kontroll). Overlevelsesraten etter UV-behandlingen indikerte at det blant de tre CPF-lignende genene var ett funksjonelt fotolyase-gen. Dette genet ga en overlevelse på over 98% etter behandling med blått lys sammenlignet med kontrollen. Fylogenetisk analyse viste at genet tilhørte klasse I cyclobutane pyrimidine dimer (CPD) fotolyase. Aksjonsspekteret ble vist *in vitro* å være fra 365 til 454 nm, noe som stemmer helt med lysspekteret for gjenoppretting av sporespiring hos UV-skadet *P. neolycopersici*. Kvantitativ RT-PCR viste at uttrykket av fotolyase-genet hos konidiesporer av *P. neolycopersici* ble indusert av kort behandling med UV (topp på 254 nm). Uttrykket var maksimalt etter 4 timer i påfølgende mørke, og rødt lys etter behandlingen med UV (topp på 254 nm) reduserte uttrykket.

Fem isolater av *P. neolycopersici* ble testet for sporespiring etter behandling med UV (topp på 254 nm) etterfulgt av inkubasjon i mørke eller i blått lys. Isolatene var fra

Norge og Nederland. Det var en variasjon i effekten av UV på spirehemming og i hvor stor grad blått lys gjenopprettet spiringen. To av isolatene responderte sterkere enn de tre andre. Genomisk DNA fra de fem isolatene ble ekstrahert, og fotolyase-genet ble PCR-amplifisert ved «primer walking». Amplifiserte PCR-fragment ble sekvensert med Sanger-sekvensering og analysert for variasjoner. Det var ingen variasjon i fotolyase-genet blant de fem isolatene.

Funnene i dette studiet gir oss viktige kriterier for bedre design av optisk-basert behandling mot meldugg ved riktig valg av bølgelengder, behandlingstidspunkt og -varighet.

LIST OF ARTICLES

This thesis is based on the following articles, which are referred to by their Roman numerals.

Paper I

Wavelength dependent recovery of UV-mediated damage: Tying up the loose ends of optical based powdery mildew management
Suthaparan, A., Pathak, R., Solhaug, K. A., Gislerød, H. R.
Journal of Photochemistry & Photobiology, B: Biology. 2018; 178:631-640

Paper II

Genome-wide identification and characterization of photoreceptor genes in powdery mildews (*Pseudoidium neolycopersici*, *Podosphaera xanthii*, and *Podosphaera aphanis*)
Pathak, R., Sundaram, A. Y. M., Suthaparan, A.
(Draft manuscript)

Paper III

Functional characterization of *Pseudoidium neolycopersici* photolyase reveals mechanisms behind the efficacy of nighttime UV on powdery mildew suppression
Pathak, R., Ergon, Å., Stensvand, A., Gislerød, H. R., Solhaug, K. A., Davidson, L. C., Suthaparan, A.
Frontiers in Microbiology. 2020; 11:1091

Paper IV

Variation in UV-mediated damage recovery among *Pseudoidium neolycopersici* isolates: possible mechanisms
Pathak, R., Suthaparan, A.
Phytofrontiers. 2021; 1:219-228

ABBREVIATIONS

PM	Powdery mildew
DMI	Di methyl inhibitors
IDM	Integrated disease management
UV	Ultraviolet
CPD	Cyclobutane pyrimidine dimer
(6-4) PP	6-4 photoproduct
PHR	Photoreactivation
CPF	Cryptochrome/photolyase family
CRY	Cryptochrome
CRY-DASH	Cryptochrome (Drosophila, Arabidopsis, Synechocystis, Human)
PHY	Phytochrome
UVR-8	UV resistance locus-8
LB	Luria-Bertani broth
Amp	Ampicillin
Kan	Kanamycin
IPTG	Isopropyl β-D-1-thiogalactopyranoside
PnPhr	Pseudoidium neolycopersici photoreactivation
LED	Light emitting diodes

1. INTRODUCTION

Powdery mildew (PM) is one of the most common and widespread fungal disease, which causes serious damage to economically important crops as well as ornamentals. Powdery mildews are Ascomycetes, belong to largest powdery mildew order Erysiphales and infect nearly 10,000 species of plants (18). These fungi are considered to evolved 100 million years ago, and there are nearly 18 genera including 700 species of powdery mildews spread all over the world (11, 99). These plant pathogenic fungi are obligate biotroph in nature, need a living host for their survival and reproduction. This is the major limitation in conducting research on powdery mildews from genetic and molecular points of view (37). Interestingly, powdery mildews are host specific or only able to infect a narrow host range, which means *Erysiphe necator*, that causes powdery mildew in grapes and linden does not infect lilac. Similarly, *Erysiphe syringae* attacks lilac but does not infect turfgrass (93).

Powdery mildew is easily recognizable, and its characteristics symptoms (Fig. 1) include white powder like growth (mycelium, conidiophores, and spores) predominantly on the leaves but stems, petioles, sepals are also infected. In some cases, like strawberry and grapes, fruits also get severe infection (7, 31, 54, 68). Unlike other fungi powdery mildews grow epiphytically (39). Symptoms usually seen on the upper surface of lower leaves, and as the disease becomes severe the underside of the leaves are also get affected (71). When disease gets older, patches become dense and turned to grey surrounded by chlorosis. Gradually, leaves turn twisted, distorted, wilted and finally fall off (27).

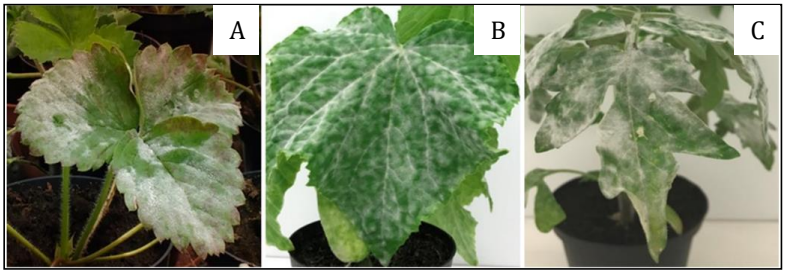

Fig. 1. Powdery mildew symptoms appeared as white powdery patches on the adaxial surfaces of leaves on the host plant. *Podosphaera aphanis* on strawberry (A),

Podosphaera xanthii on cucumber (B), and *Pseudoidium neolycopersici* on tomato (C). Photos: R. Pathak.

1.1. Powdery mildew disease development, infection, and its effects on yields

In powdery mildews, life cycle can involve both sexual (teleomorph) and asexual (anamorph), but asexual cycle is the predominant mode of reproduction and occurs via development and dispersal of conidia (37, 99). These conidia are the primary source of inoculum and can be easily dislodged by wind and water to a healthy host (27). Conidia make attachment to the hydrophobic plant surface within few minutes after deposition by excreting adhesive matrix, and germination of conidia occurs within 3 – 5 hours after deposition on the leaf surface, forming one or two germ tubes (Fig. 2a, b) (54). Germ tube elongates and formed a lobed shaped structure, called appressoria (Fig. 2c). From appressoria, an infection peg (penetration peg) forms, which uses a combination of enzymatic degradation and mechanical force to penetrate the host cell wall and cuticle (Fig. 2d) (39). In successful infection, this penetration peg creates a multilobed haustoria into the epidermal layer, and further continues to grow to form secondary hyphae (Fig. 2e – g) (54). These haustoria are the feeding structures through which fungi absorb all the essential nutrients from its host to grow and survive (71). On the host surface, formation of secondary hyphae and conidiophores lead to appear as the characteristic symptoms of white powdery patches of the disease and found on the exterior parts of the plants. The whole life cycle includes formation of conidia, release or dispersal of conidia, infection and formation of new conidia (90). The complete life cycle takes 72 – 96 hours, but the development of visible disease symptoms takes up to 7 to 10 days.

Sexual reproduction (which rarely occurs in greenhouse production systems) takes place through the formation of sexual fruiting bodies, ascocarp (formerly known as cleistothecia). Each ascocarp contain several asci, which bear ascospores. Ascocarps can overwinter (18), and act as a source of inoculum via discharging ascospores when the environmental conditions are in favour of pathogen development. In some cases, it

can overwinter as mycelium in dormant buds of their hosts. Overwintering as mycelium has been reported in powdery mildew of apple, grape, lilac, and plum (146).

Disease severity primarily depends on the host plant and climatic conditions. Powdery mildews are favored by wide fluctuations of day and night temperatures as well as relative humidity. Low relative humidity during the day and high relative humidity during the night favors the disease. Relative humidity below 80% is optimal for germination but higher humidity (> 80%) reduce the disease severity because appressoria formation is gradually reduced at this level. Temperature ranges from 20 – 25°C is optimal for PM infection (50).

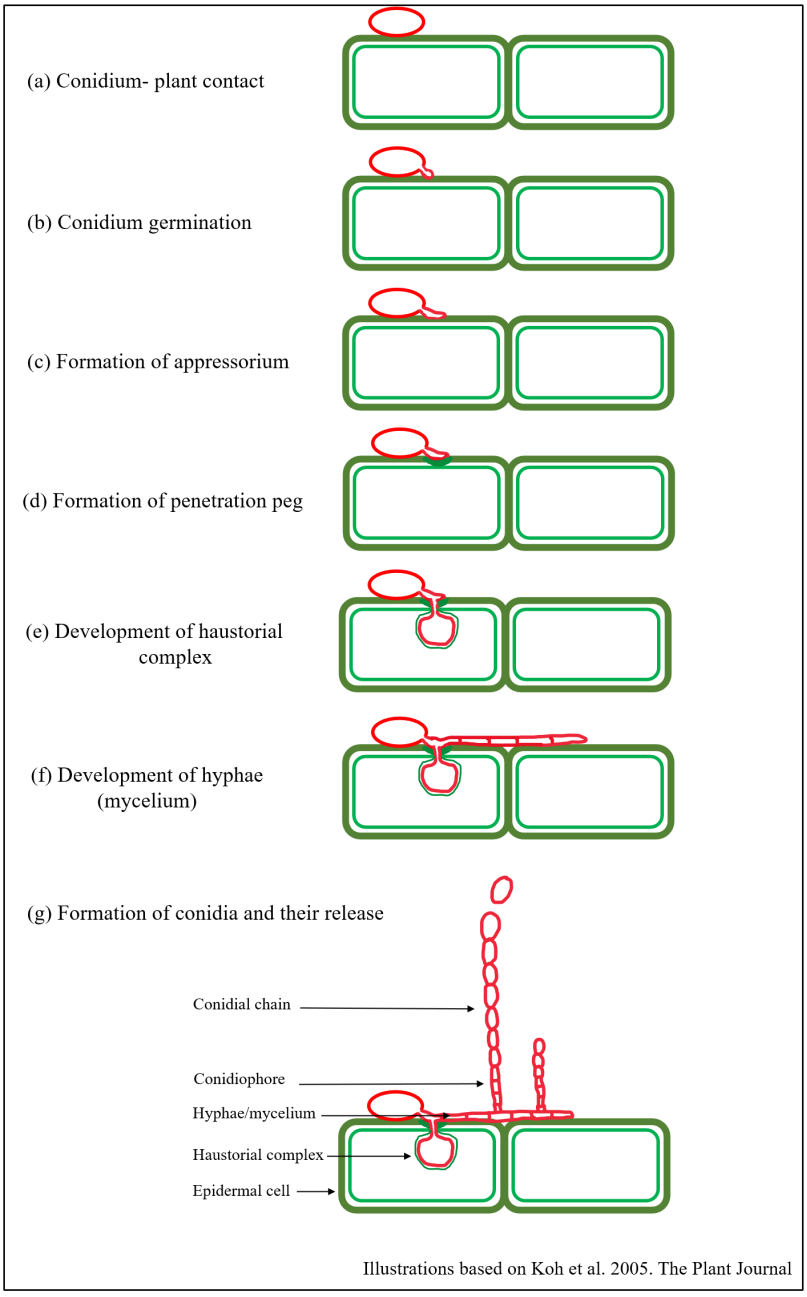

Fig. 2. Diagrammatic representation of the different stages of powdery mildew disease development on the host epidermis.

Powdery mildews have become most conspicuous plant pathogenic fungi to agronomically important crops including cereals, vegetables and fruits, grown in the fields as well as in the greenhouses (59). Powdery mildew majorly attack leaves of the plants, which limits the photosynthetic activity and lead to the drastic reduction in yields and total biomass (16, 36, 99). In case of tomato, mildew affects the aerial plant parts except fruit. As the disease becomes severe leaves fall off and expose fruits to sunburn, which further decrease the aesthetic and nutritional value of the crop with compromised fruit flavor (30). However, yield reduction and low fruit quality depends on the degree of disease severity (74).

1.2. Management of powdery mildews in protected cultivation

The controlled environment conditions are optimal for plant and pathogen development. The monoculture of high economic value crops in high density creates an ideal conditions for development of disease, and severe economic losses if pathogen inoculum enters into the production unit. In powdery mildews, asexual cycle is the predominant mode of reproduction in greenhouse production systems, and occurs via development and dispersal of conidia. Different preventive and therapeutic approaches can be used to manage powdery mildews, including use of resistant varieties, cultural practices, chemical or fungicide treatments or an integrated disease management (IDM) by using a combination of several strategies (151).

1.2.1. Resistant cultivars

One of the elementary approach for powdery mildew disease management is to grow resistant or tolerant varieties. Currently development of resistant cultivars has become increasingly important, which has been made possible by continuous breeding programmes. Genetic resistance can be achieved in different ways (47). Identification of molecular markers, which are closely linked to resistance genes, is a key factor for resistance breeding (71) or by the impairment of powdery mildew susceptible genes (47). Genetic resistance has become an important attribute, which leads to the increased production of high quality crops with low fungicide application (92). In most cases, resistance is usually conferred by a single dominant gene, but recessive genes have also

been reported (92). Resistant cultivars have been developed in number of crops, but in case of fruits and vegetables their use is limited. All cultivars and hybrids of tomato, which are available worldwide, have now attained susceptibility to powdery mildew (59).

1.2.2. Cultural control

Greenhouse provides an ideal environment to powdery mildew, therefore maintaining a proper hygiene and sanitation is a fundamental requirement to prevent infection. It is very important to maintain a balanced climate, mostly when climate is changing between warm and cold, which favours the powdery mildew development. Most common practice to prevent powdery mildew infection is to use early maturing varieties or plant early in the growing season, which allows early harvest. Early harvest are often less affected by mildews compared to the late harvest crops (32). Other prophylactic measures includes destruction of infected plants, and removal of any plant debris and weeds as they can be served as alternate host for PM as well as other pests (12). Pruning crops is helpful to improve light penetration and air circulation in lower canopies. Avoid shading of the crops and provide good air circulation between crops are also beneficial. Powdery mildew infection also increases with the availability of soil nitrogen content due to its effect on succulent growth of plants. A slow release fertilizer could be a good alternative (30). Crop rotation is not a viable practice against powdery mildews. However, careful farming methods cannot be applied as an only method to prevent infection but are more effective, if used routinely in combination with the other control methods such as resistant cultivars and chemicals.

1.2.3. Chemical control

For the management of powdery mildews, application of foliar fungicides continues to be a major practice (45). Prolonged use of fungicides developed resistance against the disease, and it has been reported that many PM fungi have developed resistance to six fungicide groups; benzimidazoles, morpholines, hydroxypyrimidines, demethylation inhibitors, phosphorothioates, and quinine outside inhibitors (78). Demethylation inhibitors (DMI) are one of the most important fungicides against

powdery mildews, but these are no longer effective and resistance to DMI was reported in *Podosphaera xanthii* (92). Benomyl and thiophanate both were found ineffective against *P. xanthii* during seven years of study from 2001–2007 (67). Number of active ingredients including benomyl, bitertanol, bupirimate, carbendazim, fenarimol, pyrazophos, thiabendazole, triforine, and sulfur were found effective against *Pseudoidium neolycopersici*, although the efficacy of every chemical may vary. In another study, Quinoxyfen, a quinoline fungicide was found to be effective in germination inhibition of *P. neolycopersici* conidia (54).

Some conventional fungicides containing sulfur, copper or mineral oil as an active ingredient are least toxic (77). Except oils, these compounds provide only prevention but oils such as Sunspray, neem oil, jojoba oil work as eradicants. Sulfur has been used to prevent powdery mildews for centuries. Vaporized sulfur formulated with surfactant provides excellent control of powdery mildew in greenhouses (30). Most of them are approved for organic production. However, appropriate timing of application of fungicides is critical, therefore disease monitoring is a primary requirement. Early detection of the disease will reduce the application number of foliar fungicide sprays (21).

Most fungicides, effective in controlling powdery mildews are systemic and have a single-site mode of action, means they are active at only one point in a metabolic pathway of a pathogen, and therefore more likely at risk for resistance development, compared to other fungicides (60, 67). In some countries, most of the fungicides, which are effective against powdery mildews are no longer registered to use in greenhouse cultivation systems because of restrictions and regulations (59).

1.2.4. Limitations in management options available in practice

Every method has their own limitations such as careful farming methods do not provide adequate disease control. In case of fungicide treatments, most of them not effective because of development of resistance in powdery mildew strains as a result from their repeated applications of fungicides (59). Resistant or tolerant varieties have been developed for many crops, but with limited use. Also environment concerns and public attitude towards the use of fungicides are the two major issues (32). Due to all

these constraints associated with fungicides and resistant cultivars, it is necessary to investigate an environmentally friendly alternative, which leads to the reduction of chemical fungicides usage against powdery mildews.

1.3. Light as an alternative

Light is one of the paramount environmental factor required by almost all the organisms on Earth for their metabolism and development (91). Photosynthetic organisms use light as a major source of energy and plays a crucial role in optimizing light-dependent energy conservation in addition to utilize light as a signal for environmental cues. Non-photosynthetic organisms use light only as a signal to anticipate about their surrounding environment in order to adapt with the environmental changes, and for synchronization of biological clocks to the length of the day (101).

Optical radiation is a part of electromagnetic spectrum between microwaves and X-rays, which includes ultraviolet (UV), visible light (VL) and infrared (IR) regions. The photobiological effects of these regions depend on their frequency, wavelength and mechanism of action (117). Apart from the beneficial effects, optical radiations particularly UV radiations can have deleterious effects on living organisms (28).

Previous studies have shown that UV radiation has a practical potential with high efficacy in controlling powdery mildews compared to other wavelength ranges within the optical radiation (51, 64, 120). It was described that spore germination and mycelial growth was negatively affected by UV-B (295 nm) in grape powdery mildew, *Uncinula necator* (64). Recently, It has been reported that UV-C (254 nm) compromises the conidial germination and appressoria formation in *Blumeria graminis,* cause of barley powdery mildew (153). In another study, a low dose UV-C (254 nm) irradiation provided an effective control against strawberry powdery mildew, *Podosphaera aphanis* (51, 136). Short wavelength UV (< 290 nm) treatment showed significant reduction in conidial germination of tomato powdery mildew, *Pseudoidium neolycopersici* in a dose dependent manner (123). UV-B (broad spectrum, peak at 313 nm) inhibited multiple stages of pathogen development; germination, infection, colony expansion, and sporulation in *Podosphaera xanthii*, cause of cucumber powdery mildew (120).

Manipulation in environmental conditions including day length (125) and spectral quality of the light (126, 139) may be an alternative strategy to control powdery mildews at greenhouse level. However, the efficacy of UV depends on the wavelength, irradiance level, duration of exposure, and complexity of organism exposed (123). UV dosage, in terms of intensity and duration should be optimized for the pathogen eradication while taking host plants into consideration. Dosage requirement should be sufficient to kill pathogen, but at the same time should not have any negative/phytotoxic effects on the host plants itself (120, 124).

Short wavelength UV represents clean and environmentally safe substitute to chemical fungicides that could be applied at greenhouse level. Therefore, UV radiations offer an interesting possibilities to be used as an alternative to chemical fungicides in disease management (123). Recent advances in technology are rapidly exploited in horticulture industry to provide protection against various diseases, especially in protected cultivation where all the environmental parameters are fully controlled and regulated (29).

1.4. Photoreceptors

For having any action, the photons of optical radiation that hits on the matter need to be absorbed. All living organisms are able to detect light through specialized molecules called photoreceptors (44). These photoreceptors molecules absorb photon energy through light absorbing chromophores, which then transduce this photon energy into a cell to initiate a biological response (25). Both plants and fungal kingdoms are capable of sensing light over the entire spectrum, ranging from ultraviolet to far-red light (44, 94). Plants possess different photoreceptors required for the regulation of plant growth, development and the entrainment of the circadian clocks. The major classes of photoreceptors have been identified and characterized in plants. These include Light-oxygen-voltage (LOV), phototropins, cryptochromes, rhodopsins, phytochromes, and a recently identified UV resistance locus-8 (UVR8) (44, 83).

1.4.1. Photoreception in Fungi

Fungi represent the third group of macroscopic eukaryotes, which are sibling kingdom to animals (48). Being non-photosynthetic organisms, fungi sense light via photoreceptors and respond to their surrounding environment (24, 35). Light is the one of the most important signals, which regulates various physiological processes in fungi including formation of asexual/sexual structures, regulation of secondary metabolism, and the circadian clock via range of photoreceptors (24-26, 94). In fungi, red light sensing is achieved by bilin binding phytochromes, and the retinal based opsin systems are responsible for green light sensing. Further, blue light sensing is achieved by a flavin based photoreceptors; white collar proteins and cryptochrome/photolyase family (94, 101, 148) (Fig. 3). Most of the current knowledge about fungal photoreceptors comes from the model filamentous fungi, *Neurospora* crassa, and with limited information on functional role confirmations from *Aspergillus nidulans* (26).

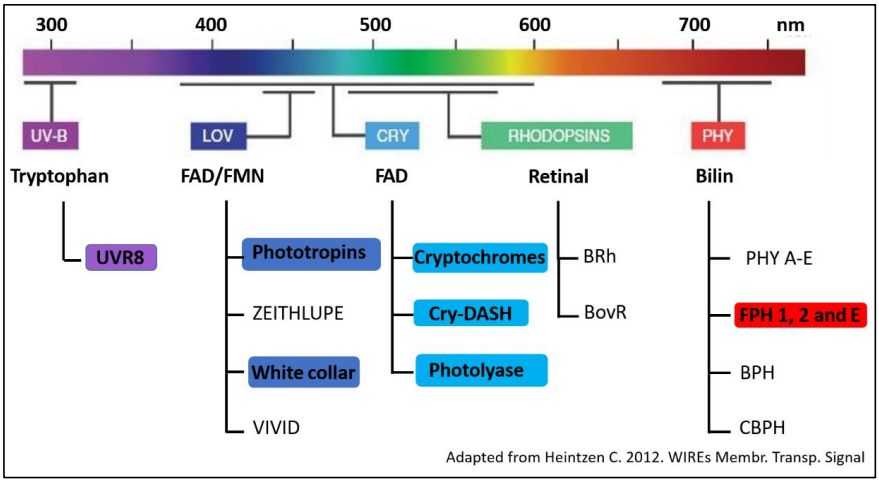

Fig. 3. The different classes of photoreceptors present in fungi respective to their absorption within the UV/visible spectrum of light. Coloured highlighted boxes represents photoreceptors in powdery mildews.

1.4.1.1. Phytochrome photoreceptors

Aspergillus nidulans has led the role in explaining red light responses in fungi (44). Phytochromes are red/far-red light absorbing photoreceptors contains a linear tetrapyrrole chromophore (bilin) for light sensing (94, 148). Phytochromes are characterized by an N-terminal PAS/GAF/PHY domain and a C-terminal output domain. In fungi, bilin covalently binds to the PAS domain in N-terminal (44). The chromophore undergoes photoconversion by switching between two stable interchangeable forms: Pr (red light absorbing) and Pfr (far-red light absorbing) (148). First fungal phytochrome, FphA was characterized in *A. nidulans* and responsible to repress the sexual development under red light conditions (13). In *N. crassa*, two phytochromes (PHY-1 and PHY-2) have been reported. These photoreceptors were hypothesized to have other roles that needs to be investigated as *N. crassa* exclusively reacts to only blue light (26, 33).

1.4.1.2. Opsin photoreceptors

Green light sensing is achieved by rhodopsins. Rhodopsins are membrane bound proteins with seven transmembrane α-helices (7TM) composed of a retinal chromophore covalently bound to an opsin apoprotein via conserved lysine residue (148). Two types of opsins are reported, type I are microbial (bacteria, archaea, fungi) opsins and serves as light controlled ion transporters or sensory receptors. Type II opsins are the primary receptors for vision in vertebrates (35, 94). The first eukaryotic type I rhodopsin was discovered in filamentous fungi, *N. crassa* opsin-1 (NOP-1). NOP-1 was found to bind with all trans retinals (101). In *N. crassa*, deletion of *nop-1* gene does not lead to any photoresponsive defects, but this deletion does however lead to a light dependent morphological difference when mitochondrial ATP synthesis is impaired. This suggests that NOP-1 may play a role in light dependent proton pump rather than a sensory receptor (35, 48). Opsin related proteins (ORPs) are widely distributed in other fungi but their biological roles have yet to be investigated (35, 101).

1.4.1.3. Light-oxygen-voltage (LOV) photoreceptors

Blue light responses are one of the best-studied responses in fungi, and most fungi respond to blue light (26, 101). LOV photoreceptors are the blue light photoreceptors contain flavin chromophore (FMN or FAD). They share a conserved domain with proteins that sense Light, Oxygen, and Voltage (LOV) (44). The first blue light photoreceptor was reported in *N. crassa*, is WC-1 (white collar). In *N. crassa*, blue light responses include induction of sporulation, hyphae growth, carotenoid synthesis, and entrainment of circadian clock (24, 25, 72). WC-1 photoreceptor contains a single LOV domain followed by two PAS domains and a zinc finger at C-terminus, which interacts with the specific DNA sequences. LOV domain binds to flavin chromophore. WC-1 operates together with the WC-2, they interact together to form a white collar complex (WCC). LOV domain together with a zinc finger allows WCC to acts as transcriptional regulator, and promotes the expression of *frq* (frequency) gene in the dark (26, 33, 148). In addition, a single LOV domain containing small photoreceptor protein VIVID (VVD) acts as a regulator of WCC and plays an important role in mediating photoadaptive responses (25, 26, 112). Similar *wc* genes are also described in other fungi (24). In *Aspergillus nidulans,* blue light alone induces asexual cycle and is perceived by WC-1 and WC-2 homologs, LreA and LreB respectively (101). However, their transcriptional activities have not been studied in detail (26).

1.4.1.4. Cryptochrome/Photolyase Family (CPF) photoreceptors

Cryptochromes and photolyases are blue light photoreceptors, which are evolutionary related flavoproteins, but perform different physiological functions (48, 105). Photolyases repair the DNA damages caused by UV while cryptochromes are responsible to synchronize the circadian clock in animals. While in plants, cryptochromes entrain circadian rhythms to mediate variety of light responses such as regulation of growth and development in response to blue light (79, 105). Cryptochromes together with the photolyases constitute a large superfamily, known as cryptochrome/photolyase family (CPF) (79). According to their functions, this superfamily includes CPD photolyases, (6-4) photolyases, cryptochrome-DASH (CRY-

DASH) and cryptochromes (55, 79, 137). CPF members are found widely distributed throughout the biological kingdom from archaebacteria to mammals (22, 105).

Cryptochrome photoreceptors were first identified in plants, where they are involved in various blue light mediated phototropic responses ranging from regulation of flowering, seedling growth, and entrainment of circadian clocks (1, 44). Cryptochromes share high degree of sequence homology, and structurally similar to photolyases. Cryptochromes and photolyases contain a catalytic chromophore (FAD), and a second photoantenna chromophore. However, during evolution cryptochromes have lost their ability to repair DNA damage caused by UV, and majorly involved in blue light signaling (44, 79). Evolutionary studies suggested that classical cryptochromes and CRY-DASH most likely emerged from a common photolyase ancestor (79). Cryptochrome genes have also been described in Fungi. In fungi, all the cryptochromes identified to date, belong to DASH type of cryptochromes. CRY-DASH have a primary role in DNA damage repair (44). It has been reported recently that cryptochrome (CRY) partially regulates the circadian clock in *N. crassa* as CRY is necessary for the oscillator activity of CDO (CRY-dependent oscillator) in constant light conditions (85). In *A. nidulans*, CRYA is the photolyase/cryptochrome like protein encoded by a *cryA* gene has shown DNA repair activity, and also shown regulatory roles like suppression of sexual development under UV-A light (9). Hence, showed combined characteristics of photolyase and classical cryptochrome.

1.5. Photolyase

DNA photolyases are considered to be the most evolutionary ancient DNA repair enzymes (79, 137). Photolyase is known as photon powered nanomachine, which repairs the DNA damage caused by UV (200 – 300 nm) using photons absorbed within near UV/blue light (350 – 500 nm) as an energy source (106, 107). Photolyase was first discovered by Claud S. (Stan) Rupert in 1958 (107). Photolyases are widely distributed in all three kingdoms of life (archaea, bacteria, eukaryota) but are absent in placental mammals including mice and humans (103). It has been reported that during the course of evolution (over 170 million years ago) when mammals split into placentals and

marsupials, former have lost photolyase mediated repair system and latter retained it (62, 80).

Photolyases are monomeric proteins of molecular mass 50 – 70 kDa (~400 – 600 amino acid residues), contains two non-covalently bound chromophores/cofactors: two electron reduced FAD (Flavin adenine dinucleotide) which is a catalytic cofactor, common to all CPF members, and a second cofactor is either methenyltetrahydrofolate (MTHF) or 8-hydroxy-7,8-didemethyl-5-deazariboflavin (8-HDF) that acts as a photoantenna chromophore (103, 106, 108, 132) (Fig. 4).

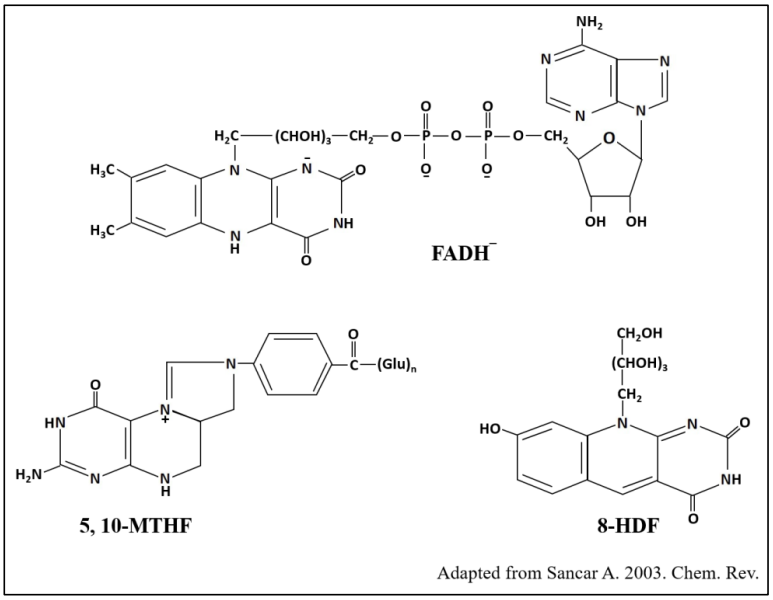

Fig. 4. Structures of chromophores present in cryptochrome/photolyase family photoreceptors. A common catalytic chromophore, flavin adenine dinucleotide ($FADH^-$), and photoantenna chromophores; methenyltetrahydrofolate (5,10-MTHF) and 8-hydroxy-5-deazaflavin (8-HDF).

Photolyase/cryptochromes proteins are distributed sporadically among species in the Ascomycetes, Basidiomycetes and Mucoromycotina (48). Photolyases are present in essentially all the species, where they are involved in light mediated DNA damage

repair (35). First regulatory role of photolyase was reported in *Trichoderma atroviride*. In *T. atroviride*, CPD photolyase (PHR1) possess photorepair properties, and also regulates its own photoinduction, which requires a White Collar (WC) homolog- BLR (blue light regulator) (10). Similarly, the photolyase ortholog in *Aspergillus nidulans*-CryA showed dual function. It is not only capable of DNA repair but also acts as a suppressor of a sexual development under UV-A light (9).

1.5.1. Ultraviolet and DNA damage

Ultraviolet radiation (100 – 400 nm) is a short wavelength part of electromagnetic spectrum, which is further subdivided into four distinct spectral areas- UV-A (315 – 400 nm), UV-B (280 – 315 nm), UV-C (200 – 280 nm) and vacuum UV (100 – 200 nm) (147). UV-C and short wavelength part of UV-B are absorbed by stratospheric ozone layer, only wavelengths greater than 290 nm can reach the Earth's surface (34). Continuous depletion of stratospheric ozone layer due to the release of atmospheric pollutants results in the increase of incidence UV radiations on Earth's surface (98).

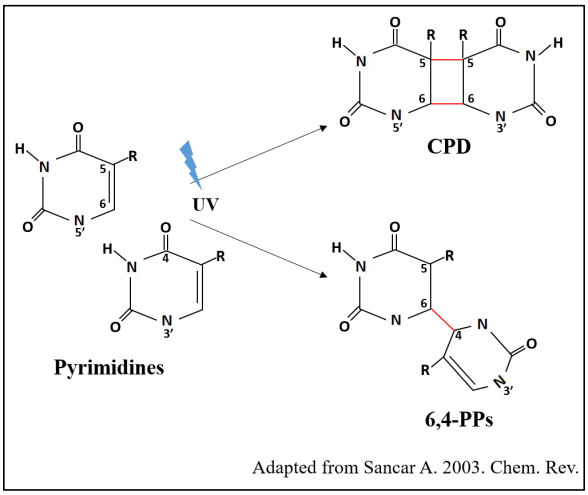

Fig. 5. Structures of two major ultraviolet induced DNA damages/lesions formed between two adjacent pyrimidine residues; cyclobutane pyrimidine dimer (CPD), and 6-4 photoproducts (6-4 PP).

UV radiations have deleterious effects on all life forms ranging from single-celled bacteria to humans and plants. UV-C in particular, is known for its highly germicidal properties and has been used to prevent and treat localized infections in early stages of development (28) as well as in disinfecting the drinking water (133). UV radiations introduce several biological effects on biota such as growth inhibition, cell survival, protein degradation, inactivation of photosynthetic machinery, and damages to biological molecules- DNA and proteins (53). UV-C (200 – 280 nm) and UV-B (280 – 315 nm) radiations are strongly absorbed by DNA and can induce lethal mutations and/or kill simple organisms once absorbed (140). Thus, the cellular DNA is a key target, which is affected by UV radiations and kill the pathogen by directly damaging its DNA (116). These damages in the cellular DNA are formed by inducing structural changes in the DNA (28). UV radiations are responsible for two major types of damages or lesions in the DNA, which are formed between two adjacent pyrimidine residues and these are cyclobutane pyrimidines (CPDs) and pyrimidine-pyrimidone (6-4) photoproducts (Fig. 5) (107). CPDs constitute about 80 – 90%, while (6-4) photoproducts constitute only 10 – 20% (106). CPDs are generated by a formation a cyclobutane ring involving two covalent bonds between C_5 and C_6 of two adjacent pyrimidine residues (C5–C5' and C6–C6') on the same DNA strand, whereas (6-4) photoproducts formed by joining C_6 of the 5' base to the C_4 of the 3' base of two adjacent pyrimidine residues (106).

These lesions are deleterious if they are left unrepaired as they block replication and transcription, which leads to the cell cycle arrest and ultimately cause cell death (34). If DNA damages are not repaired, they can result in genomic instability, which can affect the organism's development and ageing process. Moreover, loss of genomic integrity is one of the major cause of neurological disorder and cancer (40). Hence, maintaining the genomic integrity is essential for every organism's survival and for the inheritance of traits to their offspring (89).

1.5.2. Photolyase-mediated DNA damage repair mechanism

In the year 1949, Prof. Albert Kelner observed an interesting phenomenon in *Streptomyces griseus* that UV treated dead bacteria were recovered again, when exposed to the visible light. This phenomenon was termed as photoreactivation (56, 107). Later

the same phenomenon was also reported in *Escherichia coli*, *Penicillium notatum*, and *Saccharomyces cerevisiae* (57).

Photolyase mediated DNA damage repair or photoreactivation, perhaps one of the simplest and oldest repair method because of the involvement of a single enzyme (116). Ultraviolet light induces two major DNA damages or lesions, cyclobutane pyrimidine dimers (CPDs) and (6-4) photoproducts [(6-4) PPs], which are formed between two adjacent pyrimidine bases usually thymines, (T<>T) or (Pyr<>Pyr). These are potentially mutagenic, and lethal to organisms (107, 116, 140). Photolyases repair these damages by reversing CPDs to their normal conformation (monomers) by using near UV/blue light (350 – 500 nm) as an energy source (107, 108). Reaction mechanism of photolyase enzyme has been extensively studied in detail using *E. coli* photolyase (103, 104, 107). The reaction mechanism of photoreactivation is carried out as follows (Fig. 6).

(i) Substrate recognition and binding

Photolyase is extremely efficient in recognizing the cyclobutane pyrimidine dimers in the DNA. It can differentiate dimers from a huge excess of non-dimer pyrimidine bases, which are present next to each other as doublets (TT) (140). In *E. coli*, there are only ~10 – 20 molecules of photolyase per cell (43, 108). Photolyase recognizes the CPD (Pyr<>Pyr) in the DNA and bind to backbone of the damaged strand via ionic interactions (55, 107). The binding of the photolyase to the dimer occurs in a light-independent manner (103, 132). The photolyase flips out the dimer into the center of its active site cavity, where dimer is in the close proximity with the flavin, and forms a stable enzyme-substrate complex with high affinity (55, 132). Photolyase remains bound to the dimer until it gets exposed to the photoreactivating light (350 – 500 nm) (132).

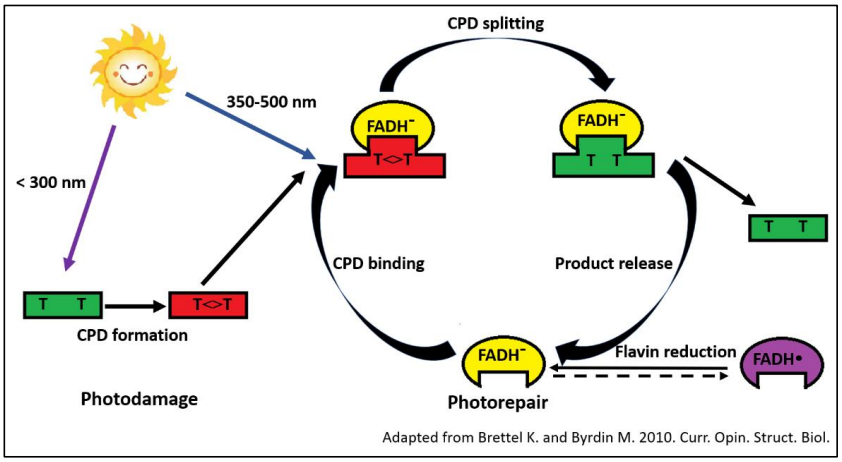

Fig. 6. Mechanism of photoreactivation. Short wavelength UV (< 300 nm) induced the formation of cyclobutane pyrimidine dimer (CPD) between two adjacent pyrimidine bases on the same DNA strand. Photolyase absorbs the photons in near UV/blue light (350 – 500 nm) as an energy source, splits the CPD (T<>T) into two canonical pyrimidine bases (T T) and then dissociates from the DNA.

(ii) Catalysis

Catalysis reaction initiated by light (350 – 500 nm) which is essential for cycloreversion of the cyclobutane ring formed between two pyrimidines (T<>T) (103). When enzyme-substrate complex exposed to light, photoantenna cofactor (MTHF or 8-HDF) absorbs the photon, and achieves a high energy excited singlet state (132). Photoantenna molecule transfers this excitation energy to the fully reduced flavin cofactor ($FADH^-$) by Förster dipole-dipole resonance energy transfer (55, 132). $FADH^-$ is a catalytically active form of flavin which is necessary for catalysis (103). The excited flavin subsequently donates an electron to the Pyr<>Pyr, where cyclobutane ring of the dimer splits via rearrangement of the bonds (C5–C5' and C6–C6') and generates two canonical pyrimidine monomers (20, 55, 103). The photolyase enzyme and the products dissociates, and finally an electron transferred back to the flavin to restore its catalytic competent form ($FADH^-$) ready for next cycle of catalysis (55, 132).

1.5.3. Photolyases classes

On the basis of their substrate binding specificity and function, photolyases are distinguished as CPD photolyase and (6-4) photolyase (132). CPD photolyase binds and repairs cyclobutane pyrimidine dimers (CPDs) in single or double stranded DNA, and (6-4) photolyase binds and repairs (6-4) photoproducts (140).

On the basis of the type of second (photoantenna) chromophore, CPD photolyases are further classified either as folate type (MTHF) or deazaflavin/flavin type (8-HDF) (103, 106) (Fig. 4). The folate (MTHF) type photolyases are found in most of the species; *Escherichia coli*, *Neurospora crassa* and *Saccharomyces cerevisiae* while the deazaflavin (8-HDF) type photolyases are present in limited number of species; *Anacystis nidulans*, *Streptomyces griseus* (103, 110).

Depending on their amino acid sequence similarity, CPD photolyases are further divided into class I, class II, and class III photolyases (137). Class I CPD photolyases are classic DNA photolyases mostly found in prokaryotes, simple eukaryotes and fungi (*E. coli*, *A. nidulans*, *N. crassa*) (140). Class II CPD photolyases include higher organisms from animals and plants, which are closely related to *Drosophila melanogaster* and *Arabidopsis thaliana*, but also include some microbial photolyases (140). Class III CPD photolyases are bacterial photolyases, which are phylogenetically close to class I CPDs and plant cryptochromes (137).

1.6. Other mechanisms of repair of UV-induced DNA damages

DNA is the key target, which gets encountered with DNA damages at cellular level that either results from endogenous (cellular metabolic processes) or exogenous (environmental factors) sources (40). Endogenous factors like hydrolysis and oxidation reactions (ROS), and exogenous factors like ionizing radiation (IR), ultraviolet (UV) radiation (mainly UV-B, 280 – 315 nm), and various other chemical agents are responsible for DNA damages (40, 98).

There are mechanisms other than photoreactivation, which are also involved in the repair of DNA damages caused by UV. CPD photolyases and (6-4) photolyases specifically recognize CPDs or (6-4) PPs respectively, but not both because they are not

able to recognize DNA damages which are different in structures (other than CPDs or 6-4 PPS). The other DNA repair mechanisms for UV induced damages are (i) Nucleotide excision repair, and (ii) Repair by UV endonuclease.

(i) Nucleotide excision repair (NER)

NER is the complex multistep process, which is one of the most versatile repair mechanisms found in both prokaryotes and eukaryotes (40, 98). It is light independent and also known as dark repair (98). NER removes wide range of lesions including bulky DNA adducts caused by chemicals and pyrimidines dimers caused by UV radiation (40). In *E. coli*, NER is controlled by *uvr* genes (*uvrA*, *uvrB*, and *uvrC*). UvrA, B, C proteins act together and make a dual incision at the damage site with precise distances. The resulting gap is filled by DNA polymerase I, and repaired patch is ligated by DNA ligase (107). In mammalian NER, over 30 different proteins are involved in recognition and repair of a damage in the DNA (116, 135).

(ii) Repair by UV endonuclease (UVDE)

An additional mechanism to repair UV induced DNA damages involves an enzyme known as UV damage endonuclease (UVDE) as they recognize and incise DNA 5' to the dimer (81, 116). These enzymes generally found in UV resistant organisms like *Micrococcus luteus* (76). UV endonucleases perform a novel form of excision repair by introducing a nick at the 5' of the pyrimidine dimer followed by the cleavage of phosphodiester bond at AP (apurinic/apyrimidinic) site. Similar enzymes have been described in eukaryotes, *Schizosaccharomyces pombe* and *N. crassa* (17, 41). These enzymes recognize both CPDs and (6-4) PPs, and introduce a nick immediately at 5' of the damage (116). In bacteriophage T4, *denV* gene encodes for similar enzyme (T4 endonuclease V) but it recognizes only CPD dimers. In bacteriophage, there is an interaction between mechanisms of repair by endonuclease and NER, where endonuclease first cleaves the fragment containing CPD, which further take over by NER and restore DNA to its original form (61).

1.7. An Overview of Tomato Crop

Tomato (*Solanum lycopersicum* L., formerly *Lycopersicum esculentum* Mill.) is one of the major horticultural crop, cultivated in more than 150 countries around the world with an estimated global production of approximately 180 million tons according FAOSTAT, 2019 (5). Commercial tomato belongs to genus *Lycopersicon* within a diverse family Solanaceae, which also includes eggplant, potatoes, peppers, and tobacco (131).

Tomato is considered a tender warm season crop with a growing period of 90 to 150 days. It is a perennial crop in its native habitat, but grown as an annual in temperate climate. Although tomatoes thrive in temperature ranges from 10°C to 30°C, but they are very intolerant to frost and cannot grow in shade (131). Tomato plants are either determinate or indeterminate. Most field tomatoes are determinate plants, and are early matured with short growing season while indeterminate plants have longer production season of 9 to 10 months, and are ideal for greenhouse production but require constant maintenance (102). Tomato has a huge fresh market, but a large production contributes to processed market in the form of various products such as sauce, salsa, soup, ketchup, pickle, sun-dried tomatoes, and other prepared foods, globally (131). In Europe, most of the part of tomato production goes to the processing sector (4).

1.7.1. Tomato Production in Norway

Norway is located on the latitude and longitude of 62°N and 10°E in the North-Western Europe. North Atlantic warm air currents with colder interior, and increased precipitation along the coast maintained the temperate climate on the west coast of Norway. This create a relatively mild climate, which allows the commercial horticulture possible even in the northern part of Norway (3). The day length varies from 6 to 19 h in the southern part, and from zero to 24 h in the northern most part of Norway (6). Because of very limited growing season (140 to 160 days) with an average temperature of above 6 °C, field grown crops are very limited in Norway (3).

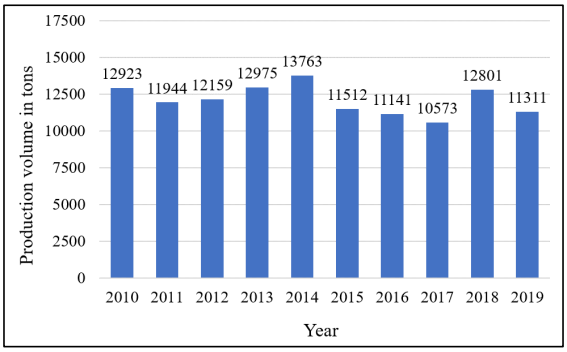

Fig. 7. Total tomato production (in tons) recorded for last ten years in Norway. Data was collected from FAOSTAT (Food and Agriculture Organization of the United Nations).

In Norway, tomatoes were introduced in 1855 at Christiania, and were first ever grown in 1890 in Rogaland, which is situated in the south-west of Norway. The first commercial production was done in the heated greenhouse in the year 1932 (38, 87). Finnøy in Rogaland is particularly known for tomato production, and it made possible because of its fertile soil and mild climate (38). In Norway, around 85% of the tomato production comes from Rogaland (2). Greenhouse production is a major source of commercial horticulture in Norway with approximately around 200 hectares (ha) of total greenhouse area calculated by the year 2010 (3). Out of the total area, half is dedicated for vegetables and half for ornamentals. From the total vegetable area nearly 390 decares (daa) (equal to 39 hectare) is used for tomato production in 2019 (personal information from A. Sand, Norwegian grower association). Total tomato production in Norway was recorded 11311 tons in 2019 (Fig. 7) (5).

In Norway, tomatoes have been the most sold product in the fresh vegetables in recent years with an annual consumption of 7.3 kg annual per capita and out of this 1/3 produced in Norway (75). In Norway, all the tomato production is intended for domestic fresh market, not for processed food because of high production cost that comes from heated glass houses and artificial light for year-round production. It is the second most product which is imported in Norway (14). In order to compete with the imported varieties, it is necessary to maintain the high quality as well as availability. Therefore, intensive research efforts are centered on the disease free growing environment, and quality with minimal use of chemicals.

1.7.1.1. Cultivation system and growth conditions

In many countries like Norway, where one wants to grow crops which need a warmer climate and more control of the environmental factors, greenhouse production is the only alternative to crop cultivation. Therefore, soilless cultivation in greenhouses are the major means of commercial tomato production in Norway. Tomatoes are grown on rockwool or an organic media such as peat or coir in gullies, so that plants are raised above from the ground (131). The cropping season usually starts by planting tomato seedlings from the end of January to the beginning of March with the use of just natural light and ends around November. With the addition of artificial light, the planting normally takes place in December and the crop ends in November. The plants are fertilized with a fully compound nutrient solution (pH 5.5–6.2 and conductivity 2.5–3.0 mS/cm) many times a day, depending on the time of the year, weather, and the developmental stage of the crop. Irrigation and fertilization programs are used to regulate the balance between vegetative and generative growth (87).

Greenhouse climate is a major factor, which influences the productivity and quality of greenhouse crops (115). Microclimate plays a significant role on the different developmental stages of the tomato plant. Hence, maintaining an environment in a greenhouse, which promotes an optimal production is really crucial. The most important environmental factors that influence the growth of tomato in greenhouse are light, CO_2, temperature, and relative humidity (RH) (114).

In Norway, about half of the tomato production is done with the use of artificial light usually 200 W/m^2 for 18 h/day. Carbon-di-oxide is also an important factor for greenhouse tomato production as CO_2 enrichment increase the plant growth and fruit set. CO_2 is usually added to a level of 800–1000 μmol mol^{-1} to the greenhouse air, which increases production to 30% compared to the CO_2 level of the outside air of 400 μmol mol^{-1} (138). Air and root temperatures both are important for tomato production and quality. Different studies are available for temperature required for each specific growth and developmental stage of a plant (114). For greenhouse tomatoes, a day temperature of 18°C–20°C and night temperature of 16°C–17°C are preferred (102). Solar radiations also contribute to the temperature in greenhouses; hence this needs to be taken into consideration.

RH is another important factor, crucial for plant growth, and critical in maintaining to optimum levels. The RH usually vary in the greenhouses; depending on the season, geographical location, and the greenhouse system used (15). The microclimate around the plants; especially inside a dense canopy can be very different (higher RH) than the rest of the greenhouse (84). Optimum relative humidity levels for tomato plants is in between 80–90 % during the day and 65–75 % during the night (19).

One of the major problem in the greenhouses is the moisture buildup because of higher RH, which can have a negative effect on the plant growth and can also lead to risk for powdery mildew development. Active and passive ventilation systems can be used to remove the excessive moisture (19, 42, 134). In addition to environmental factors, disease management and prevention are another important aspects in greenhouse cultivation of tomatoes.

1.7.2. Diseases in Greenhouse Tomato

The controlled environmental conditions in the greenhouse support optimum plant growth and development, which improves yield. However, similar conditions also provide an excellent environment for outbreak of pest and diseases if entered into the production system. Diseases are the major limiting factor, which significantly reduces the yield and cause severe economic losses (111).

Soil cultured tomato crops are more often invaded by nematodes, early blight (*Alternaria solani*), late blight (*Phytophthora infestans*), gray mold (*Botrytis cinerea*), leaf mold (*Passalora fulva*), fusarium wilt (*Fusarium oxysporum*), verticillium wilt (*Verticillium* sp.), and various bacteria and viruses while soilless cultures are often encountered with leaf mold, gray mold, root bacteria, and viruses (111). Therefore, greenhouse environment is not completely sterile environment or immune to diseases and pests instead it requires regular attention to maintain good sanitation by developing prevention programs.

1.8. Powdery Mildew in Tomato

Out of several diseases, powdery mildew is very common in greenhouse tomato production worldwide. It is usually very aggressive in susceptible cultivars, in combination moderate temperature and high relative humidity of greenhouse environment makes it more devastating if not properly managed. Powdery mildew in tomato can be caused by i) *Leveillula taurica*, ii) *Oidium lycopersici*, and iii) *Pseudoidium neolycopersici* (31, 63, 70, 142). *L. taurica* is hemi-endophytic with branched conidiophores that emerge through stomata, caused severe damages in tomatoes, and various other crops specially in tropical countries with dry and warmer climate (31, 142).

Based on morphological comparison and molecular analysis, ectophytic powdery mildew pathogens have been reported earlier as two different species i) *Oidium lycopersici*, and ii) *Pseudoidium neolycopersici*. *O. lycopersici* is common in Australia, and *P. neolycopersici*, which is widespread in Asia, Africa, Europe, Northern, and Southern America (70). A taxon with catenate conidia was named as *O. lycopersici*, and a taxon with non-catenate conidia as *P. neolycopersici* (58). Australian isolate always formed conidia in chains, while *P. neolycopersici* forms either single conidia or pseudochains of 2–6 conidia (54, 70). However, the true taxonomic determination of *P. neolycopersici* is still unclear due to the lack of the teleomorph (sexual) stage as it has not been found in tomato powdery mildew to date (54, 69, 70).

The origin of *P. neolycopersici* is still unknown suggested that it may have jumped hosts by acquiring several pathogenicity factors (54). The highly polyphagous nature of *P. neolycopersici* is a potential risk to horticulture industry especially greenhouse cultivation (142). The disease was first reported nearly 30 years ago in Southern England, UK in 1986 (31, 54). The causative agent of the disease is *Pseudoidium neolycopersici* (syn. *Oidium neolycopersici*) belongs to order Erysiphales (37, 58). The disease has gained economic importance as it poses a major threat predominantly on greenhouse grown tomatoes, and field grown tomato crops throughout Europe and America (54).

The powdery mildew caused by *P. neolycopersici* affects adaxial surfaces of leaves and stems of tomatoes and superficial mycelium gives the characteristic symptoms of

white powdery pustules (54). As the disease becomes aggressive, mildewed leaves cause considerable defoliation. This results in impaired photosynthesis, which ultimately leads to diminished yields (82). There are three key phases in the PM disease development, germination usually occurs at 3 – 6 h after inoculation (hai), appressorium formation at 6 – 8 hai, and penetration at approximately 11 hai (54). Conidia are easily dispersed by stronger winds (1.0 m/s) from conidiophores apex without forming pseudochains and deposited on the leaf surfaces (86). The disease becomes severe during spring months in the greenhouses when environmental conditions, particularly relative humidity and temperature, are ideal for pathogen to thrive and most favorable for conidial germination (31).

Although sexual stage of reproduction has not been reported yet in this fungi, available data suggested that there is a considerable variation in the host ranges, pathogenicity and virulence of different strains (52, 65). An extensive host range study revealed that members of 13 families were alternate hosts of *P. neolycopersici,* suggesting existence of different pathotypes (66, 68, 142). However, the natural occurrence of *P. neolycopersici* on the plants other than tomato has not been proven so far (52). Overall, the host range of *P. neolycopersici* is still rather inconsistent.

2. OBJECTIVES OF THE PRESENT STUDY

Powdery mildew is the most catastrophic disease in greenhouse tomatoes (70). Two possible ways have been proposed to control powdery mildews- fungicides, and breeding for resistance cultivars. In greenhouse tomatoes, sulfur vapour or synthetic fungicides are most commonly used for the disease management of powdery mildews (70). However, use of chemicals and fungicides cause adverse effects on biota associated with powdery mildews and, lethal to potential biocontrol agents that can be used against various pests. Intensive use of fungicides may also develop resistance populations of a pathogen (127).

Extensive breeding programs have been implemented because almost all the commercial tomato cultivars are susceptible to *P. neolycopersici* (68, 113). In addition, after extensive screening of available tomato cultivars with no effective sources of resistance to *P. neolycopersici*, wild tomato germplasms were also used as valuable sources of resistance (54, 68). Breeding is the safest choice for disease management with no environmental impact, and use of resistant cultivars also reduces the cost of fungicide applications. However, there are limitations as breeding is very time consuming with relatively low success rate. Therefore, these limitations and consumers choice in the modern world of "go green" inclined interest towards finding an alternative, which is environmentally friendly.

Manipulation of greenhouse environment may be an alternative approach for powdery mildew disease management. There has been limited research on the effects of different environmental conditions in *P. neolycopersici.* Previous studies have shown that short wavelength ultraviolet (< 290 nm) are potentially effective in controlling powdery mildews in different crops at greenhouse level (119, 120, 124). However, the efficiency of UV treatment is dependent on the specific wavelength, dose (intensity × duration), application time of the day, and the background light spectral quality. UV (250 – 290 nm) alone or in combination with the red light (635 – 680 nm) have shown to be the most effective in mitigating powdery mildews (119, 120, 124). The efficacy of UV in powdery mildew suppression was significantly reduced under UV-A and blue light wavelengths (350 – 500 nm) (120). This indicated the involvement of DNA repair mechanism, which is mediated by blue light photoreceptor; photolyase.

Photoreceptors genes are well characterized in filamentous fungi like *Neurospora crassa* and *Aspergillus nidulans* (26, 33, 72, 95). However, there are no reports on the presence of photoreceptor genes in any powdery mildew fungi to date. Recent advancements in sequencing technologies enabled genome and transcriptome sequenced for some fungi. Recent studies with Illumina HiSeq RNA sequencing for *Erysiphe necator*, causal agent of grapevine powdery mildew revealed the expression of genes similar to all major classes of photoreceptor genes present in higher plants.

The main goal of the present study is to optimize the optical based powdery mildew management as an environmentally friendly alternative by exploring photoreceptors in powdery mildews with objectives of i) genome-wide identification of the photoreceptor genes in three PM fungi, ii) functional characterization of photolyase, and explore its role in the efficacy of nighttime UV treatment in *P. neolycopersici*, and iii) the role of strains/isolates in potential variation of the nighttime UV efficacy in *P. neolycopersici*

Paper I

Wavelength dependent recovery of UV-mediated damage: Tying up the loose ends of optical based powdery mildew management.

Paper II

Genome-wide identification and characterization of photoreceptor genes in powdery mildews (*Pseudoidium neolycopersici*, *Podosphaera xanthii*, and *Podosphaera aphanis*).

Paper III

Functional characterization of *Pseudoidium neolycopersici* photolyase reveals mechanisms behind the efficacy of nighttime UV on powdery suppression.

Paper IV

Variation in UV-mediated damage recovery among *Pseudoidium neolycopersici* isolates: possible mechanisms.

3. MATERIAL AND METHODS

3.1. Petri dish level experiments in controlled environment chambers

All experiments were conducted at Petri dish level with i) cleaned isolates of *P. neolycopersici* or ii) wild and mutant stains of *Escherichia coli*.

Tomato leaves having active colonies of *P*. *neolycopersici* were collected from four different locations in Norway, and one from The Netherlands. Cleaned isolates were prepared individually from all these collections by sequential transfer of single conidium to surface disinfected tomato leaves of cv. Espero placed on Petri dishes containing water agar. Inoculated leaves were maintained in controlled environment chamber with 16 h photoperiod with an irradiance of 50 – 60 µmol m^{-2} s^{-1} provided by high-pressure mercury (HPM) lamps (Powerstar HQI-BT 400 W/D day light; OSRAM GmbH). Temperature and relative air humidity (RH) were maintained as 20 ± 2°C and 75 ± 5%. Colonies of eight- to nine-day-old developed from these clean isolates were transferred to tomato plants cv. Espero maintained in five different controlled environment chambers with similar environmental conditions described above. For inoculation of healthy tomato plants, diseased leaves were shaken thoroughly in distilled water with Tween-20 (20 µl/l) and the resultant conidial suspensions were sprayed on the foliage of 2-week-old healthy tomato plants maintained in the controlled environment chambers.

To examine the effect of optical wavelengths applied subsequent to nighttime UV treatment on inhibition of conidial germination and recovery experiments were conducted with the 'As' isolate collected from Akershus, Norway. Conidia of eight- to nine-day-old inoculum was dusted on 1% (w/v) water agar in 3.5 cm Petri dishes. After dusting, the Petri dishes were either exposed to non-UV (control) or UV treatment without lids. Immediately after treatments, Petri dishes were sealed and transferred into the controlled environment chambers with different incubation wavelengths (subsequent wavelength after UV treatment).

For brief UV treatment, wavelength ranges from 254 nm to 313 nm were provided by following radiation sources; 254 nm peak (45 cm length tube, model- TUV

15W/G 15 T8, Philips; Holland), 283 nm peak (XeBr Excimer lamps, model- SUS844, Ushio; Japan), 310 nm peak (120 cm fluorescent tubes model- MedSun Therapy narrow band UV-B 40W, LightTech; Dunakeszi, Hungary), and broad spectrum UV with peak at 313 nm (120 cm UV-B fluorescent tubes model UV-B-313EL, Q-Panel Lab Products; Cleveland, OH). The level of irradiance at sample level was maintained as 8 ± 0.2 µmol m^{-2} s^{-1}. Durations of UV exposure were set as 30, 60, 120 or 240 s. UV treated samples were incubated with either (i) 16 h of incubation with optical radiation followed by 8 h dark, or (ii) 8 h dark incubation followed by incubation of 16 h with optical radiation.

For incubation wavelengths, optical radiations with peak and ranges of 310 nm (290 – 350 nm) (120 cm fluorescent tubes model- MedSun Therapy narrow band UV-B 40W, LightTech; Dunakeszi, Hungary), 365 nm (320 – 443 nm) (120 cm fluorescent tubes, ES UV-A 365 nm 40W, LightTech; Dunakeszi, Hungary), 400 nm (375 – 465 nm) (RAY22 UV-A LEDs, Fluence Bioengineering; Austin, TX), 454 nm (410 – 500 nm) (15W GreenPower LED module HF blue, Philips; The Netherlands), 523 nm (470 – 600 nm) (162W High-Power LED grow light, Sola-co; Grimstad, Norway), 660 nm (600 – 700 nm) (10W GreenPower LED module HF deep red, Philips; The Netherlands), or 730 nm (650 – 780 nm) (10W GreenPower LED module HF far-red, Philips; The Netherlands) were used with irradiance of 50 ± 5 µmol m^{-2} s^{-1}.

Twenty-four hours after inoculation, samples were examined under light microscope, and 50 conidia were assessed for conidia germination. For each treatment three replicate Petri dishes were used, and experiment was repeated twice. These experiments were designed with randomized complete block design (RCBD).

3.2. Genomic DNA extraction from powdery mildew

Conidia from 10- to 14-day-old, cleaned colonies of *P. neolycopersici* (As isolate), *P. xanthii*, and *P. aphanis* were dusted on water agar surface. The inoculated water agar surfaces were gently scrapped with microscopic glass slide. Scraped samples were transferred into 2 ml Eppendorf tube and flash frozen in liquid nitrogen.

Genomic DNA was extracted using a method by H. L. Robinson et al. (100) with slight modifications. Genomic DNA quality and quantity was checked by NanoDrop™ 2000 and agarose gel (0.8%) electrophoresis respectively. Next generation sequencing

was performed on NextSeq 500 (Illumina, USA) using mid-output 150 bp paired end run, and draft genomes for *P. neolycopersici* (As isolate), *P. xanthii* and *P. aphanis* were assembled and annotated.

3.3. Cloning and photoreactivation assay of *P. neolycopersici* CPF-like genes

Based on the sequence information of the draft genome of *P. neolycopersici* (As isolate), coding region of three CPF-like genes (OINE01015670_T110144, OINE01000912_T103440, and OINE01005061_T102555) were codon optimized, synthesized by GenScript, USA with respective names of PN5670, PN0912, and PN5061 for OINE01015670_T110144, OINE01000912_T103440 and, OINE01005061_T10255. PN5670, PN0912, and PN5061 genes were cloned separately at SphI and XmaI restriction sites in pQE-30Xa vector (Amp^R) with N-terminal 6X His-tag and later named as pQE-30Xa_PN5670, pQE-30Xa_PN0912 and, pQE-30Xa_PN5061 respectively.

For survival assays, *E. coli* strains, wild type KY1056 photolyase-proficient (*recA56*, *phr*$^+$), and mutant strain KY1225 photolyase-deficient (*recA56*, *phr*$^-$) were used. Both strains were first transformed with pREP4 (Kan^R) repressor plasmid, which carries a lac repressor that tightly regulates lac promoter controlled expression of recombinant proteins in pQE-30Xa vector. Prior to photoreactivation assay, it was tested that UV-C (254 nm, 2 ± 0.2 µmol m^{-2} s^{-1}) for 10 s was sufficient to have a significant effect on cell survival of *E. coli* KY1056 and KY1225 strains. *E. coli* strains, KY1056 and KY1225 that has already been transformed with pREP4 plasmid, were transformed again with pQE-30Xa vectors with or without inserts (prepared above) and generated following constructs- (i) KY1056_pQE-30Xa (empty vector), (ii) KY1225_pQE-30Xa (empty vector), (iii) KY1225_pQE-30Xa_PN5670, (iv) KY1225_pQE-30Xa_PN0912, and (v) KY1225_pQE-30Xa_PN5061, where KY1056_pQE-30Xa and KY1225_pQE-30Xa were used as a positive and negative control respectively.

For qualitative survival assay, following transformation with above constructs, plates were exposed to no UV (control) or UV-C (254 nm, 2 ± 0.2 µmol m^{-2} s^{-1}) for 10 s. Immediately after treatment, plates were incubated in the dark or blue light (454 nm, 25 ± 5 µmol m^{-2} s^{-1}) for 2 h at 25°C followed by incubation at 37°C in dark for overnight.

Next day, plates were assessed for surviving colony. The construct (KY1225_pQE-30Xa_PN0912) which showed photoreactivation activity was further used for quantitative survival assay together with positive (KY1056_pQE-30Xa) and negative (KY1225_pQE-30Xa) controls.

3.4 Action spectra of *P. neolycopersici* photolyase

Action spectra of *P. neolycopersici* photolyase was performed in a similar manner as described in section 3.3 for quantitative survival assay. The only difference, here we have used five different incubation conditions (dark, 365 nm, 400 nm, 454 nm and 525 nm). Immediately after treatment, no UV (control) or UV (254 nm, 2 ± 0.2 µmol m^{-2} s^{-1}) for 10 s, plates were transferred to complete dark or one of four different incubation wavelengths, all with irradiance 25 ± 5 µmol m^{-2} s^{-1} for 2 h at 25°C followed by incubation in dark at 37°C for overnight. Plates were assessed for surviving colony on the following day. Three replicate Petri dishes per treatment were used and experiment was repeated twice.

3.5 Quantitative Real-time PCR for photolyase gene expression

To study the photolyase gene (OINE01000912_T103440) expression, a separate Petri dish level experiment was carried out in controlled environment chambers. Production and maintenance of *P. neolycopersici* inoculum was done as explained in section 3.1. Conidia of 9-day-old inoculum was dusted on a 2% (w/v) agar in Petri dishes. After dusting conidia, Petri dishes (without lids) were exposed to no-UV (control) or UV (254 nm, 8 ± 0.2 µmol m^{-2} s^{-1}) for 30 s. Immediately after treatment, Petri dishes were incubated in three different incubation conditions; (i) dark, (ii) UV-A/blue light (peak 400 nm, 50 ± 5 µmol m^{-2} s^{-1}) or (iii) red light (peak 660 nm, 50 ± 5 µmol m^{-2} s^{-1}). During incubation, samples were collected at three time points; (i) 30 s, (ii) 4 h or (iii) 8 h. Samples from three replicate Petri dishes (biological replicate) were collected.

Total RNA was extracted using Plant RNA reagent (Invitrogen, USA) followed by DNase treatment (Turbo DNA free™ kit, Invitrogen, USA) and purification (PureLink RNA kit, Ambion, USA) using manufacturer's protocol. RNA quality and quantity was

checked by BioAnalyzer 2100 (Agilent Technologies Inc., USA) and Nano Drop™ 2000 (Thermo Fisher Scientific, USA) respectively. cDNA was synthesized with Superscript™ IV VILO Master Mix (Invitrogen, USA) from 500 ng for each RNA sample. Real-time PCR was performed using SYBR™ Select Master Mix (Thermo Fisher Scientific, USA) on 7500 Fast Real-Time PCR system (Applied Biosystems, USA) with three technical replicates per cDNA sample. Alpha tubulin gene (OINE01013217_T107300) was used as an internal control. Photolyase gene expression was calculated relative to the non-UV treated control samples by applying the $2^{-(\Delta\Delta Ct)}$ method (73).

4. MAIN RESULTS AND DISCUSSION

Under controlled environmental conditions, within the tested wavelengths (254, 283, 310 and broad spectrum UV peak at 313 nm) ultraviolet wavelengths 254 nm and 283 nm for 30 s exposure followed by dark incubation have significant effect (germination inhibition) on conidia germination, only less than 10% of conidia germinated compared to non-UV treated dark control (100%), and conidia germination was almost negligible when UV exposure duration was increased to 4 min. Under broad spectrum UV (peak at 313 nm) conidia germination was significantly lower and dependent on the duration of exposure, which is about 60% and 35% with exposure durations of 1 min and 2 to 4 min respectively. With UV 310 nm, there was no reduction observed in conidia germination with ≤ 4 min exposure duration, and therefore it was found ineffective, when applied for less time (≤ 4 min.) in germination inhibition of conidia. Within the tested wavelength and dose ranges of optical radiation (310 – 730 nm) germination of above UV treated conidia was significantly higher (> 73%) when incubated subsequently in 350 nm to 500 nm range (germination recovery) compared to the incubation in dark (< 26%). Moreover, for effective UV treatment to reduce conidia germination, the lapse time (dark period) between nighttime UV treatment and subsequent UV-A/blue light exposure should be more than 4 h (Paper I).

Whole genome sequencing of *P. neolycopersici*, *P. xanthii,* and *P. aphanis* exhibited the assembled genome sizes of approximately 67 Mbp, 203 Mbp, and 156 Mbp respectively, which were estimated within the 158 – 282 Mbp. The draft genome assemblies generated 20061, 86938, and 63866 total number of scaffolds with N_{50} of 9966, 11293, and 7903 bp in *P. neolycopersici*, *P. xanthii* and, *P. aphanis* respectively. To evaluate the completeness of assembled genomes, we conducted core eukaryotic genome mapping approach (CEGMA). This was further verified by BUSCO (benchmarking universal single copy orthologs). Both generated similar results. *P. neolycopersici* genome assembly showed 242 complete highly conserved core eukaryotic genes (CEGs) out of 246 (98.37 %) which was increased to 100% when considering at least a partial match. The summary statistics of assemblies are described in Table 1 of Paper II. Genome annotation revealed the presence of all major classes of photoreceptors in *P. neolycopersici*, *P. xanthii,* and *P. aphanis.* Three genes were identified from blue light photoreceptors, cryptochrome/photolyase family in *P.*

neolycopersici, *P. xanthii,* and *P. aphanis*. The three CPF-like genes were OINE01015670_T110144, OINE01000912_T103440, and OINE01005061_T102555 in *P. neolycopersici* (Paper II).

In *P. neolycopersici*, gene ON0912 (OINE01000912_T103440) expressed in *E. coli* (*phr* mutant) showed photoreactivation activity of UV-C (254 nm) treated cells on subsequent exposure to blue light (454 nm). Therefore, one among three cryptochrome/photolyase family (CPF)-like genes, ON0912 was identified as a potential photolyase (*PnPHR1*). Phylogenetic analysis demonstrated that it belonged to class I CPD photolyase. The protein structure prediction suggested that *PnPHR1* possess FAD and MTHF chromophores. *PnPHR1* showed an action spectra ranges from 365 nm to 454 nm within tested wavelength ranges 365 nm to 523 nm. The photolyase (*PnPHR1*) gene expression was significantly higher in UV-C (peak at 254 nm) treated samples within 30s, independent of incubation wavelength. The maximum expression was attained at 4 h after UV-C treatment. The *PnPHR1* gene expression was significantly higher in UV-C treated followed by dark and UV-A/blue light (400 nm) incubation at all sampling time points (30 s, 4 h, and 8 h) compared to red light (660 nm) incubation. The *PnPHR1* gene expression of UV-C treated samples was dropped to the same level as non-UV control samples, when incubated in red light (Paper III).

The five different isolates (As, Vf, Fn, Sn, and Nl) of *P. neolycopersici* collected from different locations in Norway and the Netherlands showed variation in their germination recovery within blue light (454 nm) incubation of brief UV-C (254 nm) treated conidia. The two isolates (Fn and Nl) showed more tolerance to UV-C treatment compared to the other three (As, Vf, and Sn) isolates. The nucleotide sequences of three cryptochrome/photolyase family (CPF)-like genes in all five isolates showed no variations, and were highly conserved at nucleotide levels. Amino acid sequence analysis revealed protruding N-terminal end (134 amino acid residues long) in photolyase, and C-terminal extensions in putative cryptochrome and CRY-DASH genes. Amino acid sequence alignment also showed three crucial residues (W277, M345, N378) as well as tryptophan triad (W306, W359, W382) among three CPF genes (Paper IV).

Optical radiations have several beneficial effects, but there are potential hazards associated particularly with ultraviolet radiations on living organisms. However, the

degree of manifestation of UV radiations varies, depending on the wavelength, intensity, duration of exposure and complexity of an organism exposed (128, 141). Since powdery mildews do not have UV screening mechanisms, therefore they are more vulnerable to UV radiation than plants.

In previous studies, the effect of nighttime UV treatment on powdery mildew pathogen developmental stages, and disease severity has been reported in various crops (120-122, 124). In present study, we have determined the spectral efficiency within the optical region on the recovery of UV-mediated damage on *P. neolycopersici* conidia (germination recovery), and also determined the dose and lapse time of the wavelength applied after UV treatment and gave minimum recovery. The present study further confirmed that UV wavelength range 250 – 280 nm at low dose is effective in germination inhibition of *P. neolycopersici* conidia, which was reported earlier (122). UV wavelengths above 290 nm can be effective in germination inhibition, if applied at higher doses. In the present study as in case of 310 nm, which was effective when applied for >2 h (Paper I). Based on effects of UV on the infection process of *P. neolycopersici*, UV has been classified as effective (250 – 280 nm), transition (290 – 310 nm), and ineffective (310 – 400 nm) range (122). The effect of short wavelength UV was described earlier in a study on grape powdery mildew. It was reported that disease severity of grape powdery mildew, *E. necator* was increased by 20% to 40%, when short wavelength UV (< 400 nm) was filtered out from the solar radiation using artificial shading compared to the fruits, which were exposed to the unfiltered solar radiation (8). Ultraviolet kills pathogens by directly damaging their cellular DNA and when damage is extensive, it directs the cell to apoptosis. Ultraviolet radiations induce two major DNA damages; cyclobutane pyrimidine dimers (CPDs) and (6-4) photoproducts (6-4PPs). These damages are potentially lethal to organisms, and prevent DNA replication and transcription processes and if these damages are left unrepaired, they ultimately cause cell death (98, 107). The main focus of the present study is to determine the wavelength range, which is responsible for the recovery of UV-mediated germination inhibition of *P. neolycopersici* conidia. In this study, germination recovery of UV treated conidia was significantly effective above 310 – 454 nm range (Paper I). This suggested that powdery mildew has its own DNA damage repair mechanism, which is light-dependent and active within 350 – 500 nm. This range is identical to the action range of Photolyase, a DNA damage repair enzyme, which repairs the damages in the DNA induced by UV (107). UV

wavelengths 254 nm and 283 nm were equally effective in UV-mediated effect on germination (germination inhibition) if the samples were subsequently incubated in the dark (this study). However, UV-mediated effect on germination is dependent on the effective UV wavelength and its dose, when samples are subsequently incubated in the optical radiation > 310 nm to 454 nm. This demonstrated that the UV-mediated damage recovery (germination recovery) was not only dependent on the subsequent incubation wavelength but also on the wavelength and dose of the effective UV. Previous study on cucumber powdery mildew showed that application of effective UV either alone or in combination with red light was effective against powdery mildew disease suppression, but efficacy of UV was reduced in presence of background UV-A or blue light (120). For effective UV treatment to achieve the lowest germination recovery, the present study showed that the lapse time (dark period) between effective UV treatment and blue light (applicable to wavelength ranges > 310 nm to 454 nm) exposure should be > 4 h. This suggested that if the samples did not receive potential recovery wavelengths (> 310 nm to 454 nm) within 4 h after effective UV treatment, the repair mechanism (which leads to germination recovery) could not execute. Therefore, cells undergo apoptosis (Paper I).

The results of Paper I suggested the presence of photolyase like gene, which is responsible for germination recovery of UV mediated germination inhibition in *P. neolycopersici* conidia. This developed the need of whole genome sequencing of *P. neolycopersici*, which was not documented in previous studies. In the present study, the estimated genome sizes of *P. neolycopersici* (~249 Mb) and *P. xanthii* (~281 Mb) were remarkably larger than the estimated genome size of wheat powdery mildew, *Blumeria graminis* f. sp. *tritici* (~180 Mb) and other ascomycete fungi, whose genome sizes are comparatively smaller (~30 to 60 Mb) (97, 143). Previous study showed that PM genomes are estimated in size ranges from 120 to 222 Mb. This significant variations in the genome sizes of three powdery mildews is suggestive of high differential transposon activities in their genomes (143). It has been demonstrated that transposable elements contribute to genome evolution and expansion, and also played essential roles in wide range of biological events (development, differentiation, regulation) (149). In addition to variations in transposable elements, sequencing platforms and assembly pipelines used may also influence this variation in genome sizes. In this study, the number of protein coding transcripts is remarkably variable among three PM genomes. In *P.*

aphanis, and *P.* xanthii about 13025, and 6562 protein coding genes were annotated respectively while only 2888 protein coding genes were annotated in *P. neolycopersici* (Table 1, Paper II). Earlier studies showed that PMs generally possess fewer protein coding genes (6,000 to 7,000) compared to other fungi due to its obligate biotrophic nature. Barley and wheat PM have approximately 6525 to 7239 genes, which is approximately half than the number of genes present in closely related ascomycetes such as *Botrytis cinerea* (11707 genes) (143). The comparatively low gene density, and the inability of PM to grow in axenic conditions suggested that mildew genomes may lack genes, which are typically present in autotrophic ascomycetes (118). These genomic hallmarks; genome size inflation, extensive gene reshuffling correlated with expansion in (retro-)transposon number, and gene losses tends to be associated with the obligate biotrophic lifestyle of powdery mildews (118). This genome-specific gene loss may also contribute to host-specialization of PM fungi and/or reflect the impact of host metabolisms on respective PM pathogens (143). The functional annotation of *P. neolycopersici*, *P. xanthii*, and *P. aphanis* genomes revealed the presence of all major classes of photoreceptor genes; cryptochrome, photolyase, white collar (WC), phototropin, phytochrome, and UVR8. The expression of genes similar to cryptochrome, photolyase (light-dependent DNA repair), phytochrome, and white collar was also confirmed in a recent study on grapevine PM, *Erysiphe necator* using next generation sequencing (120). These photoreceptors have been functionally characterized in several other organisms including fungi (26, 46, 88, 148). The presence of these photoreceptors in PMs genomes suggested that like other fungi, PM may sense light over a broad spectrum of light ranges from ultraviolet to far-red light. Most fungi, which are photoresponsive are sensitive to light at near UV-A to blue (~ 400–495 nm) range (35). The near UV-A/blue light is perceived by a protein family composed of cryptochromes and photolyases family (CPF) genes, which are highly conserved across the entire fungal kingdom (148). The CPF genes are involved in various blue light mediated responses, and have been studied extensively in different species (46, 109). The three CPF-like genes were identified in each PM fungi; *P. neolycopersici*, *P. xanthii*, and *P. aphanis* (Paper II).

The three CPF-like genes (PN5670, PN0912 and, PN5061) identified in *P. neolycopersici* were transformed in *phr* mutant (photolyase deficient) cells showed cell survival of UV (254 nm) treated *E. coli*, when incubated in blue light (454 nm) while UV

treated *E. coli* incubated in dark showed no cell survival. Therefore, in *P. neolycopersici* among three CPF-like genes, one gene showed photoreactivation (photorepair) activity, responsible for survival of UV treated cells under blue light incubation. The other two genes, which do not show photoreactivation activity, they could be putative cryptochrome and CRY-DASH, other members of CPF. Their functional roles need to be investigated. The photoreactivation is an exclusive property, which is unique to photolyase or photoreactivation (PHR) enzyme. Photolyase repairs the UV induced DNA damages by absorbing photons within near UV/blue light (300 – 500 nm) as an energy source (106). Photolyase repairs dimers by splitting the cyclobutane ring and monomerizes the pyrimidine dimer into two canonical pyrimidines, and thus restore the original conformation of DNA (103). Our phylogenetic analysis results showed that *P. neolycopersici* is a class I CPD DNA photolyase on the basis of sequence similarity with all the other available photolyases. Class I photolyases are widespread in micro-organisms whereas class II photolyases are found in higher organisms. Most bacteria such as *E. coli*, *Streptomyces griseus*, *Thermus thermophilus*; yeast *Saccharomyces cerevisiae* and fungi *Neurospora crassa*, *Trichoderma atroviride* possess class I photolyases (137). The protein structure prediction suggested the presence of FAD and MTHF as a catalytic and photoantenna chromophores respectively. However, our result of absorption and fluorescence spectra of heterologously expressed photolyase protein only showed a presence of reduced FAD ($FADH^-$) as only chromophore, and did not predict the presence of second photoantenna chromophore. Photolyase is a well-studied enzyme, absorbs wavelengths within 300 – 500 nm for its functional activity, and these wavelengths are not absorbed by DNA or polypeptides, therefore it is evident from results of cell survival assay that *P. neolycopersici* photolyase definitely contain an additional chromophore, which absorbs within 300 – 500 nm range and carried out photoreactivation (108). It has been reported that FAD is the only chromophore identified when photolyase is heterologously expressed as most of the MTHF lost during protein purification steps. In the present study, photolyase action spectra was achieved within 365 – 454 nm (UV-A/blue light) and UV-A seems more efficient for recovery compared to blue light (Paper III). Similar results were obtained for action spectra of germination recovery within UV-A/blue light of UV treated conidia (Paper I). Gene expression studies showed that *P. neolycopersici* photolyase gene expression was induced by UV-C alone. Our results suggest that UV-C triggers the transcriptional

activation of photolyase gene. It has been reported that *E. coli phr* gene expression is induced by the formation of pyrimidine dimers (49). This explanation clearly suggests UV-C is responsible for transcriptional activation of photolyase gene, but its protein activity/function (photoreactivation) requires the absorption of photons within near-UV or blue light (300 – 500 nm). This further explains the increased efficacy of UV-C against powdery mildew disease when used in combination with the red light (660 nm), which is unable to activate the photolyase protein and further represses photolyase gene expression (Paper III).

The photolyase gene from five isolates collected from different regions in Norway and The Netherlands were highly conserved, and there were no variation observed in their nucleotide sequences. Although photolyase gene is conserved, five isolates responded differently to the similar doses of brief UV-C (254 nm) treatment, and showed difference in their germination recovery within blue (454 nm) light. Difference in germination recovery patterns could be dependent on the type and number of additional photoantenna chromophore present, which in turn will vary in their absorption and action spectrum. The variation in UV tolerance in fungal isolates resonates to their natural adaptations to the environmental conditions of their habitat. Every organism adapt to their daily optical environment, and therefore optimize their genomic and proteomic features to survive in their habitat (152). One of the possible explanation for variation in UV response, is the base composition, especially dinucleotide (NN) composition of a species. UV induces a dominant lesions- CPDs, which are formed between two adjacent pyrimidine (TT) nucleotides (103). Therefore, a high pyrimidine content in a genome will form high CPDs which lead to the higher cell death because of low damage repair efficiency of photolyase protein. Analyzing the sensitivity or tolerance of any pathogen to UV is an important step in UV-mediated disease management. This will allow us to identify an effective dose for UV treatment against pathogen, and plan for accurate disease management programs. In addition, the expression level of photolyase and translation efficiency may also affect the photolyase mediated UV damage recovery. Further studies on promoter architecture and transcription binding sites may explain this variation. Amino acid sequence alignment analysis of CPF genes (Fig. 3, Paper IV) revealed three critical residues (W277, M345, N378) which are found to be distributed in this superfamily, trp277 (W277) is crucial for substrate binding and plays a role in CPD splitting. Met345 (M345) is restricted to

CPD photolyase as it discriminates CPD photolyases from rest of the superfamily. Asn378 (N378) is highly conserved in the whole superfamily as it stabilizes the neutral FAD radical (144). A tryptophan triad (Trp triad) was found be conserved in photolyase family including class I, class II CPD photolyases and (6-4) photolyases and also provide an alternative electron-transfer pathway (W306 → W359 → W382 → FADH•) (140, 150). Protruding N-terminal end in *P. neolycopersici* photolyase showed significant similarity in amino acid residues to a sequence, which is a known cleavage site that enables a transport of mitochondrial leucyl-tRNA synthetase in mitochondria in *N. crassa* (23). These protruding N-terminal ends are also present in *S. cerevisiae* photolyase. Therefore, *S. cerevisiae* photolyase able to repair dimers in nuclei as well as in mitochondria. This suggested that protruding N-terminal ends contain a sequence that might be a putative signal sequence required for subcellular localization of a photolyase (145). These protruding N-terminals are characteristics to only fungal photolyases, and are not present in bacteria. The Cry C-terminal ends (CCE) were also observed in cryptochromes and CRY-DASH of *P. neolycopersici*. Their roles in *P. neolycopersici* require further investigation.

5. GENERAL CONCLUSIONS AND FURTHER PERSPECTIVES

- Fungi that causing powdery mildews in tomato, cucumber, and strawberry have genes representative to all major classes of photoreceptors reported so far in living organisms.
- One among the three CPF genes identified in *P. neolycopersici* is photolyase and have functions as light dependent (350 nm – 500 nm range) repair of UV induced DNA damages.
- The UV-A/blue light (365 nm – 454 nm) is the action spectra of *P. neolycopersici* photolyase, responsible for the germination recovery of UV treated *P. neolycopersici* conidia.
- Chance of recovery of the UV exposed powdery mildews decreased with increased time lapse for subsequent UV-A/blue light exposure (at least 4 h).
- Regardless of highly conserved nature of photolyase gene, five different isolates of *P. neolycopersici* have variation in UV tolerance and germination recovery process.
- In cases, where crops need longer days and necessary to have optical environment immediately after UV treatment, radiation sources with emission spectra above 510 nm can be used.
- Exploring the information of photolyase action spectra of powdery mildew will be very helpful to boost up the practical application and its efficiency of optical based powdery mildew management.

Implementation of UV irradiance systems in greenhouses for crop protection against pathogens is encouraging. This application can be extended on field-based setting to confirm the efficacy of UV on a larger scale to compare with conventional disease management methods (e.g., fungicides). Prototypes of mobile UV-C irradiation units that could pass through strawberry rows have been developed and evaluated under field conditions. Strawberry plants and their fruits are being used as a model system for field trials, but this UV-C technology may be applicable to various other crops (129). The germicidal potential of UV can become a sustainable non-chemical option for disease

management, and are not limited to only fungal pathogens, research is being conducted to use UV against arthropod pests as well (insects, mites) (130).

For UV application to be effective, the radiation needs to reach pathogen that one wants to eliminate to have direct effects. Relatively small doses of UV may not be sufficient to remove desired pathogen, but an excessive dose (intensity and duration) can damage and kill plants. Using measurements, calculations and data from trial experiments help in determining the adequate dosage for UV-C treatments to eliminate pathogens from crops. The effect of UV on pathogens may vary, and depends primarily on their complexity and tolerance to UV. Every pathosystems is different, hence the same parameters cannot be applied to another, and thus requires optimization specific only to one pathosystem. The method using UV to control powdery mildews is also dependent on the plant systems used. Since, plants have primary defense against UV by screening through epidermal flavonoids. The accurate optimization of dose, frequency and application timing could convert UV-C irradiation into one of the pivotal strategies to control powdery mildews at greenhouse level. The right dose can avoid any damage to plants as well as nutritional or aesthetic value of fruits.

The present investigation did not produce a functional confirmation of photolyase directly from *P. neolycopersici*. Host induced gene silencing (HIGS) using RNA silencing concepts has been widely used to silence the targets required for pathogen infection, and successfully used in the management of plant pathogens including powdery mildew (96). Furthermore, research is required to investigate the presence, and role of any regulatory elements including promotor analysis in the photolyase gene expression. This can resolve the enigma of variation in response to similar UV doses in *P. neolycopersici* isolates despite of highly conserved photolyase gene. Additionally, this difference can be explained by gene expression studies using quantitative RT-PCR with the samples collected after exposure to different light treatments used in the biological assay with different *P. neolycopersici* isolates. The information on photoreceptors and their functional roles in powdery mildews is still scarce. The roles of putative cryptochrome and CRY-DASH in *P. neolycopersici* yet to be investigated.

The designing of a UV array lamp is a critical aspect that could match a particular crop canopy, and target pathogen biology in determining the success of the UV

applications. Most importantly, the UV array itself is not a do it yourself project, both UV-B and UV-C can be injurious as there is a significant risk of eye and skin damage in case of exposure. Therefore, protective gears such as UV-opaque jackets, face-shields, gloves, eye gears should be used for protection and safe UV applications. In present days, modern technology advancements in the field of autonomous vehicle/robotics and LED optics technologies facilitate the manufacturing of fully automated UV-C array lights. Therefore, it has been made possible to create appropriate spectral environment for closed cultivation systems (greenhouses) for different crops. Combining the UV control strategies together with genetic improvements and good sanitation practices can create better and long term integrated disease management (IDM) programs against powdery mildew in various crops. This definitely reduce the use of fungicide applications. The present work will be extended in a new project to investigate the genetic basis of optical radiation tolerance mechanisms in gray mold, *Botrytis cinerea*. Since, gray mold have melanins, they can tolerate higher doses of UV compared to powdery mildews.

6. REFERENCES

1. Ahmad, M., Cashmore, A. 1993. HY4 gene of *Arabidopsis thaliana* encodes a protein with characteristics of a blue-light photoreceptor. Nature 366(6451):162-166.
2. Anonymous. Særheim. https://www.nibio.no/en/about-eng/addresses/saerheim
3. Anonymous. Norway. International Society for Horticultural Science. https://www.hridir.org/countries/norway/index.htm.
4. Anonymous. 2016. Europe: Tomato production, HortiDaily. https://www.hortidaily.com/article/25804/Europe-Tomato-production-rises,consumption-falls/.
5. Anonymous. 2017. FAOSTAT. Food and Agriculture Organization of the United Nations. http://www.fao.org/faostat/en/#data/QC.
6. Anonymous. 2017. Norway Weather. World Atlas. https://www.worldatlas.com/webimage/countrys/europe/norway/noweather.htm#page.
7. Asalf, B., Onofre, R. B., Gadoury, D. M., Peres, N. A., Stensvand, A. 2020. Pulsed water mists for suppression of strawberry powdery mildew. Plant Dis.105(1):71-77.
8. Austin, C. N., Wilcox, W. F. 2012. Effects of sunlight exposure on grapevine powdery mildew development. Phytopathol. 102(9):857-866.
9. Bayram, O., Biesemann, C., Krappmann, S., Galland, P., Braus, G. H. 2008. More than a repair enzyme: *Aspergillus nidulans* photolyase-like CryA is a regulator of sexual development. Mol. Biol. Cell 19(8):3254-3262.
10. Berrocal-Tito, G. M., Esquivel-Naranjo, E. U., Horwitz, B. A., Herrera-Estrella, A. 2007. *Trichoderma atroviride* PHR1, a fungal photolyase responsible for DNA repair, autoregulates its own photoinduction. Eukaryot. Cell 6(9):1682.
11. Bindschedler, L. V., Panstruga, R., Spanu, P. D. 2016. Mildew-Omics: How global analyses aid the understanding of life and evolution of powdery mildews. Front. Plant Sci. 7:123.
12. Blancard, D. 2012. Tomato Diseases: Identification, biology and control. Second Edition ed. CRC Press.

13. Blumenstein, A., Vienken, K., Tasler, R., Purschwitz, J., Veith, D., Frankenberg-Dinkel, N., Fischer, R. 2005. The *Aspergillus nidulans* phytochrome FphA represses sexual development in red light. Curr. Biol. 15(20):1833-1838.
14. Boon, J. K. 2018. *Fruit and Vegetable Facts*. https://www.freshplaza.com/article/2189007/norway-stable-import-market-for-fresh-fruit-and-vegetables/.
15. Bosque-Villarreal, G. A. D., Rodríguez-García, R., Zermeño-González, A., Jasso-Cantú, D. 2012. Evaluation of a physical model of climate simulation in a greenhouse with natural ventilation. Agrociencia 46(5):427-440.
16. Bowen, K. L., Everts, K. L., Leath, S. 1991. Reduction in yield of winter wheat in North Carolina due to powdery mildew and leaf rust. Phytopathol. 81:503-511.
17. Bowman, K. K., Sidik, K., Smith, C. A., Taylor, J. S., Doetsch, P. W., Freyer, G. A. 1994. A new ATP-independent DNA endonuclease from *Schizosaccharomyces pombe* that recognizes cyclobutane pyrimidine dimers and 6-4 photoproducts. Nucleic Acids Res. 22(15):3026-3032.
18. Braun, U., Cook, R., Inman, A. J., Shin, H. D. 2002. The taxonomy of powdery mildew fungi. In The powdery mildews: a comprehensive treatise. pp. 13-54. APS Press.
19. Buschermohle, M. J., Grandle, F. G. Controlling the environment in greenhouses used for tomato production. Agricultural Extension Service. The University of Tennessee.
20. Carell, T., Burgdorf, L. T., Kundu, L. M., Cichon, M. 2001. The mechanism of action of DNA photolyases. Curr. Opinion Chem. Biol. 5(5):491-498.
21. Cerkauskas, R. 2005. Tomato diseases: Powdery mildew. Factsheet. AVRDC- The World Vegetable Center 5-636.
22. Chaves, I., Pokorny, R., Byrdin, M., Hoang, N., Ritz, T., Brettel, K., Essen, L. O., van der Horst, G. T., Batschauer, A., Ahmad, M. 2011. The cryptochromes: Blue light photoreceptors in plants and animals. Ann. Rev. Plant Biol. 62(1):335-364.
23. Chow, C. M., Metzenberg, R. L., Rajbhandary, U. L. 1989. Nuclear gene for mitochondrial leucyl-tRNA synthetase of *Neurospora crassa*: isolation, sequence, chromosomal mapping, and evidence that the leu-5 locus specifies structural information. Mol. Cell. Biol. 9(11):4631-4644.

24. Corrochano, L. M. 2007. Fungal photoreceptors: sensory molecules for fungal development and behaviour. Photochem. Photobiol. Sci. 6(7):725-736.
25. Corrochano, L. M. 2011. Fungal photobiology: a synopsis. IMA fungus 2(1):25-28.
26. Corrochano, L. M. 2019. Light in the fungal world: From photoreception to gene transcription and beyond. Ann. Rev. Genet. 53(1):149-170.
27. Cunfer, B. M. 2002. Powdery Mildew. Plant Production and Protection Series. FAO. ISSN :0259-2525:13.
28. Dai, T., Vrahas, M. S., Murray, C. K., Hamblin, M. R. 2012. Ultraviolet C irradiation: an alternative antimicrobial approach to localized infections. Expert Rev. Anti Infect. Ther. 10(2):185-195.
29. Davis, P., Burns, C. 2016. Photobiology in protected horticulture. Food Energy Secur. 5(4):223-238.
30. Davis, R. M., Gubler, W. D., Koike, S. T. 2008. Powdery mildew on vegetables. Pest notes. University of California. Agriculture and Natural Resources.
31. Fletcher, J. T., Smewin, B. J., Cook, R. T. A. 1988. Tomato powdery mildew. Plant Pathol. 37(4):594-598.
32. Fondevilla, S., Rubiales, D. 2012. Powdery mildew control in pea. A review. Agron. Sustain. Dev. 32(2):401-409.
33. Froehlich, A. C., Chen, C. H., Belden, W. J., Madeti, C., Roenneberg, T., Merrow, M., Loros, J. J., Dunlap, J. C. 2010. Genetic and molecular characterization of a cryptochrome from the filamentous fungus *Neurospora crassa*. Eukaryot. Cell 9(5):738-750.
34. Frohnmeyer, H., Staiger, D. 2003. Ultraviolet-B radiation-mediated responses in plants. Balancing damage and protection. Plant Physiol. 13 (4):1420-8.
35. Fuller, K. K., Loros, J. J., Dunlap, J. C. 2015. Fungal photobiology: visible light as a signal for stress, space and time. Curr. Genet. 61(3):275-288.
36. Gadoury, D. M., Seem, R. C., Pearson, R. C., Wilcox, W. F., Dunst, R. M. 2001. Effects of powdery mildew on vine growth, yield, and quality of concord grapes. Plant Dis. 85(2):137-140.
37. Glawe, D. A. 2008. The powdery mildews: A review of the world's most familiar (yet poorly known) plant pathogens. Annu. Rev. Phytopathol. 46(1):27-51.

38. GoNorway. Finnøy. http://www.gonorway.com/norway/counties/rogaland/finn%C3%B8y/7635f8620a04e20/index.html.
39. Hacquard, S. 2014. The genomics of powdery mildew fungi: Past achievements, present status and future prospects. Adv. Bot. Res. 109-142.
40. Hakem, R. 2008. DNA-damage repair; the good, the bad, and the ugly. EMBO J. 27(4): 589-605.
41. Hamilton, K., Kirn, P., Doetsch, P. 1992. A eukaryotic DNA glycosylase/lyase recognizing ultraviolet light-induced pyrimidine dimers. Nature 356:725-728.
42. Hannusch, D. J., Boland, G. J. 1996. Interactions of air temperature, relative humidity and biological control agents on grey mold of bean. Eur. J. Plant Pathol. 102(2):133-142.
43. Harm, W., Harm, H., Rupert, C. S. 1968. Analysis of photoenzymatic repair of UV lesions in DNA by single light flashes: II. In vivo studies with *Escherichia coli* cells and bacteriophage. Mutat. Res. 6(3):371-385.
44. Heintzen, C. 2012. Plant and fungal photopigments. WIREs Membr. Transp. Signal 1:411-432.
45. Hollomon, D. W., Wheeler, I. E. 2002. Controlling powdery mildews with chemistry. In The powdery mildews: a comprehensive treatise. pp. 249-255. APS Press.
46. Huché-Thélier, L., Crespel, L., Gourrierec, J. L., Morel, P., Sakr, S., Leduc, N. 2016. Light signaling and plant responses to blue and UV radiations—Perspectives for applications in horticulture. Environ. Exp. Bot. 121:22-38.
47. Huibers, R. P., Loonen, A. E. H. M., Gao, D., Van den Ackerveken, G., Visser, R. G. F., Bai, Y. 2013. Powdery mildew resistance in tomato by impairment of SlPMR4 and SlDMR1. PloS ONE. 8(6):e67467.
48. Idnurm, A., Verma, S., Corrochano, L. M. 2010. A glimpse into the basis of vision in the kingdom Mycota. Fungal Genet. Biol. 47(11):881-892.
49. Ihara, M., Yamamoto, K., Ohnishi, T. 1987. Induction of phr gene expression by pyrimidine dimers in *Escherichia coli*. Photochem. Photobiol. 46(3):359-361.
50. Jacob, D., David, D. R., Sztjenberg, A., Elad, Y. 2008. Conditions for development of powdery mildew of tomato caused by *Oidium neolycopersici*. Phytopathol. 98(3):270-281.

51. Janisiewicz, W. J., Takeda, F., Nichols, B., Glenn, D. M., Jurick II, W. M., Camp, M. J. 2016. Use of low-dose UV-C irradiation to control powdery mildew caused by *Podosphaera aphanis* on strawberry plants. Can. J. Plant Pathol. 38(4):430-439.
52. Jankovics, T., Bai, Y., Kovács, G. M., Bardin, M., Nicot, P. C., Toyoda, H., Matsuda, Y., Niks, R. E., Kiss, L. 2008. *Oidium neolycopersici*: Intraspecific variability inferred from amplified gragment length polymorphism analysis and relationship with closely related powdery mildew fungi infecting various plant species. Phytopathol. 9(5): 529-540.
53. Jansen, M. A. K., Gaba, V., Greenberg, B. M. 1998. Higher plants and UV-B radiation: balancing damage, repair and acclimation. Trends Plant Sci. 3(4):131-135.
54. Jones, H., Whipps, J. M., Gurr, S. J. 2001. The tomato powdery mildew fungus *Oidium neolycopersici*. Mol. Plant Pathol. 2(6):303-309.
55. Kavakli, I. H., Ozturk, N., Gul, S. 2019. DNA repair by photolyases. In Adv. Protein Chem. Struct Biol. 115:1-19. Academic Press.
56. Kelner, A. 1949. Effect of visible light on the recovery of *Streptomyces griseus* conidia from ultra-violet irradiation injury. PNAS 35(2):73-79.
57. Kelner, A. 1949. Photoreactivation of ultraviolet-irradiated *Escherichia coli*, with special reference to the dose-reduction principle and to ultraviolet-induced mutation. J. Bacteriol. 58(4):511-522.
58. Kiss, L., Cook, R., Saenz, G., Cunnington, J., Takamatsu, S., Pascoe, I., Bardin, M., Nicot, P., Sato, Y., Rossman, A. 2001. Identification of two powdery mildew fungi, *Oidium neolycopersici* sp. nov. and *O. lycopersici*, infecting tomato in different parts of the world. Mycol. Res. 105:684-697.
59. Kiss, L. 2003. A review of fungal antagonists of powdery mildews and their potential as biocontrol agents. Pest Manag. Sci. 59(4):475-83.
60. Kitchen, J. L., van den Bosch, F., Paveley, N. D., Helps, J., van den Berg, F. 2016. The evolution of fungicide resistance resulting from combinations of foliar-acting systemic seed treatments and foliar-applied fungicides: A modeling analysis. PLoS ONE 11(8): e0161887.
61. Kraemer, K. H., DiGiovanna, J. J. 2002. Topical enzyme therapy for skin diseases. J. Am. Acad. Dermatol. 46(3):463-466.

62. Kumar, S., Hedges, S. B. 1998. A molecular timescale for vertebrate evolution. Nature 392:917-920.
63. Kumar, S. P., Srinivasulu, A., Babu, K. R. 2018. Symptomology of major fungal diseases on tomato and its management. J. Pharmacogn. Phytochem. 7(6):1817-1821.
64. L. Willocquet, D. C., M. Rougier, J. Fargues and M. Clerjeau. 1996. Effects of radiation, especially ultraviolet B, on conidial germination and mycelial growth of grape powdery mildew. Eur. J. Plant Pathol. 102:441-449.
65. Lebeda, A., Mieslerová, B. 2002. Variability in pathogenicity of *Oidium neolycopersici* on lycopersicon species. J. Plant Dis. Prot. 109(2):129-141.
66. Lebeda, A., Mieslerova, B., Luhová, L., Mlíčková, K. 2002. Resistance mechanisms in lycopersicon spp. to tomato powdery mildew (*Oidium neolycopersici*). Plant Prot. Sci. 38:141-144.
67. Lebeda, A., MgGrath, M. T., Sedláková, B. 2010. Fungicide resistance in cucurbit powdery mildew fungi. In Fungicides. pp. 221-246. InTech.
68. Lebeda, A., Mieslerová, B., Petřivalský, M., Luhová, L., Špundová, M., Sedlářová, M., Nožková-Hlaváčková, V., Pink, D. A. C. 2014. Resistance mechanisms of wild tomato germplasm to infection of *Oidium neolycopersici*. Eur. J. Plant Pathol. 138 (3):569-596.
69. Lebeda, A., Mieslerová, B., Jankovics, T., Kiss, L., Van der Linde, E. J. 2015. First detection of tomato powdery mildew caused by *Oidium neolycopersici* in South Africa. S. Afr. J. Bot. 99:153-157.
70. Lebeda, A., Mieslerova, B., Petrivalsky, M., Luhová, L., Spundova, M., Sedlarova, M., Nožková, V., Pink, D. 2017. Review of tomato powdery mildew – a challenging problem for researchers, breeders and growers. Acta Hort. 107-116.
71. Linde, M., Shishkoff, N. 2017. Powdery mildew. In Reference Module in Life Sciences. pp. 158-165. Elsevier.
72. Liu, Y., He, Q., Cheng, P. 2003. Photoreception in *Neurospora*: a tale of two White Collar proteins. Cell. Mol. Life Sci. 60(10):2131-2138.
73. Livak, K. J., Schmittgen, T. D. 2001. Analysis of relative gene expression data using real-time quantitative PCR and the 2−ΔΔCT method. Methods 25(4):402-408.

74. Lopez Pinar, A., Rauhut, D., Ruehl, E., Buettner, A. 2017. Effects of bunch rot (*Botrytis cinerea*) and powdery mildew (*Erysiphe necator*) fungal diseases on wine aroma. Front. Chem. 5:20-20.
75. Løvdal, T., Droogenbroeck, B. V., Eroglu, E. C., Kaniszewski, S., Agati, G., Verheul, M., Skipnes, D. 2019. Valorization of tomato surplus and waste fractions: A case study using Norway, Belgium, Poland, and Turkey as examples. Foods 8(7):229.
76. Mahler, I., Kushner, S. R., Grossman, L. 1971. In vivo role of the UV-endonuclease from *Micrococcus luteus* in the repair of DNA. Nature New Biol. 234(45):47-50.
77. McGrath, M. T. Powdery mildews on tomatoes. https://blogs.cornell.edu/livegpath/gallery/tomato/powdery-mildew-on-tomatoes/
78. McGrath, M. T. 2001. Fungicide resistance in cucurbit powdery mildew: Experiences and challenges. Plant Dis. 85(3):236-245.
79. Mei, Q., Dvornyk, V. 2015. Evolutionary history of the photolyase/cryptochrome superfamily in eukaryotes. PloS ONE 10(9):e0135940.
80. Menck, C. F. M. 2002. Shining a light on photolyases. Nature Genet. 32(3):338-339.
81. Meulenbroek, E. M., Peron Cane, C., Jala, I., Iwai, S., Moolenaar, G. F., Goosen, N., Pannu, N. S. 2013. UV damage endonuclease employs a novel dual-dinucleotide flipping mechanism to recognize different DNA lesions. Nucleic Acids Res. 41(2):1363-1371.
82. MieslerovÁ, B., Lebeda, A., Kennedy, R. 2004. Variation in *Oidium neolycopersici* development on host and non-host plant species and their tissue defence responses. Ann. Appl. Biol. 144(2):237-248.
83. Möglich, A., Yang, X., Ayers, R. A., Moffat, K. 2010. Structure and function of plant photoreceptors. Annu. Rev. Plant Biol. 61(1):21-47.
84. Mortensen, L., Gislerød, H. 2005. Effect of air humidity variation on powdery mildew and keeping quality of cut roses. Sci. Hortic. 104:49-55.
85. Nsa, I. Y., Karunarathna, N., Liu, X., Huang, H., Boetteger, B., Bell-Pedersen, D. 2015. A novel cryptochrome-dependent oscillator in *Neurospora crassa*. Genetics 199(1):233-245.
86. Oichi, W., Matsuda, Y., Nonomura, T., Toyoda, H., Xu, L., Kusakari, S. 2006. Formation of conidial pseudochains by tomato powdery mildew *Oidium neolycopersici*. Plant Dis. 90 (7):915-919.

87. Omdal, Ø. E. 2005. Tomat: *Lycopersicum esculentum* Mill. Rapport Rennesøy forsøksring veksthusrådgivning. 39 s.
88. Paik, I., Huq, E. 2019. Plant photoreceptors: Multi-functional sensory proteins and their signaling networks. Semin. Cell Dev. Biol. 92:114-121.
89. Papamichos-Chronakis, M., Peterson, C. L. 2012. Chromatin and the genome integrity network. Nature Rev. Genet. 14:62.
90. Pataky, N. R. 1988. Powdery mildew of roses. University of Illinois Extension. Department of Crop Sciences.
91. Paul, N. D., Gwynn-Jones, D. 2003. Ecological roles of solar UV radiation: towards an integrated approach. Trends Ecol. Evol. 18(1):48-55.
92. Pérez-García, A., Romero, D., Fernández-Ortuño, D., López-Ruiz, F., De Vicente, A., Torés, J. A. 2009. The powdery mildew fungus Podosphaera fusca (synonym Podosphaera xanthii), a constant threat to cucurbits. Mol Plant Pathol. 10(2):153-160.
93. Pottorff, L. P., Newman, S. 2013. Powdery mildews. Colorado State University Extension. Department of Agriculture.
94. Purschwitz, J., Müller, S., Kastner, C., Fischer, R. 2006. Seeing the rainbow: light sensing in fungi. Curr. Opi. Microbiol. 9(6):566-571.
95. Purschwitz, J., Müller, S., Kastner, C., Schöser, M., Haas, H., Espeso, E. A., Atoui, A., Calvo, A. M., Fischer, R. 2008. Functional and physical interaction of blue- and red-light sensors in *Aspergillus nidulans*. Curr. Biol. 18(4):255-259.
96. Qi, T., Guo, J., Peng, H., Liu, P., Kang, Z., Guo, J. 2019. Host-induced gene silencing: A powerful strategy to control diseases of wheat and barley. Int. J. Mol. Sci. 20(1):206.
97. Raffaele, S., Kamoun, S. 2012. Genome evolution in filamentous plant pathogens: why bigger can be better. Nat. Rev. Microbiol. 10(6):417-430.
98. Rastogi, R. P., Richa, Kumar, A., Tyagi, M. B., Sinha, R. P. 2010. Molecular mechanisms of ultraviolet radiation-induced DNA damage and repair. J. Nucleic Acids 2010:592980.
99. Ridout, C. J. 2009. Profiles in pathogenesis and mutualism: Powdery mildews. In Plant Relationships. pp. 51-68. Springer Berlin Heidelberg.
100. Robinson, H. L., Ridout, C. J., Sierotzki, H., Gisi, U., Brown, J. K. M. 2002. Isogamous, hermaphroditic inheritance of mitochondrion-encoded resistance to Qo

inhibitor fungicides in *Blumeria graminis f. sp. tritici*. Fungal Genet. Biol. 3(2):98-106.

101. Rodriguez-Romero, J., Hedtke, M., Kastner, C., Müller, S., Fischer, R. 2010. Fungi, hidden in soil or up in the air: Light makes a difference. Annu. Rev. Microbiol. 64(1):585-610.
102. Rutledge, A. D. 2015. Commercial Greenhouse Tomato Production. Agricultural Extension Service. The University of Tennessee.
103. Sancar, A. 1994. Structure and function of DNA photolyase. Biochem. 33(1):2-9.
104. Sancar, A. 2003. Structure and function of DNA photolyase and cryptochrome blue-light photoreceptors. Chem. Rev. 10(6): 2203-2238.
105. Sancar, A. 2004. Photolyase and cryptochrome blue-Light photoreceptors. In Advances in Protein Chemistry. 69:73-100. Academic Press.
106. Sancar, A. 2008. Structure and function of photolyase and in vivo enzymology: 50th anniversary. J. Biol. Chem. 283(47):32153-7.
107. Sancar, A. 2016. Mechanisms of DNA repair by photolyase and excision nuclease (Nobel lecture). Angew. Chem. Int. Ed. Engl. 5(30):8502-27.
108. Sancar, G. B., Sancar, A. 1987. Structure and function of DNA photolyases. Trends Biochem. Sci. 12:259-261.
109. Sancar, G. B. 1990. DNA photolyases: Physical properties, action mechanism, and roles in dark repair. Mutat. Res. 236(2):147-160.
110. Sancar, G. B., Sancar, A. 2006. Purification and characterization of DNA photolyases. In Methods in Enzymology. 408:121-156. Academic Press.
111. Sanoubar, R., Barbanti, L. 2017. Fungal diseases on tomato plant under greenhouse condition. Eur. J. Biol. Res.
112. Schwerdtfeger, C., Linden, H. 2003. VIVID is a flavoprotein and serves as a fungal blue light photoreceptor for photoadaptation. The EMBO journal 22(18):4846-4855.
113. Seifi, A., Gao, D., Zheng, Z., Pavan, S., Faino, L., Visser, R. G. F., Wolters, A. M. A., Bai, Y. 2014. Genetics and molecular mechanisms of resistance to powdery mildews in tomato (*Solanum lycopersicum*) and its wild relatives. Eur. J. Plant Pathol. 138(3):641-665.
114. Shamshiri, R. R., Jones, J. W., Thorp, K. R., Ahmad, D., Man, H. C., Taheri, S. 2018. Review of optimum temperature, humidity, and vapour pressure deficit for

microclimate evaluation and control in greenhouse cultivation of tomato: A review. Int. Agrophys. 32(2):287-302.

115. Shipp, L., Johansen, N., Vänninen, I., Jacobson, R. 2011. Greenhouse climate: An important consideration when developing pest management programs for greenhouse crops. Acta Hortic. 893:133-143.

116. Sinha, R. P., Häder, D. P. 2002. UV-induced DNA damage and repair: A review. Photochem. Photobiol. Sci. 1(4):225-236.

117. Sowa, P., Rutkowska-Talipska, J., Rutkowski, K., Kosztyła-Hojna, B., Rutkowski, R. 2013. Optical radiation in modern medicine. Postepy Dermatol. Alergol. 30(4):246-251.

118. Spanu, P. D., Abbott, J. C., Amselem, J., Burgis, T. A., Soanes, D. M., Stüber, K., Ver Loren van Themaat, E., Brown, J. K., Butcher, S. A., Gurr, S. J. 2010. Genome expansion and gene loss in powdery mildew fungi reveal tradeoffs in extreme parasitism. Science 330(6010):1543-6.

119. Suthaparan, A., Stensvand, A., Solhaug, K. A., Bjugstad, N., Gadoury, D. M., Gislerød, H. R. 2013. Practical application of UV-B radiation against powdery mildews under greenhouse conditions. Poster APS-MSA joint meeting. Austin, Texas.

120. Suthaparan, A., Stensvand, A., Solhaug, K. A., Torre, S., Telfer, K. H., Ruud, A. K., Mortensen, L. M., Gadoury, D. M., Seem, R. C., Gislerød, H. R. 2014. Suppression of Cucumber powdery mildew by supplemental UV-B radiation in greenhouses can be augmented or reduced by background radiation quality. Plant Dis. 98(10):1349-1357.

121. Suthaparan, A., Solhaug, K. A., Bjugstad, N., Gislerød, H. R., Gadoury, D. M., Stensvand, A. 2016. Suppression of powdery mildews by UV-B: Application frequency and timing, dose, reflectance, and automation. Plant Dis. 100(8):1643-1650.

122. Suthaparan, A., Solhaug, K. A., Stensvand, A., Gislerød, H. R. 2016. Determination of UV action spectra affecting the infection process of *Oidium neolycopersici*, the cause of tomato powdery mildew. J. Photochem. Photobiol B. 156:41-49.

123. Suthaparan, A., Pathak, R., Solhaug, K. A., Gislerod, H. R. 2018. Wavelength dependent recovery of UV-mediated damage: Tying up the loose ends of optical based powdery mildew management. J Photochem. Photobiol. 178:631-640.

124. Suthaparan, A., Stensvand, A., Solhaug, K. A., Torre, S., Mortensen, L. M., Gadoury, D. M., Seem, R. C., Gislerød, H. R. 2012. Suppression of powdery mildew (*Podosphaera pannosa*) in greenhouse roses by brief exposure to supplemental UV-B radiation. Plant Dis. 96(11):1653-1660.

125. Suthaparan, A., Stensvand, A., Torre, S., Herrero, M. L., Pettersen, R. I., Gadoury, D. M., Gislerød, H. R. 2010. Continuous lighting reduces conidial production and germinability in the rose powdery mildew pathosystem. Plant Dis. 94(3):339-344.

126. Suthaparan, A., Torre, S., Stensvand, A., Herrero, M. L., Pettersen, R. I., Gadoury, D. M., and Gislerød, H. R. 2010. Specific light-emitting diodes can suppress sporulation of *Podosphaera pannosa* on greenhouse roses. Plant Dis. 94(9):1105-1110.

127. Sutherland, A., Gubler, W., Parrella, M. 2010. Effects of fungicides on a mycophagous coccinellid may represent integration failure in disease management. Biol. Control. 54:292-299.

128. Sutherland, B. M. 1995. Action spectroscopy in complex organisms: potentials and pitfalls in predicting the impact of increased environmental UVB. J. Photochem. Photobiol. B. 31 (1):29-34.

129. Takeda, F., Janisiewicz, W. J., Smith, B. J., Nichols, B. 2019. A new approach for strawberry disease control. Eur. J. Hortic. Sci. 84(1):3-13.

130. Takeda, F., Janisiewicz, W., Short, B., Leskey, T., Stager, A. 2021. Ultraviolet-C (UV-C) for disease and pest management and automating UV-C delivery technology for strawberry. Acta Hortic. 1309:533-542.

131. Terry Kelley, W., Boyhan, G. E., Harrison, K., Sumner, P. E., Langston, D. B., Sparks, A. N., Culpepper, A. S., Hurst, W. C., Fonsah, E. G. 2010. Commercial tomato production handbook. UGA Cooperative Extension Bulletin 1312. University of Georgia.

132. Thompson, C. L., Sancar, A. 2002. Photolyase/cryptochrome blue-light photoreceptors use photon energy to repair DNA and reset the circadian clock. Oncogene 21(58):9043-9056.

133. Timmermann, L. F., Ritter, K., Hillebrandt, D., Küpper, T. 2015. Drinking water treatment with ultraviolet light for travelers – Evaluation of a mobile lightweight system. Travel Med. Infect. Dis. 13(6):466-474.

134. Tullus, A., Kupper, P., Sellin, A., Parts, L., Sõber, J., Tullus, T., Lõhmus, K., Sõber, A., Tullus, H. 2012. Climate change at northern latitudes: Rising atmospheric humidity decreases transpiration, N-uptake and growth rate of hybrid aspen. PLoS ONE 7(8): e42648.

135. Tuteja, N., Singh, M., Misra, M., Bhalla, P., Tuteja, R. 2001. Molecular mechanisms of DNA damage and repair: Progress in plants. Crit. Rev. Biochem. Mol. Biol. 36:337-97.

136. Van Delm, T., Melis, P., Stoffels, K., Baets, W. 2014. Control of powdery mildew by UV-c treatments in commercial strawberry production. Acta Hortic. 1049:679-684.

137. Vechtomova, Y. L., Telegina, T. A., Kritsky, M. S. 2020. Evolution of proteins of the DNA photolyase/cryptochrome family. Biochem. (Moscow) 85(1):131-153.

138. Verheul, M. J., Maessen, H. F. R., Panosyan, A., Naseer, M., Paponov, M., Paponov, I. A. 2020. Effects of supplemental lighting and temperature on summer production of tomato in Norway. Acta Hortic. 1296:707-714.

139. Wang, H., Jiang, Y. P., Yu, H. J., Xia, X. J., Shi, K., Zhou, Y. H., Yu, J. Q. 2010. Light quality affects incidence of powdery mildew, expression of defence-related genes and associated metabolism in cucumber plants. Eur. J. Plant Pathol. 127(1):125-135.

140. Weber, S. 2005. Light-driven enzymatic catalysis of DNA repair: A review of recent biophysical studies on photolyase. Biochem. Biophys. Acta 1707(1):1-23.

141. Weihs, P., Schmalwieser, A. W., Schauberger, G. 2013. UV effects on living organisms. In Environmental Toxicology: Selected Entries from the Encyclopedia of Sustainability Science and Technology. pp 609-688. Springer New York.

142. Whipps, J. M., Budge, S. P., Fenlon, J. S. 1998. Characteristics and host range of tomato powdery mildew. Plant Pathol. 47(1):36-48.

143. Wu, Y., Ma, X., Pan, Z., Kale, S. D., Song, Y., King, H., Zhang, Q., Presley, C., Deng, X., Wei, C. I. 2018. Comparative genome analyses reveal sequence features reflecting distinct modes of host-adaptation between dicot and monocot powdery mildew. BMC Genomics 19(1):705.

144. Xu, L., Zhu, G. 2010. The roles of several residues of *Escherichia coli* DNA photolyase in the highly efficient photo-repair of cyclobutane pyrimidine dimers. J. Nucleic Acids 2010:794782.

145. Yajima, H., Inoue, H., Oikawa, A., Yasui, A. 1991. Cloning and functional characterization of a eucaryotic DNA photolyase gene from *Neurospora crassa*. Nucleic Acids Res. 19(19): 5359-5362.
146. Yarwood, C. E. 1957. Powdery mildews. Bot. Rev. 23(4):235-301.
147. Yin, R., Dai, T., Avci, P., Jorge, A. E. S., de Melo, W. C. M. A., Vecchio, D., Huang, Y.-Y., Gupta, A., Hamblin, M. R. 2013. Light based anti-infectives: ultraviolet C irradiation, photodynamic therapy, blue light, and beyond. Curr. Opin. Pharmacol.13(5):731-762.
148. Yu, Z., Fischer, R. 2019. Light sensing and responses in fungi. Nature Rev. Microbiol. 17(1):25-36.
149. Zhang, C., Deng, W., Yan, W., Li, T. 2018. Whole genome sequence of an edible and potential medicinal fungus, *Cordyceps guangdongensis.*G3: Genes, Genomes, Genetics 8(6):1863.
150. Zhang, M., Wang, L., Zhong, D. 2017. Photolyase: Dynamics and mechanisms of repair of sun-induced DNA damage. Photochem. Photobil. 93(1):78-92.
151. Zhang, S., Mersha, Z., Vallad, G. E., Huang, C. H. 2016. Management of powdery mildew in squash by plant and alga extract biopesticides. Plant Pathol. J. 32(6):528-536.
152. Zhou, P., Wen, J., Oren, A., Chen, M., Wu, M. 2007. Genomic survey of sequence features for ultraviolet tolerance in haloarchaea (family Halobacteriaceae). Genomics 90(1):103-109.
153. Zhu, M., Riederer, M., Hildebrandt, U. 2019. UV-C irradiation compromises conidial germination, formation of appressoria, and induces transcription of three putative photolyase genes in the barley powdery mildew fungus*, Blumeria graminis f. sp. hordei*. Fungal Biol. 123(3):218-230.

Paper I

Journal of Photochemistry & Photobiology, B: Biology 178 (2018) 631–640

Contents lists available at ScienceDirect

Journal of Photochemistry & Photobiology, B: Biology

journal homepage: www.elsevier.com/locate/jphotobiol

Wavelength dependent recovery of UV-mediated damage: Tying up the loose ends of optical based powdery mildew management

Aruppillai Suthaparan[a,*], Ranjana Pathak[a], Knut Asbjørn Solhaug[b], Hans Ragnar Gislerød[a]

[a] Department of Plant Sciences, Faculty of Biosciences, Norwegian University of Life Sciences, 1432 Ås, Norway
[b] Faculty of Environmental Sciences and Natural Resource Management, Norwegian University of Life Sciences, 1432 Ås, Norway

ARTICLE INFO

Keywords:
Powdery mildew
Recovery action spectra
Ultraviolet

ABSTRACT

Controlled environment chamber experiments at Petri dish level were conducted to examine the wavelength and dose dependent efficacy of ultraviolet (UV) radiation, the recovery action potential of optical radiation applied concomitantly/subsequently to effective UV treatment, and the lapse time between UV treatment and subsequent exposure to recovery wavelength on germination efficiency of *Oidium neolycopersici* conidia. Conidia of eight- to nine-day-old colonies were dusted on water agar surface in Petri dishes and exposed to UV treatments (without lid). Immediately after UV treatments, Petri dishes were sealed and incubated in darkness or differing optical environments generated using seven different radiation sources (range 290 nm to 780 nm). Twenty-four hours after UV treatment, fifty conidia from each sample were assessed for germination. Compared to non-UV controls, < 10% of the conidia germinated after 30 s of exposure to 254 nm or 283 nm UV and subsequent dark incubation. Conidia germination was almost negligible if the exposure duration increased to 4 min. Germination was about 60% with broad spectrum UV after 1 min of exposure, and about 35% after 2 to 4 min of exposure. There was no reduction of conidia germination with the exposure of ≤ 4 min with 310 nm. With the tested wavelength and dose ranges, germination recovery was effective in the 350 nm to 500 nm range. Germination efficiency of conidia treated with effective UV was significantly higher (> 73%) if incubated subsequently in the 350 nm to 500 nm range (germination recovery). Furthermore, germination recovery depends on the characteristics of UV treatment (wavelength, and duration of exposure) and the lapse time between UV treatment and subsequent exposure to optical radiation in the recovery range. The findings of this study provide key criteria for wavelength selection, combination and application time in the optical radiation range, enabling improved design of optical based management strategies against powdery mildews.

1. Introduction

Optical radiation is comprised of the ultraviolet (UV), visible and infrared parts of the electromagnetic spectrum. These regions play key roles in growth, development and survival of living organisms in the biosphere. While photosynthetic organisms use optical radiation as a source of energy as well as an environmental cue [1], non-photosynthetic organisms use these radiation regions primarily as an environmental cue to anticipate environmental changes [2,3].

Notwithstanding its beneficial effects, optical radiation can have deleterious effects on living organisms; in particular, UV radiation is known for its potentially harmful effect on living organisms. Depending on wavelength, irradiance level, duration of exposure, as well as the complexity of the organisms, UV can induce mutations and/or kill simple organisms if it is absorbed by DNA [4]; this characteristic has been used for disinfection of water and air. Use of UV against phytopathogens is limited due to its phytotoxic effect on host plants, primarily because the dose optimum for efficient disease control is generally phytotoxic in host plants.

Recent studies have focused on optimizing UV against phytopathogens by wavelength, application time of day, frequency of application and growth light conditions. Brief application of UV during night-time was effective against powdery mildews in a wide range of crops with no phytotoxicity [5,8,12]. Based on its effect on the infection process of *Oidium neolycopersici*, the cause of powdery mildew in tomato, UV has been classified as effective (250–280 nm), transition (290–310 nm) and ineffective (310–400 nm) [6]. Concomitant/subsequent application of full spectrum grow light significantly reduced the powdery mildew control efficiency of UV on cucumber [7,8]. While application of effective UV in combination with red light enhances its disease control efficiency, combination with blue or UV-A significantly reduced its efficiency [7,8]. This indicated light mediated recovery. The

* Corresponding author.
E-mail address: aruppillai.suthaparan@nmbu.no (A. Suthaparan).

https://doi.org/10.1016/j.jphotobiol.2017.12.018
Received 29 September 2017; Received in revised form 12 December 2017; Accepted 15 December 2017
Available online 18 December 2017
1011-1344/

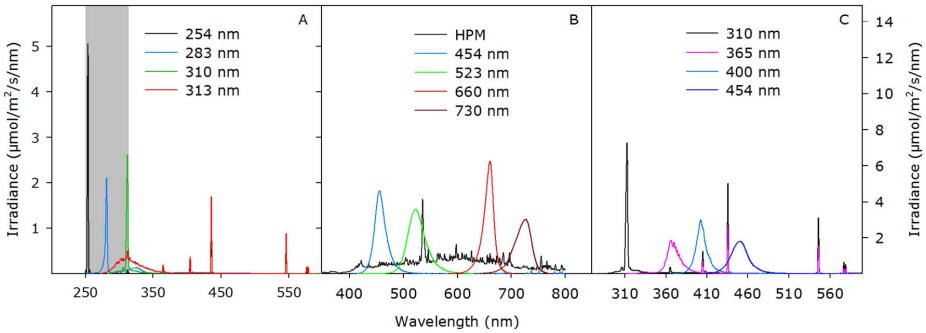

Fig. 1. Spectral distribution of the optical radiation sources measured at 1 nm wavelength intervals for (A) Ultraviolet (UV)-C fluorescent tube (peak at 254 nm), XeBr Excimer lamps (peak at 283 nm), narrow band UV-B fluorescent tubes (peak at 310 nm), broad band UV fluorescent tubes (peak at 313 nm) used for brief night-time UV treatment, and (B and C) high pressure mercury lamps (HPM), and light emitting diodes (LEDs) used in recovery incubation of *Oidium neolycopersici* conidia. Gray shade indicates the 250 nm to 315 nm wavelength range.

light dependent role of photolyase in repair of UV-induced DNA lesions has been well documented in plants and *Escherichia coli*. The 360 nm to 420 nm spectral region has been reported to be efficient for photolyase dependent recovery in higher plants for a wide range of species [9]. However, little is known about fungi and there are no reports on fungi that cause powdery mildews.

Powdery mildews are widespread diseases among all plants caused by a group of diverse fungal pathogens belonging to the order Erysiphales in the phylum Ascomycota [10,11]. Because of its obligate biotrophic nature, it was difficult to prove the existence of a self-repair mechanism in powdery mildew fungi. *O. neolycopersici*, the causal agent of powdery mildew in tomato is one of the few powdery mildew fungi that have high potential for germination of conidia on water agar surface (> 90%). A recent study using various ranges of UV wavelengths and doses on germination of *O. neolycopersici* conidia on water agar showed that UV had a direct effect on the germination process [6]. However, this study did not investigate the effect of concomitant/subsequent optical radiation on the germination inhibition efficacy of effective UV. With the exception of protected cultivation, the sun is the sole source of energy for plant photosynthesis, and the solar radiation that reaches the terrestrial surface is largely optical radiation. It is important to determine the impact of optical radiation, correlated to wavelength and dose, on the disease control efficacy of effective UV.

A series of experiments were conducted in controlled environment chambers to determine the i) optimum wavelength-dose combination for germination inhibition in the UV range ≤ 315 nm with minimal phytotoxicity, ii) concomitant/subsequent application of optical radiation wavelengths and doses on germination recovery of UV treated conidia (recovery action spectra), iii) lapse time between brief night-time UV treatment and subsequent optical incubation on germination recovery of *O. neolycopersici* conidia.

2. Materials and Methods

2.1. Production and Maintenance of Plants and Pathogen Isolate

Powdery mildew susceptible tomato plants cultivar (cv.) Espero were propagated by sowing seeds in 12 cm diameter plastic pots filled with standard peat growth medium, and maintained in glasshouse compartments as described previously [8]. Healthy and vigorously growing plants were transferred to a controlled environment inoculum chamber with temperature and relative humidity (RH) of 20 ± 1 °C and 75 ± 5%, respectively. A daily light cycle of 16 h with an irradiance of 60 ± 10 µmol/m^2/s was provided using high-pressure mercury (HPM) (Powerstar HQI-BT 400 W/D day light; OSRAM GmbH) lamps.

Colonies of *O. neolycopersici* were obtained by sequential transfers of the conidia from a tomato leaf containing powdery mildew to clean leaf disks in Petri dishes, and then to clean plants in the inoculum chamber as described previously [8]. Pathogen inoculum was renewed weekly by spraying conidial suspensions onto healthy tomato plants, and eight- to nine-day-old fresh inoculum was used in each experiment as described previously [6].

2.2. Experimental Setup

Petri dish level experiments with randomized complete block design (RCBD) were conducted in controlled environment experiment chambers with an air temperature of 20 ± 1 °C and RH of 75 ± 5%. Each experiment was conducted twice in succession (with three Petri dishes in each treatment) and considered as block in data analysis. To avoid interference between optical treatments, each treatment was implemented in a separate controlled environment chamber. All treatments within the block (experiment repeat) were randomly assigned to separate controlled environment chambers. Petri dishes receiving same treatments in each study were assigned randomly. *O. neolycopersici* conidia from fresh inoculum were dusted on the surface of water agar (1% w/v) in 3.5 cm diameter Petri dishes and exposed briefly to either non-UV dark or UV treatment without lid. Immediately after non-UV or UV treatment, Petri dishes were sealed with parafilm and incubated in experiment chambers until assessment. As positive control, conidia on water agar with sealed Petri dishes were incubated in experiment chambers with 8 h dark followed by 16 h of growth light (60 ± 10 µmol/m^2/s) supplied using HPM lamps.

2.3. Environmental Conditions and Recording

For brief UV treatments, 8 ± 0.2 µmol/m^2/s of UV irradiance (≤ 315 nm) at Petri dish level were applied with wavelength peaks at 254 nm (45 cm length tube, model - TUV 15W/G 15 T8, Philips; Holland), 283 nm (XeBr Excimer lamps, model SUS844, Ushio, Japan), 310 nm (120 cm fluorescent tubes, model - MedSun Therapy narrow band UV-B 40W, LightTech; Dunakeszi, Hungary), and broad-spectrum UV with peak at 313 nm (120 cm UV-B fluorescent tubes, model UV-B-313EL; Q-Panel Lab Products, Cleveland, OH) (Fig. 1A).

For incubation treatments, optical radiation in the 290 nm to 780 nm range was applied with wavelength peaks at 310 nm (120 cm fluorescent tubes, model - MedSun Therapy narrow band UV-B 40W, LightTech; Dunakeszi, Hungary), 365 nm (120 cm fluorescent tubes, ES UV-A 365 nm 40W, LightTech, Dunakeszi, Hungary), 400 nm (RAY22 UV-A LEDs, Fluence Bioengineering, Austin, TX), 454 nm (15 W GreenPower LED module HF blue; Philips, The Netherlands), 523 nm

(162 W High-Power LED grow light; Sola-co, Grimstad, Norway), 660 nm (10 W GreenPower LED module HF deep red; Philips, The Netherlands), and 730 nm (10 W GreenPower LED module HF far-red; Philips, The Netherlands) (Fig. 1B & C). For incubation of positive control Petri dishes, HPM lamps similar to those described above were used (Fig. 1B).

A Priva greenhouse computer (Priva, Zijlweg, The Netherlands), with dry and wet bulb thermo sensors deployed at Petri dish/plant level in each chamber, was used to record air temperature and RH at 5 min intervals. An Optronic model 756 spectroradiometer (Optronic Laboratories, Orlando, FL, USA) was used for measurement of spectral composition and irradiance level of the optical radiation sources (UV–Visible-Infrared).

2.4. Effect of Brief UV on Germination, Nuclear Division and Cytotoxicity of O. neolycopersici Conidia

Two-factor (UV wavelengths and exposure durations) experiments were conducted to study the effect of different UV wavelengths and exposure durations on germination, nuclear division and cytotoxicity. Conidia of *O. neolycopersici* were exposed to UV photons of 8 ± 0.2 μmol/m^2/s from 254 nm, 283 nm, 310 nm or broad spectrum 313 nm UV sources. The exposure durations were 30, 60, 120 or 240 s. Immediately after UV treatment, Petri dishes were sealed and incubated in darkness for 24 h. Germination, nuclear division and cytotoxicity were assessed independently.

2.5. Effect of Incubation Wavelength (454 nm to 730 nm) on Germination Efficiency of Conidia Treated With Brief UV

Experiments were performed to examine the potential of incubation wavelength (blue to far-red range) on the germination efficiency (germination recovery) of *O. neolycopersici* conidia treated briefly with UV photons of 8 ± 0.2 μmol/m^2/s. Experiments were conducted as three factors (UV wavelength, duration of UV exposure, and subsequent incubation wavelength) with different levels for each factors. Conidia were exposed to UV photons from 254 nm, or 283 nm or broad spectrum 313 nm UV radiation sources. The duration of exposure was 30, 60, 120 or 240 s. Immediately after UV treatment, Petri dishes were sealed and incubated with 50 ± 5 μmol/m^2/s irradiance supplied by i) blue (peak 454 nm, and range 410–500 nm), or ii) green (peak 523 nm, and range 470–600 nm), or iii) red (peak 660 nm, and range 600–700 nm), or iv) far-red (peak 730 nm, and range 650–780 nm) (Fig. 1B) for 16 h followed by 8 h of darkness (daily light integral (DLI) of 2.88 mol/m^2/day). Twenty four hours after UV treatment, samples were examined for germination of conidia.

An independent experiment similar to that described above was performed with a slight modification to the incubation. Immediately after UV treatment, sealed Petri dishes were incubated in the dark for 8 h followed by 16 h of blue or green or red or far-red light. Twenty four hours after UV treatment, samples were examined for germination of conidia.

2.6. Effect of Incubation Wavelength (310 nm to 454 nm) and Irradiance Levels on Germination Efficiency of Conidia Treated With Brief UV

Two independent experiments were conducted as described above on i) incubation of brief UV treated Petri dishes to 16 h of optical radiation followed by 8 h dark or, ii) incubation of brief UV treated Petri dishes to 8 h dark followed by 16 h of optical radiation. However, the wavelengths of the optical radiation sources with peak and range for incubation were 310 nm (290–350 nm), 365 nm (320–443 nm), 400 nm (375–465 nm) or 454 nm (410–500 nm) (Fig. 1C) with an irradiance of 50 ± 5 μmol/m^2/s (incubation DLI of 2.88 mol/m^2/day).

Similar experiments were conducted using an irradiance of 25 ± 5 μmol/m^2/s for the incubation radiation (incubation DLI = 1.44 mol/m^2/day).

2.7. Effect of Incubation Wavelength (310 nm to 454 nm) and Dose on Germination Efficiency of Conidia Treated With Brief UV

Based on the results of the experiments explained above in Sections 2.5 and 2.6, incubation wavelengths of 310 nm to 454 nm were selected with an irradiance of 50 ± 5 μmol/m^2/s and the incubation duration of 8 h as the longest incubation period (incubation DLI = 1.44 mol/m^2/day). A three-factor (UV, subsequent incubation wavelength, and duration of incubation) experiment was performed to examine the dose response of germination recovery (germination efficiency) in the 310 nm to 454 nm incubation wavelength range. Conidia of *O. neolycopersici* were dusted on a water agar surface as explained above and exposed with either i) dark (non-UV), or ii) highly effective UV wavelength of 254 nm for 30 s. Immediately after non-UV or UV treatment, Petri dishes were sealed and incubated with an irradiance of 50 ± 5 μmol/m^2/s provided by wavelengths of i) 310 nm, or ii) 365 nm, or iii) 400 nm, or iv) 454 nm with incubation duration of i) 0 h, ii) 2 h, iii) 4 h, or iv) 8 h. Conidia germination was assessed 24 h after inoculation as explained above.

2.8. Effect of Lapse Time Between Night-time UV Treatment and Subsequent Blue Light

Experiment was conducted to determine the required minimum time period between UV treatment and subsequent exposure to recovery wavelengths (< 310 nm to < 500 nm) (lapse time) to have significant reduction in conidia germination.

Based on the results of the experiment explained above in Section 2.7, a representative wavelength of 454 nm with an irradiance of 50 ± 5 μmol/m^2/s and incubation duration of 2 h was selected.

Conidia were exposed to 30 s with either i) dark (non-UV), or ii) highly effective UV wavelength of 254 nm. Immediately after non-UV or UV treatment, Petri dishes were sealed and incubated with one of the following dark periods (lapse time between UV treatment and subsequent blue light) of i) 0 h, ii) 2 h, iii) 4 h, iv) 6 h, or v) 8 h. Immediately after dark incubation, all samples were treated with 2 h of blue light (50 ± 5 μmol/m^2/s) with peak wavelength at 454 nm followed by darkness until assessment. Conidia germination was assessed 24 h after inoculation as explained above.

2.9. Preparation of Slides and Microscopic Assessments

All microscopic assessments were conducted 24 h after inoculation. A piece of water agar taken from the centre of each Petri dish was mounted on glass slides. For germination assessment, a drop of sterilized distilled water was added to the piece of water agar and covered with a cover slip. Fifty conidia/germlings were examined in each sample, and conidia with germ tubes equal to or longer than the conidial width were counted as germinated.

For nuclear staining, a few drops of freshly prepared staining solution containing 50 mM Tris/malic acid, pH 5.2, 20 mg/ml of Polyvinylpyrrolidone (PVP40), 0.4% TritonX-100 (v/v), 15% (v/v) Glycerol, 4% formaldehyde (v/v), and 0.6 μg/ml DAPI (4′,5-Diamidina-2-Phenylindole, Life Technologies AS) were added to a piece of water agar. Samples were covered with coverslips and incubated at 4 °C for 30 min in darkness. Ten colony-forming units (CFU) (conidia/germlings) were examined in each sample (piece of water agar) and the number of CFU having more than one nuclei were quantified using a fluorescent microscope (Leica DM 5000B equipped with Leica DFC 425 camera and Leica Application Suit software) with excitation and emission wavelengths of 340–380 nm and 425 nm, respectively. Fluorescence and differential interference contrast images acquired simultaneously and overlay with ImageJ software version 1.46r.

For cytotoxicity assessment, a drop of filter (0.2 μM)-sterilized MTT

(3-(4,5-dimethylthiazol-2-yl)-2,5-diphenyltetrazolium bromide, Life Technologies As) solution (0.5 mg MTT dissolved in 1 ml PBS (pH = 7.2)) was added to the water agar piece on a glass slide and covered with a cover slip. Samples were incubated at 37 °C for 2 h. Fifty CFU were examined in each sample under a light microscope, and colourless CFU were counted for cytotoxicity. Germination efficiency (inverse of UV efficacy) was calculated using the following formula

$$\text{Germination efficiency} = \frac{Y}{X} \times 100$$

where X is the mean number of conidia germinated with positive control, Y is the number of conidia germinated with treatment. Efficiency for nuclear division and cytotoxicity were calculated similarly.

2.10. Data Analysis

Analysis of variance for germination efficiency of *O. neolycopersici* conidia was performed using the general linear model (Minitab Version 17.0, Minitab Corp., State College, PA, USA). Treatment means were separated using Tukey's pairwise comparison at P = 0.05. Figures and trend analysis with non-linear exponential decay (single, 2 parameter) model fit were performed using SigmaPlot 10 (Systat Software, Inc., Chicago, IL, USA). Prior to analysis, data were checked for homogeneity of variances.

3. Results

3.1. Effect of Brief UV on Germination, Nuclear Division and Cytotoxicity of O. neolycopersici Conidia

UV wavelength, and UV wavelength × exposure duration interaction had a significant effect on conidia germination efficiency (P < 0.0001). This was significantly lower (≤ 7%) when exposed to UV wavelengths of 254 nm and 283 nm independent of the duration of exposure, compared with conidia germination (88–95%) exposed to UV wavelength of 310 nm. Conidia germination efficiency was significantly lower with UV from broad-spectrum UV-B lamps with peak at 313 nm, dependent on the duration of exposure (59–60% with exposed duration of 30 s or 1 min, and 25–28% with exposed duration of 2 to 4 min), compared with conidia germination at narrow wavelength of 310 nm (Fig. 2A, D).

The UV wavelength had a significant effect on nuclear division (P < 0.0001). The number of conidia with more than one nuclei was significantly lowest (0.6) with UV of 254 and 283 nm (independent of the tested duration of exposure), and low (44) with broad-spectrum UV with peak at 313 nm, compared with the narrow wavelength of 310 nm (96) (Fig. 2B, E).

UV wavelength, and UV wavelength × exposure duration interaction had a significant effect on the conidia cytotoxicity (P < 0.0001). The number of conidia showing cytotoxicity was significantly highest at 254 and 283 nm (dependent of the duration of exposure), compared with 310 nm (Fig. 2C, F).

3.2. Effect of Incubation Wavelength (454 nm to 730 nm) on Germination Efficiency of Conidia Treated With Brief UV

3.2.1. Brief UV Followed by 16 h Incubation Followed by 8 h Darkness

UV wavelength (Adjusted mean square (AMS) = 7539.5, F = 64.8), incubation wavelength (AMS = 6543.3, F = 56.3), and all interactions of UV wavelength × duration of UV exposure (AMS = 492.5, F = 4.2), UV wavelength × incubation wavelength (1274.1, F = 11), UV wavelength × duration of UV exposure × incubation wavelength (AMS = 494.1, F = 4.3), all had a significant effect on the germination efficiency of conidia (P < 0.0001).

Considering the effect of incubation wavelengths (as main factor) on germination efficiency of all UV treated conidia, significantly highest germination efficiency (69%) was observed with an incubation wavelength of 454 nm compared with all other incubation wavelengths.

UV wavelengths of 254 nm or 283 nm with exposed duration ≤ 60 s followed by incubation with 454 nm showed germination efficiency ≥ 80%.

UV wavelengths of 254 nm or 283 nm with all exposed duration of ≥ 60 s showed significantly low germination efficiency (< 16%), if samples were incubated with either dark or wavelengths > 523 nm.

Samples treated with broad spectrum UV showed < 50% of germination efficiency, if the duration of exposure was ≥ 120 s followed by incubation with dark or wavelengths > 523 nm (Fig. 3A–D).

3.2.2. Brief UV Followed by 8 h Darkness Followed by 16 h Incubation

UV wavelength (AMS = 6914.2, F = 78.9, P < 0.0001), duration of UV exposure (AMS = 259.6, F = 3, P = 0.032), incubation wavelength (AMS = 236.5, F = 2.7, P = 0.031), UV wavelength × duration of UV exposure (AMS = 915.7, F = 10.5, P < 0.0001), UV wavelength × incubation wavelength (AMS = 224.6, F = 2.6, P = 0.01), and UV wavelength × duration of UV exposure × incubation wavelength (AMS = 268.3, F = 3.1, P < 0.0001), all had a significant effect on conidia germination.

Significantly highest germination efficiency (37.8%, mean of all UV treated conidia) was observed with an incubation wavelength of 454 nm (if considered as main factor) compared with all other incubation wavelengths.

UV wavelengths of 254 nm with an exposed duration of 30 s showed germination efficiency of 27.6%, if the incubation wavelength was 454 nm. The germination efficiency reduced to 3.3% with 60 s of UV exposure. Similarly, conidia germination efficiency was 51.4% and 17.2% with UV wavelength of 283 nm.

UV wavelengths of 254 nm or 283 nm with all exposed duration of ≥ 60 s showed significantly low germination efficiency (< 15%), if samples were incubated with either dark or wavelengths ≥ 523 nm.

Samples treated with broad spectrum UV showed germination efficiency > 75% with all durations of UV exposure with an incubation wavelength of 454 nm (Fig. 4A–D).

3.3. Effect of Incubation Wavelength (310 nm to 454 nm) on Germination Efficiency of Conidia Treated With Brief UV

3.3.1. Brief UV Followed by 16 h Incubation Followed by 8 h Darkness

UV wavelength (AMS = 12,951.3, F = 200.1, P < 0.0001), duration of UV exposure (AMS = 326.3, F = 5, P = 0.002), incubation wavelength (AMS = 12,605.1, F = 194.7, P < 0.0001), interactions of UV wavelength × duration of UV exposure (AMS = 1102.6, F = 17, P < 0.0001), UV wavelength × incubation wavelength (AMS = 2511.5, F = 38.8, P < 0.0001), duration of UV exposure × incubation wavelength (AMS = 3107.6, F = 48, P < 0.0001), and UV wavelength × duration of UV exposure × incubation wavelength (AMS = 1512.2, F = 23.4, P < 0.0001), all had a significant effect on conidia germination.

Germination efficiency of conidia treated with UV (mean of all UV treatments with incubation wavelength as main factor) was significantly higher (73–76%) with incubation wavelengths of 365 nm, 400 nm or 454 nm, compared to incubation in complete darkness (25.2%). The significantly lowest germination efficiency was observed with incubation under 310 nm (0.1%).

UV wavelengths of 254 nm or 283 nm with exposed duration ≤ 60 s followed by incubation with ≥ 365 nm showed germination efficiency > 77%.

UV wavelengths of 254 nm or 283 nm or broad spectrum UV with all exposed duration showed significantly low germination efficiency (< 1%), if samples were incubated with 310 nm wavelength (Fig. 5A–D).

Germination efficiency was similar, even though the irradiance level of the incubation wavelength was reduced to 25 μmol/m^2/s (data not

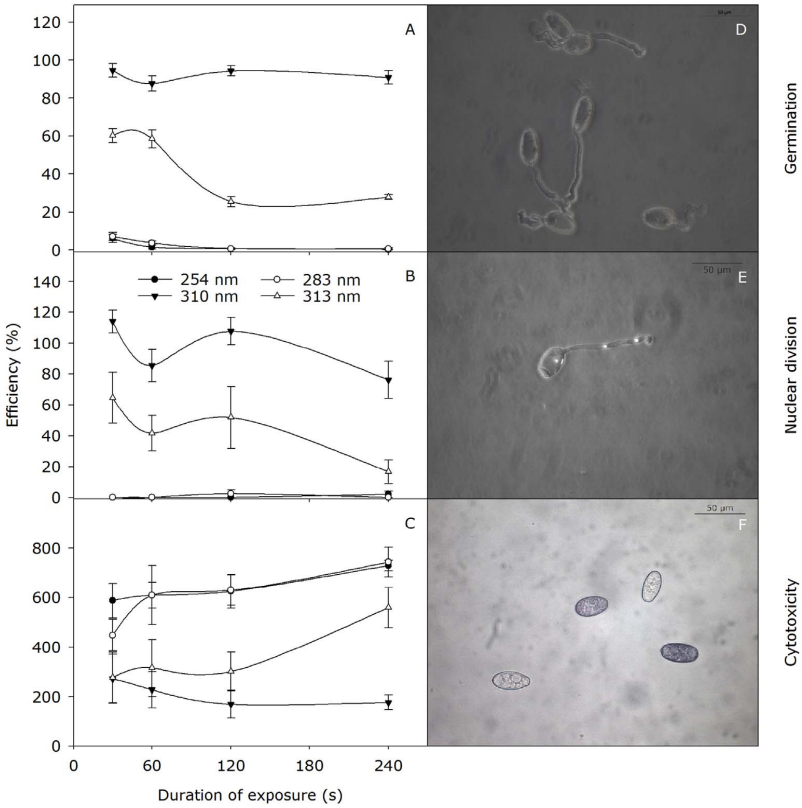

Fig. 2. Wavelength dependent effect of UV irradiances (8 ± 0.2 µmol/m^2/s) on efficiency of germination (A, D), nuclear division (B, E), and cytotoxicity (C, F) of *Oidium neolycopersici* conidia on water agar exposed to near monochromatic UV of 254 nm, 283 nm, 310 nm or broad-spectrum UV with peak at 313 nm (described in Fig. 1A) applied to 30, 60, 120 or 240 s. Immediately after UV treatment samples were incubated under darkness for 24 h (A, B, C). Representative images of germlings (D), germlings with nucleus (E), and cytotoxic (non-stained colourless)-non cytotoxic (conidia stained in purple) conidia (F). Efficiency values were calculated as described in Materials and Methods. Each value is the mean ± standard error of two repeated experiments each with three replicate Petri dishes (n = 6). (For interpretation of the references to colour in this figure legend, the reader is referred to the web version of this article.)

shown).

3.3.2. Brief UV Followed by 8 h Dark Followed by 16 h Incubation

UV wavelength (AMS = 16,523.2, F = 324.5, P < 0.0001), incubation wavelength (AMS = 991.9, F = 19.5, P < 0.0001), interactions among UV wavelength × duration of UV exposure (AMS = 1192.8, F = 23.4, P < 0.0001), UV wavelength × incubation wavelength (AMS = 1610.1, F = 31.6, P < 0.0001), duration of UV exposure × incubation wavelength (AMS = 262.8, F = 5.2, P < 0.0001), and UV wavelength × duration of UV exposure × incubation wavelength (AMS = 992, F = 19.5, P < 0.0001), all had a significant effect on germination efficiency.

Considering incubation wavelength as main factor, germination efficiency of UV treated conidia (mean germination efficiency from all UV treatments) with incubation wavelengths of 365 nm to 454 nm showed a significantly high germination efficiency (41.4–43.3%), compared with complete dark incubation (24.9%). Conidia germination efficiency was lowest with incubation wavelength 310 nm (4.9%), compared with complete darkness.

Samples treated with UV wavelengths of 254 nm with all tested duration of exposure and incubation wavelengths showed < 30% of germination efficiency. On the other hand, samples treated with 283 nm UV with exposed duration of 30 s and 60 s showed germination efficiency of 68.7% and 36.7% respectively with all incubation wavelengths ≥ 365 nm.

UV wavelengths of 254 nm or 283 nm or broad spectrum UV with all exposed duration showed significantly low germination efficiency (< 34%), if samples were incubated with 310 nm wavelength (Fig. 6A–D).

The germination efficiency was similar, even though the irradiance level of the incubation wavelength was reduced to 25 µmol/m^2/s (data not shown).

3.4. Effect of Incubation Wavelength (310 nm to 454 nm) and Dose on Germination Efficiency of Conidia Treated With Brief UV

UV treatment (AMS = 44,676, F = 387.1, P < 0.0001), incubation dose (recovery dose) (AMS = 16,275.7, F = 141, P < 0.0001), UV treatment × incubation dose (AMS = 16,114.7, F = 139.6, P < 0.0001), incubation wavelength × incubation dose (AMS = 6633.5, F = 57.5, P < 0.0001), all had a significant effect on conidia germination efficiency. All non-UV treated samples showed germination efficiency > 78% with all incubation wavelength and doses, except samples incubated with 310 nm wavelengths for ≥ 2 h. Almost no conidia germinated, if the non-UV treated samples were incubated with 310 nm wavelength for ≥ 4 h.

All UV treated samples showed low germination efficiency (< 9%), if they were incubated with any wavelength for 0 h (UV treatment followed by dark incubation). UV treated samples incubated with 310 nm wavelength for 2 h showed germination efficiency of 34.5%, and the germination efficiency decreased with increased incubation dose.

All UV treated samples incubated with wavelengths ≥ 365 nm for ≥ 2 h showed germination efficiency of > 80% (Fig. 7A–D).

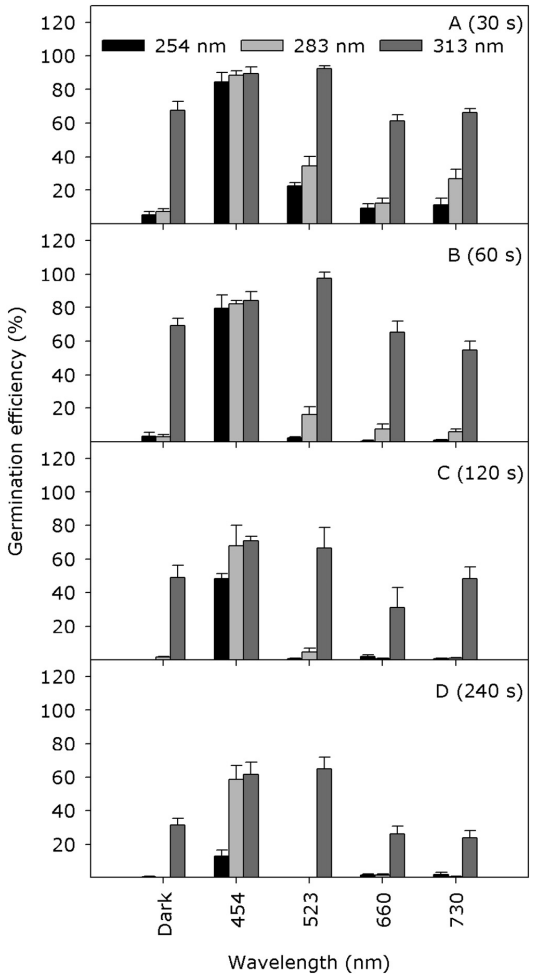

Fig. 3. The effect of incubation wavelengths (454 nm to 730 nm as described in Fig. 1B) applied subsequently to different doses of brief UV treatment on germination efficiency of *Oidium neolycopersici* conidia. Conidia dusted on water agar surface were first exposed to near monochromatic UV of 254 nm, 283 nm, or broad-spectrum UV with peak at 313 nm (described in Fig. 1A) for (A) 30 s, (B) 60 s, (C) 120 s, or (D) 240 s. Immediately after UV treatment, samples were incubated with 16 h of specific light of 50 ± 5 μmol/m^2/s (described in Fig. 1B) followed by 8 h dark. Germination efficiency was calculated as described in Materials and Methods. Each value is the mean ± standard error of two repeated experiments each with three replicate Petri dishes (n = 6).

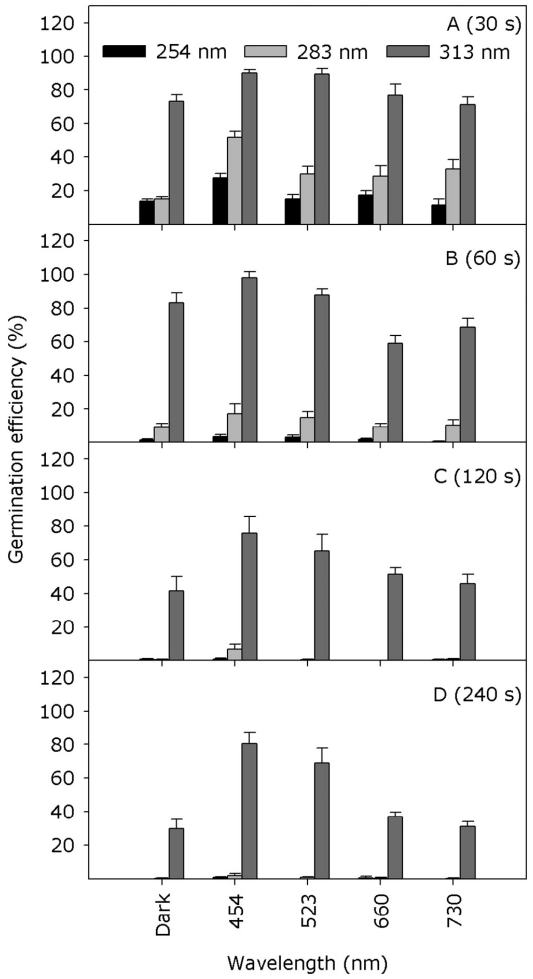

Fig. 4. The effect of incubation wavelength (454 nm to 730 nm as described in Fig. 1B) applied after 8 h of dark from the application of different doses of brief UV treatment on germination efficiency of *Oidium neolycopersici* conidia. Conidia dusted on water agar surface were first exposed to near monochromatic UV of 254 nm, 283 nm, or broad-spectrum UV with peak at 313 nm (described in Fig. 1A) for (A) 30 s, (B) 60 s, (C) 120 s, or (D) 240 s. Immediately after UV treatment, samples were incubated with 8 h of dark followed by 16 h of specific light (described in Fig. 1B) with an irradiance of 50 ± 5 μmol/m^2/s. Germination efficiency was calculated as described in Materials and Methods. Each value is the mean ± standard error of two repeated experiments each with three replicate Petri dishes (n = 6).

3.5. *Effect of Lapse Time Between Night-time UV Treatment and Subsequent Blue Light*

UV treatment (AMS = 1054.5, F = 16.5, P < 0.0001) and UV treatment × dark period before blue light (lapse time) (AMS = 2878.2, F = 45.2, P < 0.0001) both had a significant effect on conidia germination efficiency. Lapse time showed no effect on germination efficiency of non-UV control (103%) (mean conidia germination efficiency of all non-UV treated samples independent of lapse time). On the other hand, conidia germination efficiency was significantly lowest (32.7%) for samples treated with 254 nm for 30 s (mean conidia germination efficiency of all UV treated samples independent of lapse time). Among the UV treated samples, germination efficiency was significantly highest for samples incubated immediately (lapse time = 0 h) with 2 h of blue light (85.1%). The germination efficiency was significantly lowest (7.8 to 13.4%) when UV treated samples were incubated with 6 h or 8 h of dark period (lapse time of 6 h or 8 h) followed by 2 h of blue light (Fig. 8), and there was no significant difference between 6 h and 8 h of lapse time on germination efficiency. For the lowest germination efficiency, the lapse time between UV treatment and the subsequent blue light should be > 4 h. Non-linear model fit yielded an exponential decrease in germination efficiency in relation to increased lapse time (dark period) before blue light.

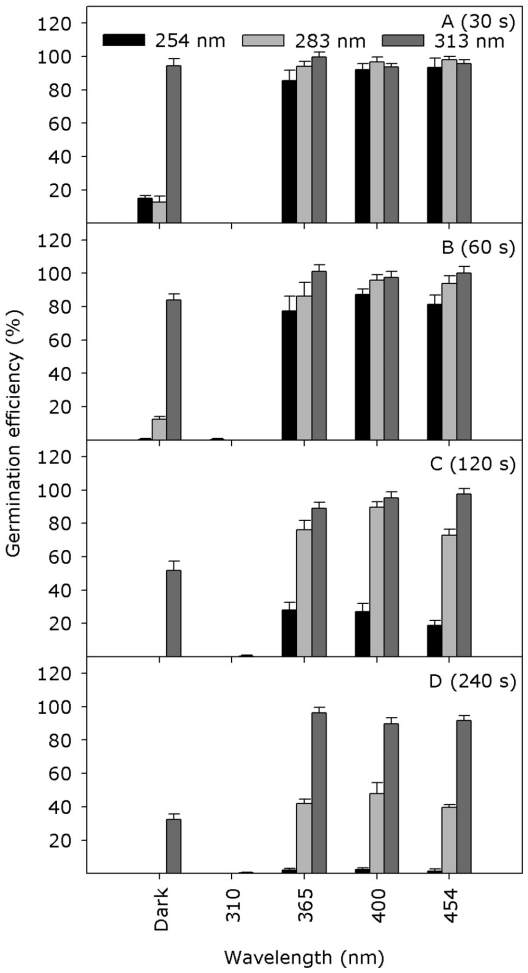

Fig. 5. The effect of incubation wavelength (described in Fig. 1C) applied subsequently to different doses of brief UV treatment on germination efficiency of *Oidium neolycopersici* conidia. All other details are as explained in Fig. 3 except the incubation wavelengths from 310 nm to 454 nm (described in Fig. 1C).

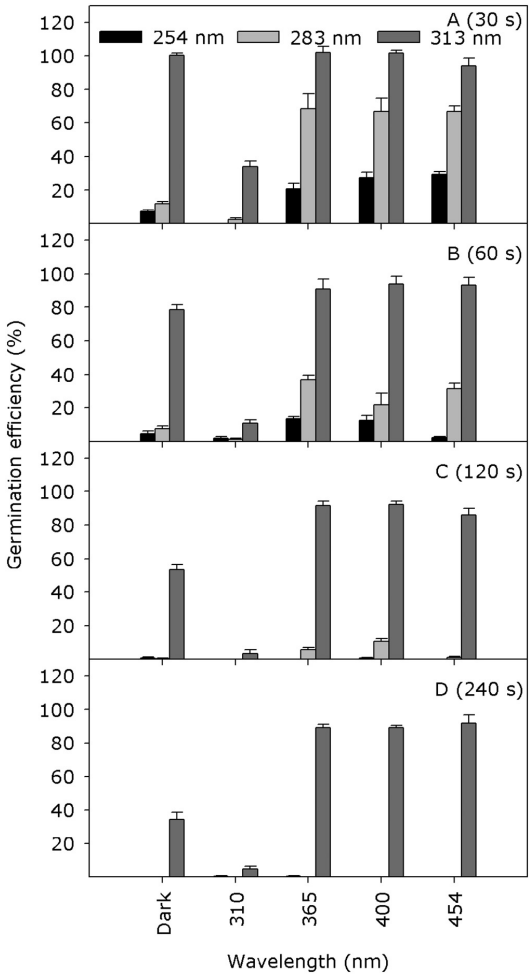

Fig. 6. The effect of incubation wavelength (described in Fig. 1C) applied after 8 h of dark from the application of different doses of brief UV treatment on germination efficiency of *Oidium neolycopersici* conidia. All other details are as explained in Fig. 4 except the incubation wavelengths from 310 nm to 454 nm (described in Fig. 1C).

4. Discussion

The effect of night-time UV on pathogen developmental stages and severity of powdery mildews in a range of crops has been reported in our previous studies [5,6,8,12]. This study focused on determining the spectral efficiency in the optical region on recovery of UV mediated damage in *O. neolycopersici* conidia. Furthermore, this study also determined the dose and lapse time of the wavelength which, applied after night-time UV treatment, gave minimal recovery. This study confirmed our previous findings that the effective UV range for germination inhibition of conidia is from 250 to 280 nm at low dose [6]. However, significantly low germination efficiency of conidia exposed to 310 nm wavelength for > 2 h showed that the efficacy could be achieved with wavelengths above 290 nm if applied at high dose. This supports the previous reports that powdery mildew severity on grape fruits is increased by 20% to 40% when 90% of the UV radiation from the solar spectrum is filtered out (< 400 nm) compared with the severity on fruits exposed to unfiltered solar radiation [13]. UV impacts on growth, development and stress responses of living organisms via alterations in membrane protein, DNA, photosystem II, enzyme synthesis, production of growth regulators, and reactive oxygen species [14–18]. Depending on the wavelength, dose, and the complexity of the organism, UV can kill, induce mutations, or act as a signal [4]. The present study has demonstrated the direct effect of UV on conidial germination, nuclear division and cytotoxicity. Absorption of high-energy UV photons has been shown to induce two major lesions of cyclobutane pyrimidine dimers (CPDs) and pyrimidine-pyrimidone (6–4) photoproducts (6-4PPs) [19–21] in addition to their related Dewar valence isomers, between the adjacent pyrimidines on the same DNA strand. The existence of such lesions may disrupt the action of DNA polymerase and thereby prevent genome replication [22,23] and RNA polymerase, thereby altering the relative transcription profile [24] which leads to cell cycle arrest.

The present study showed that the *O. neolycopersici* has its own

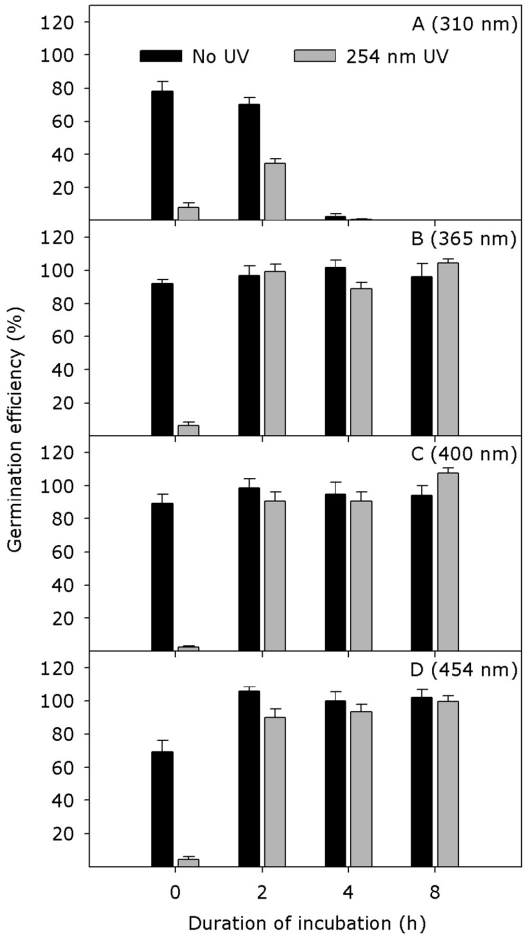

Fig. 7. The effect of incubation wavelengths (310 nm to 454 nm) and duration of incubation applied subsequently to either non-UV or UV treatment on germination efficiency of *Oidium neolycopersici* conidia. Conidia dusted on water agar were treated with either non-UV or UV of 254 nm wavelength (8 ± 0.2 μmol/m^2/s) for 30 s followed by incubation wavelengths of (A) 310 nm, (B) 365 nm, (C) 400 nm or (D) 454 nm with an irradiance of 50 ± 5 μmol/m^2/s. Germination efficiency was calculated as described in Materials and Methods. Each value is the mean ± standard error of two repeated experiments each with three replicate Petri dishes (n = 6).

optical dependent repair machinery for UV-mediated damage. In the tested wavelengths in the optical range, the UV damage recovery action for *O. neolycopersici* conidia is limited from above 310 nm to 454 nm. This range is close to the photolyase action spectra reported for a wide range of species, with 360 nm to 420 nm in higher plants [9]. Three major mechanisms of DNA damage repair have been identified so far including excision repair (ER), photorepair (photoreactivation) and recombination repair [25]. Enzyme (photolyase) mediated photorepair is a major mechanism in all forms of life except placental mammals [26] and a few other species [27] which use UV-A to blue wavelengths (350 to 450 nm) as an energy source [28]. Photolyases can be classified as CPD photolyase, 6-4PP photolyase, and Cry-DASH based on substrate. Photolyase binds to the backbone of the damaged DNA strand via ionic interactions [29], and catalyzes monomerization of the UV-induced pyrimidine dimers by utilizing photon energy in the UV-A to blue range.

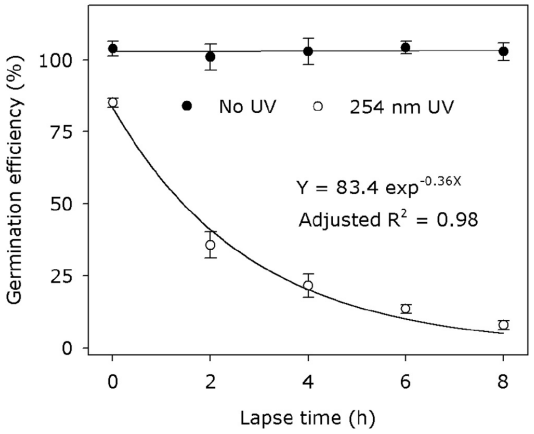

Fig. 8. The potential of blue light related to its application time after night-time UV treatment (lapse time) on germination efficiency of *Oidium neolycopersici* conidia. Conidia of *O. neolycopersici* were dusted on a water agar surface as explained above and exposed to 30 s with either i) dark (non-UV), or ii) highly effective UV wavelength of 254 nm. Petri dishes were sealed and incubated with one of the following dark periods of i) 0 h, ii) 2 h, iii) 4 h, iv) 6 h, or v) 8 h. Immediately after dark incubation, samples were treated with 2 h of blue light (50 ± 5 μmol/m^2/s) with peak wavelength at 454 nm followed by dark until assessment. Conidia germination was assessed 24 h after inoculation. Germination efficiency was calculated as described in Materials and Methods. Each value is the mean ± standard error of two repeated experiments each with three replicate Petri dishes (n = 6).

The UV-mediated effect on germination efficiency of conidia was equally effective in the effective range (254 nm and 283 nm in this study) if samples were subsequently incubated under darkness. However, the UV-mediated effect on germination efficiency was dependent on the wavelength and dose of effective UV if samples were subsequently exposed to incubation wavelengths of above 310 nm to 454 nm. This showed that the UV-mediated damage recovery efficiency was not only dependent on subsequent incubation wavelength but also on the wavelength and dose of the effective UV. A possible reason could be i) UV wavelength-dependent differences in distribution pattern of the twelve possible UV-mediated dimeric photo lesions, or ii) UV wavelength-dependent quantitative differences in the photo lesions. It has been reported that the distribution pattern of the twelve possible UV-mediated dimeric photo lesions were similar in isolated and cellular DNA at exposure to low doses of either UV-C or UV-B [30]. Furthermore, it has been reported that UV-mediated DNA lesions are wavelength dependent following the pattern of increased lesions with decreasing wavelengths from UV-A to UV-C [31,32]. While UV-C and UV-B induce CPDs, 6-4PPs and their related Dewar valence isomers, UV-A can induce only CPDs, and can convert 6-4PPs to Dewar valence isomers but cannot induce 6-4PPs [33].

The present study showed that UV treatment at 254 nm followed by incubation in darkness or incubation with 310 nm for a minimum of 4 h gave the significantly lowest germination efficiency. This result further confirms the existence of a photolyase (like) mechanism and its key role in the recovery of UV-mediated damage.

To achieve the lowest germination efficiency (i.e. lowest damage recovery), the present study demonstrated that the lapse time between UV treatment and blue light exposure should be > 4 h (applicable to wavelength ranges of > 310 nm to 454 nm). This indicated that the repair mechanism will become ineffective if the samples do not receive potential recovery wavelengths within 4 h from the effective UV treatment. The persistence of UV-mediated lesions for > 4 h can disrupt key intercellular process, which can ultimately lead to cell death. This is in accordance with our previous reports of sustaining/increasing

disease control efficiency of UV with subsequent red light application, instead of blue/UV-A which reduces the UV efficiency [8,34].

Cells are constantly adjusting their structure and function (homeostasis) to accommodate changing demands and extracellular stresses, but only up to a limit. As cells encounter physiological stresses, they can undergo adaptation (achieving a new steady state and preserving viability and function) or experience cell injury if the adaptive capability of the cells is exceeded. The injury can be either reversible or irreversible, and can cause cell death if the stress is severe or persistent.

Optical radiation is an important environmental factor that governs many cellular responses in all forms of life on earth. Consequently, life forms possess different classes of photoreceptors for perception of the optical environment as a sensory cue to anticipate environmental changes to those possessed by photosynthetic organisms that also use light as a source of energy. Fungi represent the third group of macroscopic eukaryotes, and are neither photosynthetic nor capable of observing adjacent objects [35]. All of the fungal species, with a few exceptions, respond to light [3]. The majority of the exceptions are obligate pathogens with a close association with their host [35]. Powdery mildew is a widespread disease with great economic impact, and is caused by a diverse range of obligate biotrophic fungal pathogenic species all of which belong to the order Erysiphales, phylum Ascomycota [10,11]. Recently, the presence and expression of genes similar to phytochromes, cryptochromes, white collar, and photolyase were confirmed using next generation sequencing in *Erysiphe necator* [7]. Moreover, next generation high throughput sequencing of the whole genome and transcriptome performed on *O. neolycopersici*, *Podosphaera xanthii*, *Podosphaera aphanis* confirmed the presence of genes similar to all major classes of photoreceptor genes of photolyase, cryptochrome, white collar, phototropins, phytochrome and UVR8.

All living organisms have mechanisms to protect their genome from genotoxic agents including UV. Melanin in humans, various amino acid compounds in cyanobacteria, carotenoids, flavonoids or sinapic acid derivatives in plants all act as a UV screening primary line of defence via UV absorption [36]. Organisms exposed to solar radiation are typically equipped with UV absorbing pigments as a primary line of defence [36]. To cope with UV damage, plants have two layers of protection mechanisms; UV screening via accumulation of UV absorbing compounds in epidermal cells, and repair of UV-mediated damage [37]. On the other hand, powdery mildew fungi lack UV screening mechanisms leaving them more vulnerable to UV radiation than plants. Proper selection and combinations of different wavelength in optical range, right application time in relation to each other with certain minimum blue/UV-A photons in growth light applied 4 h after night-time UV treatment can enhance the practical efficiency of UV against powdery mildews.

Conflict of Interest

The authors declare that there is no conflict of interest.

Acknowledgements

This research was financed by the Research Council of Norway (projects 225080, 243732, and 256323), and PhD stipend (1207051033) to cover payroll and running expenses. The 283 nm UV XeBr Excimer lamp was kindly provided by Ushio America Inc. We are thankful for the coordination work done by Dr. David M. Gadoury and Dr. Mark Rea for the lamp from Ushio America Inc. We extended our thanks to technicians at the Centre for Controlled Environment Plant Research (SKP) for their excellent support and assistance.

Author Contributions

Aruppillai Suthaparan - Conceived, designed and performed the experiments, analyzed the data, and wrote the manuscript. Ranjana Pathak - Contributed to performing the experiments. Knut Asbjørn Solhaug, and Hans Ragnar Gislerød - Contributed to designing experiments and reviewing the manuscript.

References

[1] L. Huché-Thélier, L. Crespel, J. Le Gourrierec, P. Morel, S. Sakr, N. Leduc, Light signaling and plant responses to blue and UV radiations-perspectives for applications in horticulture, Environ. Exp. Bot. 121 (2016) 22–38.
[2] M.L. Porter, Beyond the eye: molecular evolution of extraocular photoreception, Integr. Comp. Biol. 56 (2016) 842–852.
[3] A. Idnurm, S. Verma, L.M. Corrochano, A glimpse into the basis of vision in the kingdom Mycota, Fungal Genet. Biol. 47 (2010) 881–892.
[4] B.M. Sutherland, Action spectroscopy in complex organisms: potentials and pitfalls in predicting the impact of increased environmental UVB, J. Photochem. Photobiol. B 31 (1995) 29–34.
[5] A. Suthaparan, A. Stensvand, K.A. Solhaug, S. Torre, L.M. Mortensen, D.M. Gadoury, R.C. Seem, H.R. Gislerød, Suppression of powdery mildew (*Podosphaera pannosa*) in greenhouse roses by brief exposure to supplemental UV-B radiation, Plant Dis. 96 (2012) 1653–1660.
[6] A. Suthaparan, K.A. Solhaug, A. Stensvand, H.R. Gislerød, Determination of UV action spectra affecting the infection process of *Oidium neolycopersici*, the cause of tomato powdery mildew, J. Photochem. Photobiol. B 156 (2016) 41–49.
[7] A. Suthaparan, A. Stensvand, K.A. Solhaug, S. Torre, K.H. Telfer, A.K. Ruud, L.C. Davidson, L.M. Mortensen, D.M. Gadoury, R.C. Seem, H.R. Gislerød, Suppression of cucumber powdery mildew by UV-B is affected by background light quality (abstract), Phytopathology 102 (S4) (2012) 116.
[8] A. Suthaparan, A. Stensvand, K.A. Solhaug, S. Torre, K.H. Telfer, A.K. Ruud, L.M. Mortensen, D.M. Gadoury, R.C. Seem, H.R. Gislerød, Suppression of cucumber powdery mildew by supplemental UV-B radiation in greenhouses can be augmented or reduced by background radiation quality, Plant Dis. 98 (2014) 1349–1357.
[9] W.M. Waterworth, Q. Jiang, C.E. West, M. Nikaido, C.M. Bray, Characterization of *Arabidopsis* photolyase enzymes and analysis of their role in protection from ultraviolet-B radiation, J. Exp. Bot. 53 (2002) 1005–1015.
[10] D.A. Glawe, The powdery mildews: a review of the world's most familiar (yet poorly known) plant pathogens, Annu. Rev. Phytopathol. 46 (2008) 27–51.
[11] S. Takamatsu, Origin and evolution of the powdery mildews (Ascomycota, Erysiphales), Mycoscience 54 (2013) 75–86.
[12] A. Suthaparan, K.A. Solhaug, N. Bjugstad, H.R. Gislerod, D.M. Gadoury, A. Stensvand, Suppression of powdery mildews by UV-B: application frequency and timing, dose, reflectance, and automation, Plant Dis. 100 (2016) 1643–1650.
[13] C.N. Austin, W.F. Wilcox, Effects of sunlight exposure on grapevine powdery mildew development, Phytopathology 102 (2012) 857–866.
[14] M.M. Caldwell, C.L. Ballare, J.F. Bornman, S.D. Flint, L.O. Björn, A.H. Teramura, G. Kulandaivelu, M. Tevini, Terrestrial ecosystems, increased solar ultraviolet radiation and interactions with other climatic change factors, Photochem. Photobiol. Sci. 2 (2003) 29–38.
[15] M.M. Caldwell, L.O. Bjorn, J.F. Bornman, S.D. Flint, G. Kulandaivelu, A.H. Teramura, M. Tevini, Effects of increased solar ultraviolet radiation on terrestrial ecosystems, J. Photochem. Photobiol. B 46 (1998) 40–52.
[16] B.Y. Choi, K.S. Roh, UV-B radiation affects chlorophyll and activation of Rubisco by Rubisco activase in *Canavalia ensiformis* L. leaves, J. Plant Biol. Res. 46 (2003) 117–121.
[17] E.L. Fiscus, F.L. Booker, Is increased UV-B a threat to crop photosynthesis and productivity? Photosynth. Res. 43 (1995) 81–92.
[18] S.A.H. Mackerness, C.F. John, B. Jordan, B. Thomas, Early signaling components in ultraviolet-B responses: distinct roles for different reactive oxygen species and nitric oxide, FEBS Lett. 489 (2001) 237–242.
[19] H. Frohnmeyer, D. Staiger, Ultraviolet-B radiation-mediated responses in plants. Balancing damage and protection, Plant Physiol. 133 (2003) 1420–1428.
[20] N. Tuteja, P. Ahmad, B.B. Panda, R. Tuteja, Genotoxic stress in plants: shading light on DNA damage, repair and DNA repair helicases, Mutat. Res. 681 (2009) 134–149.
[21] A.C. Kneuttinger, G. Kashiwazaki, S. Prill, K. Heil, M. Müller, T. Carell, Formation and direct repair of UV-induced dimeric DNA pyrimidine lesions, Photochem. Photobiol. 90 (2014) 1–14.
[22] G.J.S. Jenkins, B. Burlinson, J.M. Parry, The polymerase inhibition assay: a methodology for the identification of DNA-damaging agents, Mol. Carcinog. 27 (2000) 289–297.
[23] R.P. Sinha, M. Dautz, D.P. Hader, A simple and efficient method for the quantitative analysis of thymine dimers in cyanobacteria, phytoplankton and macroalgae, Acta Protozool. 40 (2001) 187–195.
[24] S. Tornaletti, D. Reines, P.C. Hanawalt, Structural characterization of RNA Polymerase II complexes arrested by a cyclobutane pyrimidine dimer in the transcribed strand of template DNA, J. Biol. Chem. 274 (1999) 24124–24130.
[25] V. Manova, D. Gruszka, DNA damage and repair in plants - from models to crops, Front. Plant Sci. 6 (2015) 1–26.
[26] J. Jans, W. Schul, Y. Sert, Y. Rijksen, H. Rebel, A.P.M. Eker, S. Nakajima, H. van Steeg, F.R. de Gruijl, A. Yasui, J.H.J. Hoeijmakers, G.T.J. van der Horst, Powerful skin cancer protection by a CPD- photolyase transgene, Curr. Biol. 15 (2005) 105–115.
[27] Q. Mei, V. Dvornyk, Evolutionary history of the photolyase/cryptochrome superfamily in eukaryotes, PLoS ONE 10 (2015) 1–20.
[28] A.B. Britt, DNA damage and repair in plants, Annu. Rev. Plant Physiol. Plant Mol. Biol. 47 (1996) 75–100.

[29] I.H. Kavakli, I. Baris, M. Tardu, S. Gul, H. Oner, S. Cal, S. Bulut, D. Yarparvar, C. Berkel, P. Ustaoglu, C. Aydin, The photolyase/cryptochrome family of proteins as DNA repair enzymes and transcriptional repressors, Photochem. Photobiol. 93 (2017) 93–103.
[30] J. Cadet, E. Sage, T. Douki, Ultraviolet radiation-mediated damage to cellular DNA, Mutat. Res. 571 (2005) 3–17.
[31] A. Besaratinia, J. Yoon, C. Schroeder, S.E. Bradforth, M. Cockburn, G.P. Pfeifer, Wavelength dependence of ultraviolet radiation-induced DNA damage as determined by laser irradiation suggests that cyclobutane pyrimidine dimers are the principal DNA lesions produced by terrestrial sunlight, FASEB J. 25 (2011) 1–13.
[32] Z. Kuluncsics, D. Perdiz, E. Brulay, B. Muel', E. Sage, Wavelength dependence of ultraviolet-induced DNA damage distribution: involvement of direct or indirect mechanisms and possible artefacts, J. Photochem. Photobiol. B 49 (1999) 71–80.
[33] J. Hu, S. Adar, The cartography of UV-induced DNA damage formation and DNA repair, Photochem. Photobiol. 93 (2017) 199–206.
[34] A. Suthaparan, K.A. Solhaug, A. Stensvand, H.R. Gislerød, Daily light integral and day light quality: potentials and pitfalls of nighttime UV treatments on cucumber powdery mildew, J. Photochem. Photobiol. B 175 (2017) 141–148.
[35] K.K. Fuller, J.J. Loros, J.C. Dunlap, Fungal photobiology: visible light as a signal for stress, space and time, Curr. Genet. 61 (2015) 275–288.
[36] R. Chasan, A ray of light on DNA repair, Cell 6 (1994) 159–161.
[37] E.J. Vonarx, H.L. Mitchell, R. Karthikeyan, I. Chatterjee, B.A. Kunz, DNA repair in higher plants, Mutat. Res. 400 (1998) 187–200.

Paper II

Genome-wide identification and characterization of photoreceptor genes in powdery mildews (*Pseudoidium neolycopersici*, *Podosphaera xanthii*, and *Podosphaera aphanis*)

Ranjana Pathak[1]; Arvind Y. M. Sundaram[2]; Aruppillai Suthaparan[1 #]

[1]Faculty of Biosciences, Norwegian University of Life Sciences, 1432 Ås, Norway.

[2]Norwegian Sequencing Centre, Department of Medical Genetics, Oslo University Hospital, 0407 Oslo, Norway.

#Corresponding author: Aruppillai Suthaparan; email: aruppillai.suthaparan@nmbu.no

Abstract

Powdery mildew (PM) is one among the top 10 important fungal diseases, widespread in crops with great economic importance. Effect of optical radiation on pathogen development of powdery mildews have been studied intensively. However, this group of phytopathogens get least attention in finding genes of photoreceptors and their biological functions if any, due to its obligate biotrophic interaction with their host. In this study, we have sequenced the genomes of *Pseudoidium neolycopersici*, *Podosphaera xanthii*, and *Podosphaera aphanis* that causes powdery mildew in economically important horticulture crops of tomato, cucumber, and strawberry respectively. The genomic DNA was isolated from 10- to 14-day-old sporulating colonies of powdery mildew, and subjected to whole genome sequencing using Illumina NextSeq 500 next generation sequencing platforms. The results showed an assembled genome sizes 66 Mb, 202 Mb, and 155 Mb with 2888, 6562, and 13025 protein coding transcripts in *Pseudoidium neolycopersici*, *Podosphaera xanthii*, and *Podosphaera aphanis* respectively. Core eukaryotic genes mapping approach (CEGMA) and benchmarking universal single copy orthologs (BUSCO) showed more than 96% of the eukaryotic orthologous groups (KOGs) aligned as complete gene copies to the scaffolds in all three fungal species. Genome annotation also revealed that the above-mentioned three powdery mildew possess putative genes similar to major class of photoreceptors genes; cryptochrome, photolyase, white collar (WC), phototropin, phytochrome, and UV resistance locus 8 (UVR8). Detailed studies targeting with each photoreceptor gene are necessary to understand its biological role, and possible exploitation of these roles to increase the effectiveness of optical based management of powdery mildews, in practice.

Keywords

Pseudoidium neolycopersici, *Podosphaera xanthii*, *Podosphaera aphanis*, powdery mildew, genome, photoreceptors

Introduction

Optical radiation, composed of ultraviolet, visible and infrared regions, is one of most important environmental factors play a key role in all domains of life on earth. Photosynthetic organisms use optical radiation as source of energy and environmental sensory cue (12, 23). On the other hand, non-photosynthetic organisms use optical radiation primarily as an environmental sensory cue to anticipate environmental changes about their surroundings (22). The molecular mechanisms used by biological systems to detect optical radiation are diverse, but generally involve a light-sensitive chromophore molecule bound to a protein (apoprotein) to form a light sensitive complex called photoreceptor (22). Upon the perception of light, emitted photons are absorbed by the chromophore, and undergoes a physicochemical and structural change that is sensed by interacting protein (19). This change in the photoreceptor stimulates a signal transduction cascade leading to alterations in gene expression and behaviour (18). At least 10 families of photoreceptor proteins including rhodopsins, cryptochromes, photoactive yellow proteins, phytochromes, phototropins, photoactivated adenylyl cyclases (PACs), and UV resistance locus 8 (UVR8) receptors have been reported in domains of life (22). In contrast to animal photoreceptors that are typically expressed in highly specialized organs, multiple photoreceptors are present throughout the plant to accurately detect, and respond to dynamic changes of optical environment such as its spectral composition, direction and duration (9).

The fungi represent the third group of macroscopic eukaryotes, and are sibling kingdom to animals (13). Fungi are neither photosynthetic nor capable of observing adjacent objects. However, among the estimated 1.5 million of fungal species, the majority of them respond to light (13). The fungal genome encode all photoreceptor genes, which are representative of major classes of photosensors known from other organisms (7, 40). All these photoreceptors, except white collar (WC) were recently discovered (13). Further, fungi use up to 11

photoreceptors and signaling cascades to control a large proportion of their genome, and therefore adapt to environmental changes (40).

However, there are exceptions like Saccharomycotina yeasts including *Saccharomyces* and *Candida*, as well as species of the dermatophytic fungi like *Malassezia*, *Trichophyton* and *Microsporum* did not respond to light (8). As many of these organisms are obligate pathogens and live in a close association with their host, it is possible that genes involved in environmental light signaling no longer provided a selective advantage to these pathogens and were lost (8).

Powdery mildew (PM) is a widespread disease with great economic importance, caused by diverse range of obligate biotrophic fungal pathogenic species all belongs to order Erysiphales, phylum of Ascomycota (10, 38). The effect of optical radiation on development of powdery mildews in wide range of crops have been reported (1, 14, 27, 31-33, 35). However, as an obligate biotrophs co-evolve with their host (38), this group of phytopathogens get least attention in finding genes of photoreceptors and their biological functions, if any. Presence and the expression of genes similar to phytochrome, cryptochrome, white collar, and photolyase was confirmed recently using next generation sequencing of grapevine powdery mildew, *Erysiphe necator* (34).

In this study, next generation high throughput sequencing of the whole genome was performed with *Pseudoidium neolycopersici*, *Podosphaera xanthii*, and *Podosphaera aphanis*, causal organisms of tomato, cucumber, and strawberry powdery mildew respectively with an objectives of identifying major classes of photoreceptor genes.

Materials and Methods

Preparation of fungal material for sequencing

Aseptic cultures of clonal isolates of *Pseudoidium neolycopersici*, *Podosphaera xanthii*, and *Podosphaera aphanis*, prepared from single conidium, were maintained in powdery mildew susceptible tomato (cv. Espero), cucumber (cv. Odeon) and strawberry (cv. korona) plants respectively as described in previous studies (35-37). Plants were maintained in a crystal-clear polypropylene round plastic box (OS140BOX/Green filter, Duchefa Biochemie B.V, The Netherlands) contained autoclaved nutrient agar medium (1.5–2.0 cm thick) prepared with complete nutrient solution containing 0.8 % agar (w/v). The boxes were placed in growth chamber at 20 ± 2°C with growth light cycle (GLC) of 16 h daily photoperiod provided with 120 cm fluorescent lamps with PPF of 75 ± 10 µmol/m^2/s (model PLD 36 W/840; Philips, The Netherlands).

Extraction and quality control of genomic DNA

Genomic DNA was extracted from 10- to 14-day-old sporulating clean colonies mentioned above. A cyclone separator tube adapter attached to the vacuum port was used to collect the ectophytic fungal tissue. Modified CTAB protocol was used to extract the DNA (25) and stored in 10 mM Tris buffer at -80°C. Quality and quantity of the gDNA were checked with gel electrophoresis (Bio-Rad, USA) and NanoDrop™ 2000 (Thermo Scientific, USA) respectively. A high quality of gDNA was used for sequencing.

Library preparation, sequencing and quality control

Library preparation, sequencing, and quality control were performed at the Norwegian Sequencing Centre, Oslo, Norway. Genomic DNA was fragmented using a Bioruptor® NGS (Diogenode, USA). Paired end libraries (150 bp) were prepared using TruSeq Nano library preparation kit (100 ng input, 10 cycles PCR) (Illumina, USA) following standard protocol. Three individual libraries were constructed for *P. neolycopersici*, *P. xanthii*, and *P.* aphanis. Individually indexed *P. aphanis* and *P. xanthii* genomic DNA libraries were pooled together

and sequenced in a NextSeq 500 (Illumina, USA) using mid-output reagents while *P. neolycopersici* was sequenced in a separate NextSeq 500 mid-output run. 150 bp paired end sequencing was employed across all the NextSeq runs.

Raw sequence data was quality-trimmed and filtered using Trimmomatic (v0.33) to remove adapters, and unqualified low quality reads and duplicates reads were filtered out, and further processed with BBMap (v34) aligner to remove Illumina spike-in PhiX (3, 5). Cleaned data from *P. aphanis*, *P. xanthii* and *P. neolycopersici* were aligned against strawberry (ftp://ftp.ncbi.nlm.nih.gov/genomes/all/GCF_000184155.1_FraVesHawaii_1.0), cucumber (ftp://ftp.ncbi.nlm.nih.gov/genomes/all/GCF_000004075.2_ASM407v2) and tomato (ftp://ftp.sgn.cornell.edu/genomes/Solanum_lycopersicum/wgs/assembly/build_2.50) genomes respectively, using BBMap to remove plant DNA contamination, and reads that did not align were used to generate PM genome assemblies.

Genome assembly and annotation

A high-quality reads were used for de novo assembly. Three individual genomes were assembled separately using assembler MaSuRCA (v3.1.3) (42) using default parameters. A core eukaryotic gene mapping approach (CEGMA v2.5) was performed to evaluate the completeness of the assemblies by analyzing the 246 core eukaryotic genes (21). The quality check of assembled genomes (genome completeness) was further assessed by benchmarking Universal Single-Copy Orthologs (BUSCO) (28).

Gene prediction and functional annotation

Gene prediction was performed with the automated pipeline MAKER2 (v2.31.9) (11) utilizing two-pass approach in order to combine data from three ab initio predictors; i) SNAP (v2006-07-28), ii) GeneMark-ES suite (v4.30), and iii) AUGUSTUS (v3.0.1) (4, 15, 30). In the first iteration of MAKER2, we combine data of all known mRNA and proteins, and the

ab initio predictions from SNAP and GeneMark-ES suite. The generated output was then used in evidence-based predictor, AUGUSTUS. The resulting gene sets were combined to achieve most comprehensive set of non-redundant reference genes.

Publicly available transcriptome assembly (GenBank: GEUO00000000.1) consisting of 37,241 transcript sequences were used as EST evidence for gene prediction in *P. xanthii* while the same was used as alternate EST evidence for *P. neolycopersici* and *P aphanis*. Fungi protein sequences classified under 'taxon identifier: 4751' in UniProt, reviewed Swiss-Prot (32,291 sequences) was used as protein homology evidence during gene prediction across all three PM genome assemblies.

Functional annotation of predicted genes was performed mainly by their sequence homology to known annotated genes, and proteins available within various databases using NCBI BLAST as the main tool. Protein coding genes predicted by MAKER2 pipeline with Annotation Edit Distance (AED) <1 were further used for functional annotation using NCBI BLAST (v2.2.29+) against Ascomycete nr database. Total 7,555,988 protein sequences were extracted from the global NCBI nr database using 'txid4890[Organism]' as the search term.

Photoreceptor gene family analysis

mRNA sequence data published in NCBI database similar to cryptochrome, photolyase, white collar (WC), phototropin, phytochrome, and UVR8 were retrieved, and blasted against the assembled genomes of *P. neolycopersici*, *P. xanthii*, and *P. aphanis*. Scaffolds/contigs with unique matches (≥ 75% coverage) were extracted by using blastx (NCBI) for comparison and phylogenetic analysis. All six reading frames were translated on the query (coding nucleotide sequence) and used to search the database for protein homology.

Results

Genome sequencing assembly/genome features

To sequence the haploid genomes of the *Pseudoidium neolycopersici*, *Podosphaera xanthii*, *Podosphaera aphanis* isolates, Illumina shotgun sequencing approach was used to generate 150 bp pair end reads with NextSeq 500 sequencers. After quality trimming and filtering, sequence reads of 79% from *P. neolycopersici*, 86% from *P. xanthii*, and 86% from *P. aphanis* were assembled into scaffolds with an assembled genome sizes of approximately 66, 202, and 155 Mb respectively. Assembly of the processed sequenced reads generated the draft genomes of *Pseudoidium neolycopersici*, *Podosphaera xanthii*, and *Podosphaera aphanis.* The assembly statistics, and genome coverage are presented in Table 1 and Fig. 1 respectively. The longest scaffold sizes are 97.6 kb, 997.7 kb, and 109.2 kb for *P. neolycopersici*, *P. xanthii*, and *P. aphanis* respectively.

To assess the quality and completeness of the assembled gene space, we applied CEGMA approach (21) to map a set of 246 core eukaryotic orthologous groups (KOGs), which are conserved across higher eukaryotes, and showed > 96% of the KOGs aligned as complete gene copies to the scaffolds in all three fungal species, and this was increased to > 99 %, when considering at least a partial match (Table 1). CEGMA results were further evaluated with BUSCO pipeline and similar results were observed (28) (Table 2). These results indicate that the sequencing approach used in this study generated relatively contiguous assemblies of the genomes for all three PM species.

Gene prediction/annotation

The simple genetic structures of fungi facilitates accurate gene prediction. Gene modeling using homology search predicted 2888 protein coding transcripts for *Pseudoidium*

neolycopersici and 6562 protein coding transcripts for *Podosphaera xanthii*, and 13025 protein coding transcripts for *Podosphaera aphanis* (Table 1). The average gene length was 1505 bp, 1316 bp, and 984 bp in *P. neolycopersici*, *P. xanthii*, and *P. aphanis* respectively (Table 1). The average gene length in *P. neolycopersici*, and *P. xanthii* were slightly higher than the average gene length in *P. aphanis.* Further, the functional annotation of 2888, 6562, and 13025 predicted non-redundant protein coding transcripts for *Pseudoidium neolycopersici*, *Podosphaera xanthii*, and *Podosphaera aphanis* respectively, were subjected to similarity analysis in blastx (NCBI).

Photoreceptor genes

We mapped all three assembled powdery mildew genomes to study the presence of photoreceptor genes. A total of 15 genes were assigned to putative photoreceptor gene families represented in Table 3. The cryptochrome, photolyase, white collar (WC), phototropin, phytochrome, and UV resistance locus 8 (UVR8) were found in genomes of *P. neolycopersici*, *P. xanthii*, and *P. aphanis*.

Discussion

In the present study, the estimated genome sizes for tomato PM (~249 Mb), and cucumber PM (~281 Mb) are remarkably larger than the genome size (~180 Mb) estimated for wheat powdery mildew, *Blumeria graminis* f. sp. *tritici* (39), and other ascomycete fungi whose genome size ranges from 30 to 60 Mb (24). Previous studies demonstrated that powdery mildew genomes are estimated in size ranges from 120 to 222 Mb (39).After genome assembly, tomato powdery mildew has relatively more compact genome compared to cucumber and strawberry PM genomes (Table 1). It has been described earlier that the transposable elements contribute to genome expansion and evolution, and played essential roles in wide range of biological events (development, differentiation, regulation) (41).

Sequencing platforms and assembly pipelines used may influence this variation, in addition to variations in transposable elements.

In the present study, the number of protein coding genes is remarkably variable among three PM fungi. Our annotation process recovered 13025, and 6562 protein coding genes in *P. aphanis* and *P.* xanthii respectively while only 2888 protein coding genes were annotated in *P. neolycopersici* (Table 1). It is known that fungi causing PMs generally possess fewer protein-coding genes (6,000 to 7,000) than other fungi due to its obligate biotrophic lifestyle. It is 6525 to 7239 genes in barley and wheat PM, which is approximately half than the number of genes present in closely related ascomycetes such as *Botrytis cinerea* (11707 genes) (39). The comparatively low gene density, and the inability of a pathogen to grow in vitro suggest that the mildew genomes may lack genes typically present in autotrophic ascomycetes (29). These genomic hallmarks; genome size inflation, extensive gene reshuffling correlated with expansion in (retro-)transposon number, and gene losses tends to be associated with the obligate biotrophy in the powdery mildews (29). Additionally, this genome-specific gene loss may contribute to host-specialization of PM fungi and/or reflect the impact of host metabolisms on respective PM pathogens (39).

Based on the functional annotation of *P. neolycopersici*, *P. xanthii*, and *P. aphanis*; cryptochrome, photolyase, white collar (WC), phototropin, phytochrome, and UVR8 were assigned to photoreceptor proteins (Table 3). The photoreceptors identified in this study, have been functionally characterized in several other organisms including fungi (7, 12, 20, 40). The presence of these photoreceptors in PMs genomes indicated that like other fungi, PM may be capable of sensing light over a broad spectrum of light, ranges from ultraviolet to far-red light. Photoreceptors have evolved into a variety of light-sensing proteins, and are highly conserved across the entire fungal kingdom. All fungi, which are photoresponsive are sensitive to light at the blue to near-UV-A (~ 400–495 nm) range (8, 26). The blue light responses are best

studied in model fungus, *Neurospora crassa* (26). The first fungal blue light LOV domain containing photoreceptor protein was isolated and characterized, was white collar-1 (WC-1), WC-1 operates with WC-2 and form white collar complex (WCC). This WC complex regulates fungal photoresponses (e.g., induction of sporulation, circadian clock control), and also acts as a transcription factor (6, 17). Another blue light photoreceptors, cryptochrome and photolyase together form a cryptochrome/photolyase family. These are flavin binding with an additional non-covalently bound chromophore (40). Photolyases have the ability to repair DNA damage caused by short wavelength UV by using UV-A/blue light as an energy source. The first fungal photolyase (PHR1) was characterized in filamentous fungus, *Trichoderma atroviride*. It repairs DNA damage, and is rapidly upregulated by blue light. In *T. atroviride*, PHR1 regulates its own photoinduction, which is the first evidence for a regulatory role of photolyase, a role usually associated with cryptochromes (2). Contrarily, the cryptochromes do not have DNA repair activity, but regulate entrainment of the circadian clock in plants and animals by using light (16). Their function in fungi is still unclear (7). The red light reception carried out via phytochrome photoreceptors, a phytochrome FphA in *Aspergillus nidulans* regulate development and accumulation of secondary metabolites (7).

The most reliable way to demonstrate a photosensory function of a protein is a multistep process. In the first step, a light-response is observed, and second is to measure the efficiency of that response over a range of wavelengths to generate an action spectrum of the response either crudely into broad color ranges (e.g., blue, green, or red), or more precisely over narrow wavelengths. In the third step, the photo sensing gene and protein are identified (e.g., from cloning, by complementation assay, bioinformatics analysis of genomes, mutant screening, protein analysis). Fourth one, the light response must be abolished by photosensor gene mutation. Fifth, the photosensory protein is purified and characterized to determine that it has the same absorption spectrum as the action spectrum in step 2, as well as enabling the

identification of the bound chromophore. Moreover, all known photosensory proteins function by interacting with a photosensitive molecule (e.g., flavins, tetrapyrroles, retinals). Sixth, the photosensor function must explain the phenotypes observed, in that it should regulate genes or proteins specifically required for the responses. Clearly, this is a multidisciplinary process and often it is partially accomplished (13).

Furthermore, research is required to investigate the functional roles of each photoreceptor in powdery mildews identified in the present study. Additionally, gene expression under different light conditions would be advantageous to understand functional role of light dependent or light-independent genes. These PM genomic resources can be a foundational information for the improvement of genetic and molecular tools to understand the molecular basis of how powdery mildew respond and behave to light, and can also be used as a reference for future studies in the field of genomics and transcriptomics.

Data availability

Data will be available online (NCBI) once the modified version of this manuscript accepted for publication.

Acknowledgements

The Norwegian Research Council (projects 225080 and 1207051033) financed this research. We thank to Karin Svinnset for her contribution in maintenance of powdery mildew isolates, and technicians at the Centre for Controlled Environment Plant Research (SKP), NMBU for their excellent support and assistance. Library preparation and sequencing was carried out by Norwegian High Throughput Sequencing Centre, Department of Medical Genetics, Oslo University Hospital, 0450 Oslo, Norway.

Author Contributions

Aruppillai Suthaparan- Conceived, designed and performed the experiments, and wrote the manuscript. Ranjana Pathak- Performed the experiments and wrote the manuscript. Arvind Y. M. Sundaram-Involved in design, performed bioinformatics and manuscript revision.

	DNA		
	Pseudoidium neolycopersici	***Podosphaera xanthii***	***Podosphaera aphanis***
# of raw reads (150 PE)	167,590,324	76,415,989	89,915,519
# of cleaned reads	150,804,907	70,598,348	82,395,014
# of reads after removing plant DNA	132,346,281	65,731,919	77,401,212
Estimated genome size	249,147,646	281,345,667	159,864,358
Assembled genome size	66,294,405	202,257,412	155,168,007
# of scaffolds	20,061	86,938	63,866
Scaffold N50	9,966	11,293	7,903
Longest scaffold (bp)	97,677	997,747	109,278
# of contigs	20,727	88,175	64,370
Contig N50	9,088	10,945	7,692
Longest contig (bp)	73,971	566,457	109,278
GC content (%)	38.97	51.72	43.27
CEGMA complete (246 COGs) (%)	98.37	97.15	96.34
CEGMA partial (246 COGs) (%)	100	99.59	99.19
# of protein coding transcripts	18,602	8,589	27,475
Average gene length (bp)	793	1,091	730
# of protein coding transcripts (AED < 1.0)	2,888	6,562	13,025
Average gene length (bp)	1,505	1,316	984

CEGMA – Core eukaryotic genes mapping approach

KOG – Eukaryotic orthologous groups

AED – Annotation Edit Distance

Table 1. Summary statistics of draft genome assemblies for *Pseudoidium neolycopersici*, *Podosphaera xanthii*, and *Podosphaera aphanis*

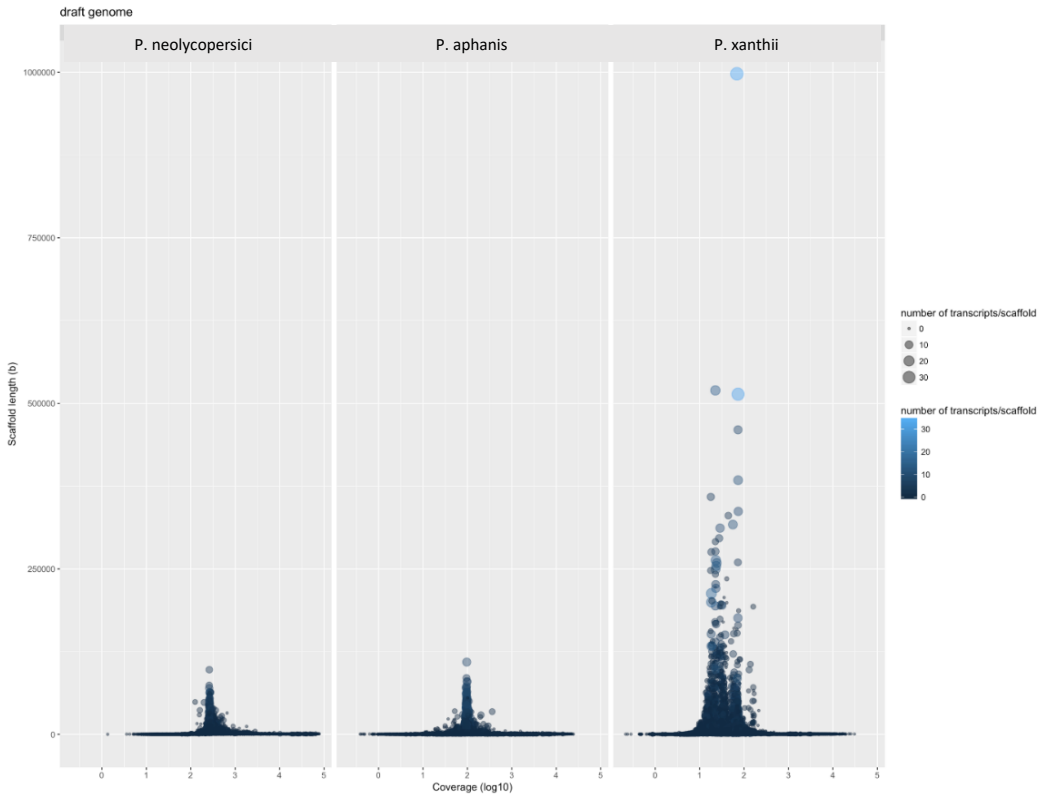

Fig. 1. Genome coverage represents the relationship between sequenced read coverage (log10) and the scaffold length across three species- *Pseudoidium neolycopersici*, *Podosphaera aphanis*, and *Podosphaera xanthii*. The size and the color (refer legend) shows the number of transcripts found in each assembled scaffold.

	Pseudoidium neolycopersici		*Podosphaera xanthii*		*Podosphaera aphanis*	
Fungi odb9						
Complete BUSCOs (C)	280	96.60%	281	96.90%	286	98.70%
Complete and single-copy BUSCOs (S)	279	96.20%	280	96.60%	267	92.10%
Complete and duplicated BUSCOs (D)	1	0.30%	1	0.30%	19	6.60%
Fragmented BUSCOs (F)	3	1.00%	5	1.70%	1	0.30%
Missing BUSCOs (M)	7	2.40%	4	1.40%	3	1.00%
Total BUSCO groups searched	290	100.00%	290	100.00%	290	100.00%
Eukaryote odb9						
Complete BUSCOs (C)	297	98.00%	294	97.00%	295	97.40%
Complete and single-copy BUSCOs (S)	297	98.00%	293	96.70%	269	88.80%
Complete and duplicated BUSCOs (D)	0	0.00%	1	0.30%	26	8.60%
Fragmented BUSCOs (F)	2	0.70%	4	1.30%	1	0.30%
Missing BUSCOs (M)	4	1.30%	5	1.70%	7	2.30%
Total BUSCO groups searched	303	100.00%	303	100.00%	303	100.00%

Table 2. Assessment of *Pseudoidium neolycopersici*, *Podosphaera xanthii*, and *Podosphaera aphanis* draft genome assemblies, and gene sets in BUSCO (Benchmarking Universal Single-Copy Orthologs).

Genes	# of seq collected from NCBI	# of seq used for Blast	>= 75% coverage	Total number of genes
CRY-Fungi	62	60	3	3
CRY-Plant	5	5	3	
PHR-Fungi	19	19	3	3
PHR-Plant	11	5	1	
Phototropin-Fungi	32	32	6	6
Phototropin-Plant	96	96	5	
PHY-Fungi	21	21	1	1
PHY-Plant	125	125	0	
UVR8-Plant	349	298	2	2

Table 3. Total number of gene sequences collected from NCBI belongs to different classes of photoreceptors of plants and fungi, number of sequences used for blast against powdery mildew genomes, and total number of photoreceptor genes predicted from powdery mildew genomes. CRY- cryptochrome, PHR- photolyase, PHOT- phototropin, PHY- phytochrome, and UVR8- UV resistance locus-8.

References

1. Amsalem, L., Freeman, S., Rav-David, D., Nitzani, Y., Sztejnberg, A., Pertot, I., Elad, Y. 2006. Effect of climatic factors on powdery mildew caused by *Sphaerotheca macularis* f.sp. *fragariae* on strawberry. Eur. J. Plant Pathol. 114:283-292.

2. Berrocal-Tito, G. M., Esquivel-Naranjo, E. U., Horwitz, B. A., Herrera-Estrella, A. 2007. *Trichoderma atroviride* PHR1, a fungal photolyase responsible for DNA repair, autoregulates its own photoinduction. Eukaryot. Cell 6(9):1682.

3. Bolger, A. M., Lohse, M., Usadel, B. 2014. Trimmomatic: a flexible trimmer for Illumina sequence data. Bioinformatics 30(15):2114-2120.

4. Borodovsky, M., Lomsadze, A. 2011. Eukaryotic gene prediction using GeneMark.hmm-E and GeneMark-ES. Curr. Protoc. Bioinformatics Chapter 4:Unit-4.6.10.

5. Bushnell, B. 2014. BBMap: A Fast, Accurate, Splice-Aware Aligner. Conference. Lawrence Berkeley National Lab, Berkeley, CA (United States).

6. Corrochano, L. M. 2011. Fungal photobiology: a synopsis. IMA fungus 2(1):25-28.

7. Corrochano, L. M. 2019. Light in the fungal world: from photoreception to gene transcription and beyond. Annu. Rev. Genet. 53(1):149-170.

8. Fuller, K. K., Loros, J. J., Dunlap, J. C. 2015. Fungal photobiology: visible light as a signal for stress, space and time. Curr. Genet. 61(3):275-288.

9. Galvao, V. C., Fankhauser, C. 2015. Sensing the light environment in plants: photoreceptors and early signaling steps. Curr. Opin. Neurobiol. 34:46-53.

10. Glawe, D. A. 2008. The powdery mildews: A review of the world's most familiar (yet poorly known) plant pathogens. Annu. Rev. Phytopathol. 46:27-51.

11. Holt, C., Yandell, M. 2011. MAKER2: an annotation pipeline and genome-database management tool for second-generation genome projects. BMC Bioinformatics 12(1):491.

12. Huché-Thélier, L., Crespel, L., Gourrierec, J. L., Morel, P., Sakr, S., Leduc, N. 2016. Light signaling and plant responses to blue and UV radiations—Perspectives for applications in horticulture. Environ. Exp. Bot. 121:22-38.

13. Idnurm, A., Verma, S., Corrochano, L. M. 2010. A glimpse into the basis of vision in the kingdom Mycota. Fungal Genet. Biol. 47(11):881-892.

14. Jacob, D., David, D. R., Sztjenberg, A., Elad, Y. 2008. Conditions for development of powdery mildew of tomato caused by *Oidium neolycopersici*. Phytopathol. 98:270-281.

15. Korf, I. 2004. Gene finding in novel genomes. BMC Bioinformatics 5(1):59.

16. Lin, C., Todo, T. 2005. The cryptochromes. Genome biology 6(5):220-220.

17. Liu, Y., He, Q., Cheng, P. 2003. Photoreception in *Neurospora*: a tale of two White Collar proteins. Cellular and Molecular Life Sciences CMLS 60(10):2131-2138.

18. Lorrain, S., Genoud, T., Fankhauser, C. 2006. Let there be light in the nucleus. Current Opinion in Plant Biology 9:509-514.

19. Losi, A. 2007. Flavin-based blue-light photosensors: A photobiophysics update. Photochemistry and Photobiology 83:1283-1300.

20. Paik, I., Huq, E. 2019. Plant photoreceptors: Multi-functional sensory proteins and their signaling networks. Seminars in Cell & Developmental Biology 92:114-121.

21. Parra, G., Bradnam, K., Korf, I. 2007. CEGMA: a pipeline to accurately annotate core genes in eukaryotic genomes. Bioinformatics 23(9):1061-1067.

22. Porter, M. L. 2016. Beyond the eye: Molecular evolution of extraocular photoreception. Integr. Comp. Biol. 56:842-852.

23. Purschwitz, J., Müller, S., Kastner, C., Fischer, R. 2006. Seeing the rainbow: light sensing in fungi. Curr. Opin. Microbiol. 9(6):566-571.

24. Raffaele, S., Kamoun, S. 2012. Genome evolution in filamentous plant pathogens: why bigger can be better. Nat. Rev. Microbiol. 10(6):417-430.

25. Robinson, H. L., Ridout, C. J., Sierotzki, H., Gisi, U., Brown, J. K. M. 2002. Isogamous, hermaphroditic inheritance of mitochondrion-encoded resistance to Qo inhibitor fungicides in *Blumeria graminis* f. sp. *tritici*. Fungal Genet. Biol. 36(2):98-106.

26. Rodriguez-Romero, J., Hedtke, M., Kastner, C., Müller, S., Fischer, R. 2010. Fungi, hidden in soil or up in the air: light makes a difference. Annu. Rev. Microbiol. 64(1):585-610.

27. Schuerger, A. C., Brown, C. S. 1997. Spectral quality affects disease development of three pathogens on hydroponically grown plants. HortScience 32:96-100.

28. Simao, F. A., Waterhouse, R. M., Loannidis, P., Kriventseva, E. V., Zdobnov, E. M. 2015. BUSCO: assessing genome assembly and annotation completeness with single-copy orthologs. Bioinformatics 31:3210-3212.

29. Spanu, P. D., Abbott, J. C., Amselem, J., Burgis, T. A., Soanes, D. M., Stüber, K., Ver Loren van Themaat, E., Brown, J. K., Butcher, S. A., Gurr, S. J., et al. 2010. Genome expansion and gene loss in powdery mildew fungi reveal tradeoffs in extreme parasitism. Science 330(6010):1543-6.

30. Stanke, M., Waack, S. 2003. Gene prediction with a hidden Markov model and a new intron submodel. Bioinformatics 19 (suppl_2): ii215-ii225.

31. Suthaparan, A., Stensvand, A., Torre, S., Herrero, M., L., Pettersen, R. I., Gadoury, D. M., Gislerød, H. R. 2010. Continuous lighting reduces conidial production and germinability in the rose powdery mildew pathosystem. Plant Dis. 94:339-344.

32. Suthaparan, A., Torre, S., Stensvand, A., Herrero, M. L., Pettersen, R. I., Gadoury, D. M., Gislerød, H. R. 2010. Specific light emitting diodes can suppress sporulation of *Podosphaera pannosa* on greenhouse roses. Plant Dis. 94:1105-1110.

33. Suthaparan, A., Stensvand, A., Solhaug, K. A., Torre, S., Mortensen, L. M., Gadoury, D. M., Seem, R. C., Gislerød, H. R. 2012. Suppression of powdery mildew (*Podosphaera pannosa*) in greenhouse roses by brief exposure to supplemental UV-B radiation. Plant Dis. 96:1653-1660.

34. Suthaparan, A., Stensvand, A., Solhaug, K. A., Torre, S., Telfer, K. H., Ruud, A. K., Davidson, L. C., Mortensen, L. M., Gadoury, D. M., Seem, R. C., et al. 2012. Suppression of cucumber powdery mildew by UV-B is affected by background light quality (abstract). Phytopathol. 102(S4):116.

35. Suthaparan, A., Stensvand, A., Solhaug, K. A., Torre, S., Telfer, K. H., Ruud, A. K., Mortensen, L. M., Gadoury, D. M., Seem, R. C., Gislerød, H. R. 2014. Suppression of cucumber powdery mildew by supplemental UV-B radiation in greenhouses can be augmented or reduced by background radiation quality. Plant Dis. 98:1349-1357.

36. Suthaparan, A., Solhaug, K. A., Bjugstad, N., Gislerod, H. R., Gadoury, D. M., Stensvand, A. 2016. Suppression of powdery mildews by UV-B: Application frequency and timing, dose, reflectance, and automation. Plant Dis. 100:1643-1650.

37. Suthaparan, A., Solhaug, K. A., Stensvand, A., Gislerød, H. R. 2016. Determination of UV action spectra affecting the infection process of *Oidium neolycopersici*, the cause of tomato powdery mildew. J. Photoch. Photobio. B. 156:41-49.

38. Takamatsu, S. 2013. Origin and evolution of the powdery mildews (Ascomycota, Erysiphales). Mycoscience 54:75-86.

39. Wu, Y., Ma, X., Pan, Z., Kale, S. D., Song, Y., King, H., Zhang, Q., Presley, C., Deng, X., Wei, C.-I., et al. 2018. Comparative genome analyses reveal sequence features reflecting distinct modes of host-adaptation between dicot and monocot powdery mildew. BMC Genomics 19(1):705.

40. Yu, Z., Fischer, R. 2019. Light sensing and responses in fungi. Nature Reviews Microbiol. 17(1):25-36.

41. Zhang, C., Deng, W., Yan, W., Li, T. 2018. Whole genome sequence of an edible and potential medicinal fungus, *Cordyceps guangdongensis*. G3: Genes,Genomes,Genetics 8(6):1863.

42. Zimin, A. V., Marc¸ais, G., Puiu, D., Roberts, M., Salzberg, S. L., Yorke, J. A. 2013. The MaSuRCA genome assembler. Bioinformatics 29:2669-2677.

Paper III

frontiers in Microbiology

ORIGINAL RESEARCH
published: 29 May 2020
doi: 10.3389/fmicb.2020.01091

Functional Characterization of *Pseudoidium neolycopersici* Photolyase Reveals Mechanisms Behind the Efficacy of Nighttime UV on Powdery Mildew Suppression

*Ranjana Pathak[1], Åshild Ergon[1], Arne Stensvand[1,2], Hans Ragnar Gislerød[1], Knut Asbjørn Solhaug[3], Lance Cadle-Davidson[4] and Aruppillai Suthaparan[1]**

[1] Department of Plant Sciences, Faculty of Biosciences, Norwegian University of Life Sciences, Ås, Norway, [2] Division of Biotechnology and Plant Health, Norwegian Institute of Bioeconomy Research, Ås, Norway, [3] Faculty of Environmental Sciences and Natural Resource Management, Norwegian University of Life Sciences, Ås, Norway, [4] Grape Genetics Research Unit, Agricultural Research Service, United States Department of Agriculture, Geneva, NY, United States

OPEN ACCESS

Edited by:
Levente Kiss,
University of Southern Queensland, Australia

Reviewed by:
Laurence Veronique Bindschedler, Royal Holloway, University of London, United Kingdom
Mirna Barsoum, RWTH Aachen University, Germany
Markus Gorfer, Austrian Institute of Technology (AIT), Austria

***Correspondence:**
Aruppillai Suthaparan
aruppillai.suthaparan@nmbu.no

Specialty section:
This article was submitted to Fungi and Their Interactions, a section of the journal Frontiers in Microbiology

Received: 13 October 2019
Accepted: 30 April 2020
Published: 29 May 2020

Citation:
Pathak R, Ergon Å, Stensvand A, Gislerød HR, Solhaug KA, Cadle-Davidson L and Suthaparan A (2020) Functional Characterization of Pseudoidium neolycopersici Photolyase Reveals Mechanisms Behind the Efficacy of Nighttime UV on Powdery Mildew Suppression. Front. Microbiol. 11:1091. doi: 10.3389/fmicb.2020.01091

Powdery mildews can be controlled by brief exposure to ultraviolet (UV) radiation with devastating effect on their developmental stages including conidia germination. The treatment effect can be impaired by subsequent exposure to UV-A/blue light. UV-A/blue light-activated photolyase may be responsible for this and therefore we tested the function of three cryptochrome/photolyase family (CPF)-like genes (OINE01015670_T110144, OINE01000912_T103440, and OINE01005061_T102555) identified in the obligate biotrophic fungus *Pseudoidium neolycopersici*, the cause of tomato powdery mildew. A photolyase-deficient mutant of *Escherichia coli* transformed with coding sequence of OINE01000912_T103440 and exposed to brief (UV)-C treatment (peak emission at 254 nm) showed photoreactivation and cell survival when exposed to subsequent blue light, indicating complementation of photolyase activity. In contrast, the same photolyase-deficient *E. coli* transformed with the coding sequences of other two CPF-like genes did not survive this treatment, even though their expression were confirmed at protein level. This confirmed that OINE01000912_T103440 is a gene encoding photolyase, here named *PnPHR1*, with functionality similar to the native photolyase in *E. coli,* and classified as a class I cyclobutane pyrimidine dimer (CPD) photolyase. Modeling of the 634-amino acid sequence of *PnPHR1* suggested that it is capable of binding flavin adenine dinucleotide (FAD) and methenyltetrahydrofolate (MTHF). However, spectroscopic data of the protein produced in an *E. coli* expression system could only reveal the presence of a reduced form of FAD, i.e., $FADH^{-}$ as an intrinsic chromophore. Within the tested wavelength range of 365–525 nm, the survival of photolyase-deficient mutant *E. coli* transformed with *PnPHR1* showed a broad action spectrum from 365 to 454 nm. This was very similar to the previously characterized action spectrum for survival of *P. neolycopersici* conidia that had been treated with UV-C. Quantitative RT-PCR revealed that the expression

of *PnPHR1* in *P. neolycopersici* conidia was induced by UV-C, and peak expression occurred 4 h after brief UV-C treatment. The expression of *PnPHR1* was repressed when incubated in red light after the UV-C treatment, but not when incubated in UV-A/blue light. The results may explain why the disease-reducing effect of short wavelength UV is impaired by exposure to UV-A and blue light.

Keywords: absorption spectra, action spectra, cryptochrome, CPD photolyase, DNA damage

INTRODUCTION

Powdery mildews are caused by obligate biotrophic fungal pathogens in the order Erysiphales. Nearly 10,000 plant species can be infected by these fungi (Glawe, 2008; Braun and Cook, 2012), and the disease can be devastating if not properly managed. Tomato powdery mildew, caused by *Pseudoidium neolycopersici* (formerly known as *Oidium neolycopersici*), is of great economic importance worldwide in greenhouse and field-grown tomatoes (Jankovics et al., 2008; Li et al., 2012). The pathogen typically thrives in protected cultivation environments where there is poor ventilation, high humidity and moderate temperatures, and it is difficult to eradicate once established. Several control measures, including fungicide treatments and breeding programs to develop resistant cultivars, are being employed for better disease management (Li et al., 2012).

Extensive research has examined the potential of different spectral qualities, irradiance levels and duration of irradiance in control of powdery mildews for a wide range of crops (Suthaparan et al., 2010, 2012a, 2016a; Van Delm et al., 2014; Janisiewicz et al., 2016). Short wavelength (<290 nm) ultraviolet radiation (UV) and red light have shown great potential against powdery mildews (Suthaparan et al., 2012a, 2014, 2016b, 2018). However, the efficacy of UV against powdery mildew varies depending on the spectral quality of the subsequent growth light. Brief exposure to UV during dark or in combination with red light showed higher disease control efficacy than exposure to UV in the presence of light with wavelengths shorter than 500 nm. Furthermore, using growth lights with an increased proportion of wavelengths below 500 nm immediately following the UV treatment decreased the efficacy of the nighttime UV treatment against powdery mildew (Suthaparan et al., 2017, 2018). This confirmed that recovery of germination in *P. neolycopersici* conidia treated with brief UV is dependent on the wavelength, and indicates the presence of possible light-mediated repair mechanisms of UV-induced damage in the powdery mildews (Suthaparan et al., 2018).

Ultraviolet has deleterious effects on all life forms, ranging from bacteria to higher plants, animals, and humans. DNA is the cellular component which is most significantly affected by UV (Weber, 2005). The predominant UV-induced DNA damage is the formation of pyrimidine dimers (Sancar, 1994). UV induces two major types of lesions in DNA, cyclobutane pyrimidine dimers (CPDs) and (6–4) photoproducts, which constitute 80–90% and 10–20% of the damage, respectively (Sinha and Häder, 2002; Sancar, 2008). If the damage is not repaired, it can result in an arrested cell cycle due to blocking of replication and transcription (Sancar, 1994). Different DNA damage repair mechanisms include nucleotide excision repair, recombination repair, mutagenic repair, and photolyase-mediated repair. Out of these, photolyase-mediated repair (also known as photoreactivation, or photorepair) is the simplest and most rapid mechanism because of the involvement of a single enzyme (Sinha and Häder, 2002). It is also the only repair mechanism regulated by light (Essen and Klar, 2006). Photolyases absorb energy in the near UV to blue regions (300–500 nm) and use this energy to catalyze the repair of CPDs and (6–4) photoproducts (Sinha and Häder, 2002; Thompson and Sancar, 2002). All photolyases contain a common catalytic cofactor, flavin adenine dinucleotide (FAD), and an additional second cofactor, which is methenyltetrahydrofolate (MTHF) in the majority of species, and 8-hydroxy-7, 8-didemethyl-5-deazariboflavin (8-HDF) in a limited number of species. Depending on their substrate binding specificity, photolyases have been categorized into CPD photolyases and (6–4) photolyases (Weber, 2005; Essen and Klar, 2006).

Photolyases have been structurally and functionally characterized in many life forms, including filamentous fungi and plants (Sancar et al., 1987b; Yajima et al., 1991; Waterworth et al., 2002). However, there are no reports on the functional characteristics of photolyases in obligate biotrophic fungi. Using next generation transcriptome sequencing of *Erysiphe necator*, the cause of grape powdery mildew, the presence and expression of putatively photo-responsive genes similar to phytochromes, cryptochromes, white collar, and photolyases have been identified (Suthaparan et al., 2012b). Preliminary analysis of whole genome and transcriptome sequencing of *P. neolycopersici* as well as *Podosphaera xanthii* and *Podosphaera aphanis*, the causal agents of powdery mildew in cucumber and strawberry, respectively, confirmed the presence of genes similar to all major classes of photoreceptors, including photolyase, cryptochrome, white collar, phototropin, phytochrome, and UVR8 (Pathak et al., 2017). Three genes similar to the blue light-absorbing cryptochrome/photolyase family (CPF)-like genes were identified in each of these three species, but the function of the gene products has not been characterized (Pathak et al., 2017). Despite a high degree of sequence homology, photolyases and cryptochromes perform two distinct functions, photolyase repair DNA damage caused by UV while cryptochromes play a key role in circadian entrainment in animals and regulate

Abbreviations: CPD, cyclobutane pyrimidine dimer; CPF, cryptochrome/photolyase family; 8-HDF, 8-hydroxy-7, 8-didemethyl-5-deazariboflavin; FAD, flavin adenine dinucleotide; IPTG, isopropyl-1-thio-D-galactopyranoside; LB, Lysogeny Broth; MTHF, methenyltetrahydrofolate; PHR, photoreactivation; UV, ultraviolet.

growth and development in plants (Thompson and Sancar, 2002; Zhang et al., 2017).

The objectives of this study were to identify the functional photolyase gene among three putative CPF-like genes in *P. neolycopersici*, to characterize its action and absorption spectra, and to test for gene induction in response to UV.

MATERIALS AND METHODS

Phylogenetic Analysis of CPF-Like Genes

Amino acid sequences of 137 CPF-like genes (**Supplementary Data S2**) were retrieved from National Centre for Biotechnology Information[1]. These were, together with predicted amino acid sequences of the three CPF-like genes from *P. neolycopersici* (OINE01015670_T110144, OINE01000912_T103440, and OINE01005061_T102555) subjected to phylogenetic analysis using the MEGAX software package (Kumar et al., 2018). Multiple sequence alignment was done by ClustalW with default parameters and an unrooted tree of sequence data was constructed by implementing neighbor-joining algorithm with 1000 bootstrap replicates.

Cloning of Putative CPF-Like Genes

The full-length coding regions of three putative CPF-like genes (OINE01015670_T110144, OINE01000912_T103440, and OINE01005061_T102555) identified in the *P. neolycopersici* genome (Suthaparan A. et al., unpublished) were PCR-amplified from cDNA (**Supplementary Table S1**), cloned into a pCR™ 2.1-TOPO® TA cloning vector (Thermo Fisher Scientific, United States) and sequenced. The sequences (NCBI GeneBank accession numbers MT277362, MT277363, and MT277364) were adapted to the codon usage in *E. coli* using OptimumGene™ and synthesized (GenScript, United States). The synthetic genes PN5670, PN0912, and PN5061, with *Sph*I and *Xma*I restriction sites, were excised and ligated into the SphI/XmaI sites of the pQE-30Xa (AmpR) expression vector with 6× His-tag at the N-terminus (Qiagen, Germany). The resulting three constructs were named pQE-30Xa_PN5670, pQE-30Xa_PN0912, and pQE-30Xa_PN5061 and maintained in *E. coli* DH5α in 15% glycerol at −80°C, for the following survival assays.

Survival Assay With Wild Type and Photolyase-Deficient *E. coli* Strains Transformed With Putative CPF-Like Genes

Two *E. coli* strains were used to test the photoreactivation activity of the three putative CPF-like genes: KY1056 (*recA56, phr*$^+$), which is photolyase-proficient, and KY1225 (*recA56, phr*$^-$), which is photolyase-deficient. The two *E. coli* host strains were first transformed with the pREP4 (Kan^R) repressor plasmid (Qiagen, Germany), carrying a lac repressor that tightly regulates the lac promoter-controlled expression of recombinant proteins in the pQE-30Xa (Amp^R) vector. The pREP4 (Kan^R) transformed strains were subsequently transformed with pQE-30Xa with and without gene inserts, resulting in the following transgenic strains: (i) KY1056_pQE-30Xa (without gene insert), (ii) KY1225_pQE-30Xa (without gene insert), (iii) KY1225_pQE-30Xa_PN5670, (iv) KY1225_pQE-30Xa_PN0912, and (v) KY1225_pQE-30Xa_PN5061. KY1056_pQE-30Xa and KY1225_pQE-30Xa were used as positive and negative controls, respectively. Transformed cultures were maintained on Lysogeny Broth (LB) agar (15% w/v) supplemented with 100 μg/ml ampicillin and 25 μg/ml kanamycin as selective antibiotics.

For all UV-C treatments described in this study, 120 cm fluorescent tubes with UV emission peak at 254 nm (120 W germicidal UV-C tubes; Light Tech, United States) were used. A preliminary experiment confirmed that exposure to UV-C (254 nm, 2 ± 0.2 μmol/m^2/s) for 10 s was sufficient to have a significant effect on survival of *E. coli* strains KY1056 and KY1225 (**Supplementary Figure S1**). For a qualitative survival assay, transgenic *E. coli* strains were grown to saturation at 28°C overnight. Fresh LB medium supplemented with selective antibiotics was inoculated using saturated colonies with the dilution of 1:100, and further grown at 28°C until they reached an optical density of 0.5 at 600 nm wavelength (OD_{600} = 0.5). To induce gene expression, isopropyl-1-thio-D-galactopyranoside (IPTG) was added to a final concentration of 20 μg/ml in the cultures, and the cultures were allowed to continue growing for an additional 4 h. Then cultures were diluted to OD_{600} = 0.05 and plated on LB agar only supplemented with required antibiotics. No IPTG was used in LB agar plates at any stage of the experiment. Immediately after plating, Petri dishes without lids were exposed to either (i) UV-C treatment (254 nm) of 2 ± 0.2 μmol m^{-2} s^{-1} for 10 s or (ii) complete darkness. Petri dishes were sealed immediately after UV-C exposure and incubated at 25°C with either, (i) 2 h of blue light with an irradiance of 25 ± 5 μmol m^{-2} s^{-1} (peak at 454 nm) (15 W GreenPower LED module HF blue; Philips, Netherlands) or (ii) 2 h of complete darkness. All samples were subsequently incubated in darkness at 37°C overnight. On the next day, plates were assessed for surviving colonies. At this stage of experiment, growing cultures of all three constructs (pQE-30Xa_PN5670, pQE-30Xa_PN0912, and pQE-30Xa_PN5061) were tested for protein expression by western blot (**Supplementary Figure S2**). It was shown that all three constructs were expressing under similar conditions used in survival assay but only pQE-30Xa_PN0912 has photolyase like activity.

Based on the results of the above qualitative survival assay, the *E. coli* strain with a functional photolyase gene (KY1225_pQE-30Xa_PN0912) was selected for the quantitative assay. KY1056_pQE-30Xa and KY1225_pQE-30Xa (both without gene inserts) were again used as positive and negative controls, respectively. The experiment was performed as described above, except that the plated bacteria were first incubated at 37°C overnight in dark without any light treatment. On the next day, single colonies were picked and transferred to new Petri dishes with LB agar containing selective antibiotics (50 colonies per Petri dish). Plates were then exposed to the different treatments as described above. On the following day, the number of surviving

[1]https://www.ncbi.nlm.nih.gov/

colonies were recorded. Four replicate plates per treatment were used, and the experiment was performed twice.

Structure Model of Putative Photolyase of *P. neolycopersici*

The amino acid sequence of the *P. neolycopersici* photolyase gene (OINE01000912_T103440) identified in the *E. coli* survival assay was used in modeling of its three-dimensional (3D) structure. A 3D structure model was generated using the protein structure and function prediction server RaptorX (Källberg et al., 2012). RaptorX can take the advantage of the sequence conservation in known photolyase proteins and generated a reliable homology model of the conserved region of the protein, based on experimentally determined structures of photolyases in Protein data bank (PDB[2]). To predict the presence of the type of second cofactor (MTHF or 8-HDF), the generated 3D structure model of *P. neolycopersici* was visualized and superimposed with photolyases from *E. coli* containing 5, 10-MTHF (PDB id: 1DNP) or *Anacystis nidulans* (PDB id: 1QNF) containing 8-HDF, using the PyMOL software (PyMOL Molecular Graphics System, Version 2.0 Schrödinger, LLC). An amino acid sequence alignment of the putative *P. neolycopersici* photolyase and the *E. coli* and *A. nidulans* photolyases was made by Clustal Omega (Sievers et al., 2011).

Expression and Purification of a Putative *P. neolycopersici* Photolyase

Expression and purification of the putative *P. neolycopersici* photolyase (PN0912) was done by GenScript (United States) as follows. pQE30-Xa_PN0912 does not yield sufficient protein for purification. Hence, the linear pET-30a (Kan^R) expression plasmid (Novagen, Germany) containing gene PN0912 with 6× His-tag at C- terminus, was used for overexpression using *E. coli* BL21 (DE3) cells. A single colony was used to inoculate 4 ml of LB containing kanamycin and incubated overnight at 37°C and 200 rpm. Four milliliter of an overnight-grown culture was used to inoculate 1 L of auto-induced medium of 5052 containing selective antibiotics, and incubated at 37°C. When an OD_{600} value of 1.2 was reached, the culture was induced with IPTG at a final concentration of 0.5 mM, and allowed to grow for 16 h at 15°C at 200 rpm. Then cells were harvested by centrifugation at 4,000 rpm for 20 min. The pellet was resuspended in a lysis buffer (50 mM Tris–HCl, 150 mM NaCl, 1 mM TCEP, pH 8.0). The cell lysate was prepared by sonication at 600 W for 10 min with 3 s bursts and 6 s cooling intervals followed by centrifugation at 13,000 rpm for 30 min at 4°C to pellet the cells. The supernatant was discarded, and inclusion bodies were collected. Protein was obtained from inclusion bodies and purified by Ni-NTA affinity chromatography according to the manufacturer's protocol (Qiagen, Germany). All the protein purification steps were carried out at 4°C to avoid any degradation. Protein fractions were analyzed on 10% SDS-PAGE (GenScript, United States) stained with Coomassie Brilliant Blue G-250 (Bio-Rad, United States), and western blot analysis was done using a mouse anti-His monoclonal antibody (GenScript, United States).

Photolyase Absorption and Action Spectra

Photolyase protein with 85% purity was subjected to spectroscopic measurements (**Supplementary Figure S3**). To identify the presence and type of chromophores responsible for photo-repair activity, the absorption, excitation and emission spectra were measured at 22°C with a Synergy H1 hybrid multi-mode plate reader (BioTek, United States). The excitation spectra (300–500 nm) of the purified protein and the denatured protein supernatant were measured at an emission wavelength of 530 nm, while the emission spectra (400–650 nm) were measured with an excitation wavelength of 370 nm. To release its chromophores, the protein was heated at 95°C for 5 min. The precipitated protein was then removed by centrifugation, and the supernatant was collected and used to measure the absorption spectrum of the released chromophores within the range of 300–550 nm wavelength. To obtain more precise information about the second chromophore (MTHF), fluorescence excitation and emission spectra were measured.

The photolyase action spectrum was determined *in vivo*. A separate, quantitative survival assay with the *E. coli* strain containing the photolyase gene (KY1225_pQE-30Xa_PN0912), was carried out in a similar manner as described in 2.3 with the exception that we here used five different incubation conditions: dark, 365, 400, 454, and 525 nm. Immediately after non-UV or UV-C (254 nm, 2 ± 0.2 μmol m^{-2} s^{-1} for 10 s) treatments, plates were transferred to complete darkness or one of the four different incubation wavelengths with an irradiance of 25 ± 5 μmol m^{-2} s^{-1} for 2 h at 25°C. After 2 h incubation in specified conditions, plates were incubated in darkness at 37°C overnight, and on the following day, the number of surviving colonies were recorded. The four incubation wavelengths were obtained from the following sources: UV-A, peak 365 nm, full width at half maximum (FWHM) 14 nm (RAY22 UV-A LEDs, Fluence Bioengineering, Austin, TX, United States); UV-A/blue, peak 400 nm, FWHM 14 nm (RAY22 UV-A LEDs, Fluence Bioengineering, Austin, TX, United States); blue, peak 454 nm, FWHM 23 nm (15 W GreenPower LED module HF blue; Philips, Netherlands) and green, peak 525 nm, FWHM 14 nm (RAY44 Green LEDs, Fluence Bioengineering, Austin, TX, United States) (**Supplementary Figure S4**).

A similar set up with slight modifications was used to study the action spectra for germination recovery of *P. neolycopersici* conidia treated with brief UV. Immediately after inoculation of *P. neolycopersici* conidia in water agar (1% w/v), Petri dishes without lids were exposed to either complete darkness (non-UV) or UV-C (peak 254 nm, 8 ± 0.2 μmol m^{-2} s^{-1} for 30 s) treatments. Immediately after treatments, plates were sealed and transferred to complete darkness or one of four different incubation wavelengths (365, 400, 454, and 525 nm) with an

[2]http://www.rcsb.org

irradiance of 50 ± 5 μmol m^{-2} s^{-1} for 16 h followed by 8 h of darkness at temperature and relative humidity (RH) of 20 ± 1°C and 75 ± 5%, respectively. Germination of conidia was assessed 24 h after inoculation (Suthaparan et al., 2018).

Analysis of Photolyase Gene Expression

Inoculum of a *P. neolycopersici* isolate (isolate was collected from Akershus county, Norway named as As_PN) was maintained on powdery mildew susceptible tomato cv. Espero, grown at a 16 h photoperiod at 20 ± 2°C and 75 ± 5% RH. For inoculation of tomato plants, diseased leaves were shaken thoroughly in distilled water containing Tween-20 (20 μl/L) and sprayed onto 2-week-old healthy plants using a handheld sprayer. Conidia of 9-day-old inoculum of *P. neolycopersici* was dusted on 2% (w/v) water agar in Petri dishes (54 dishes). After dusting, half of the dishes (27) were exposed to UV-C (254 nm, 8 ± 0.2 μmol m^{-2} s^{-1}) for 30 s without lids, and the other half were exposed to complete darkness for 30 s without lids.

Immediately after this, the Petri dishes were sealed and distributed among one of the following three different incubation treatments: (i) darkness, (ii) UV-A/blue light (peak 400 nm, 50 ± 5 μmol m^{-2} s^{-1}) (RAY22 UV-A LEDs, Fluence Bioengineering, Austin, TX, United States), or (iii) red light (peak 660 nm, 50 ± 5 μmol m^{-2} s^{-1}) (10 W GreenPower LED module HF Deep Red; Philips, Netherlands). Samples were collected at three different time points during incubation: (i) 30 s, (ii) 4 h, and (iii) 8 h. Samples from three replicate Petri dishes were collected at each time point per treatment (biological replicates). Conidia were collected into 2 ml Eppendorf tubes using a microscopy glass slide to gently scrape the surface of the water agar. Samples were flash frozen with liquid nitrogen and then stored at −80°C until use. Total RNA was extracted using the Plant RNA reagent (Invitrogen, United States) followed by DNase treatment (Turbo DNA free™ kit, Invitrogen, United States) and purification (PureLink RNA kit, Ambion, United States) as described in the manufacturer's protocol. The quantity and quality of the RNA was estimated by NanoDrop™ 2000 (Thermo Fisher Scientific, United States) and BioAnalyzer 2100 (Agilent Technologies Inc., United States). cDNA was synthesized from 500 ng of RNA using Superscript™ IV VILO Master Mix (Invitrogen, United States).

Real-time PCR was performed using SYBR™ Select Master Mix (Thermo Fisher Scientific, United States) on the 7500 Fast Real-Time PCR system (Applied Biosystems, United States). qPCR primers for *P. neolycopersici* photolyase (OINE01000912_T103440) (target gene) and alpha-tubulin gene (OINE01013217_T107300) (internal control) (**Supplementary Data S1**) were designed using Primer3 (v.0.4.0) (**Supplementary Table S1**). Standard curves were generated with one of the cDNA samples with serial dilution to a factor of 10. The following two-step PCR program of 50°C for 2 min, 95°C for 2 min, 45 cycles of 95°C for 15 s and 60°C for 1 min was used with three technical replicates per sample. Photolyase expression of *P. neolycopersici* was first normalized to alpha tubulin expression in the same sample, and then expression was calculated relative to the non-UV treated control samples, using the $2^{-(\Delta\Delta Ct)}$ method (Livak and Schmittgen, 2001).

Recording Environmental Conditions and Data Analysis

Spectral composition and level of irradiance for all radiation sources used in this study were measured by an Optronic model 756 spectroradiometer (Optronic Laboratories, Orlando, FL, United States). Air temperature and RH inside controlled environment chambers were recorded in 5 min interval using a Priva greenhouse computer coupled with dry and wet bulb thermo sensors (Priva, Zijlweg, Netherlands). Analysis of variance for fold change gene expression of *P. neolycopersici* photolyase was done by using general linear model (Minitab Version 18.0, Minitab Corp., State College, PA, United States). Treatment means were separated by Tukey's pairwise comparison at $P = 0.05$. All figures were drawn using SigmaPlot 10 (Systat Software, Inc., Chicago, IL, United States) unless otherwise specified.

RESULTS

Phylogenetic Analysis

The phylogeny results suggest that *P. neolycopersici* gene OINE01015670_T110144 was clustered within the (6-4) photolyases and animal cryptochromes and appeared to be most closely related to other fungal cryptochromes in *Fusarium oxysporum* and *Aspergillus niger*. *P. neolycopersici* OINE01000912_T103440, falls within the clade of class I CPD photolyases with high bootstrap percentage and was closely related to fungal class I CPD photolyases, particularly from *E. necator* and *Golovinomyces cichoracearum*. The third CPF-like member from *P. neolycopersici*, OINE01005061_T102555, clustered within the CRY-DASH clade, and was closely related to the fungal *Neurospora crassa* and *Botrytis cinerea* cryptochrome DASH genes and the bacterial *Vibrio cholerae* cryptochrome DASH-like gene (**Figure 1**).

Identification of a Functional Photolyase Gene of *P. neolycopersici* in *E. coli*

All three putative CPF- like genes (OINE01015670_T110144, OINE01000912_T103440, and OINE01005061_T102555) were tested for photoreactivation activity. In the qualitative survival assay, none of the tested *E. coli* strains survived when they were treated with brief UV-C followed by complete darkness. However, when the UV-C treatment was followed by 2 h in blue light (454 nm), KY1225 cells harboring the pQE-30Xa_PN0912 plasmid had a high survival rate, similar to that of the positive control. This treatment gave the lowest survival rate for KY1225 cells harboring either pQE-30Xa_PN5670 or pQE-30Xa_PN5061 plasmids, similar to that observed in the negative control (**Figure 2**).

In the quantitative survival assay, *E. coli* strain KY1225 harboring pQE-30Xa_PN0912 and the positive control had a colony survival rate of more than 98% when they were treated with UV-C followed by blue light (454 nm) incubation, whereas a survival rate of 4.5% was observed when they

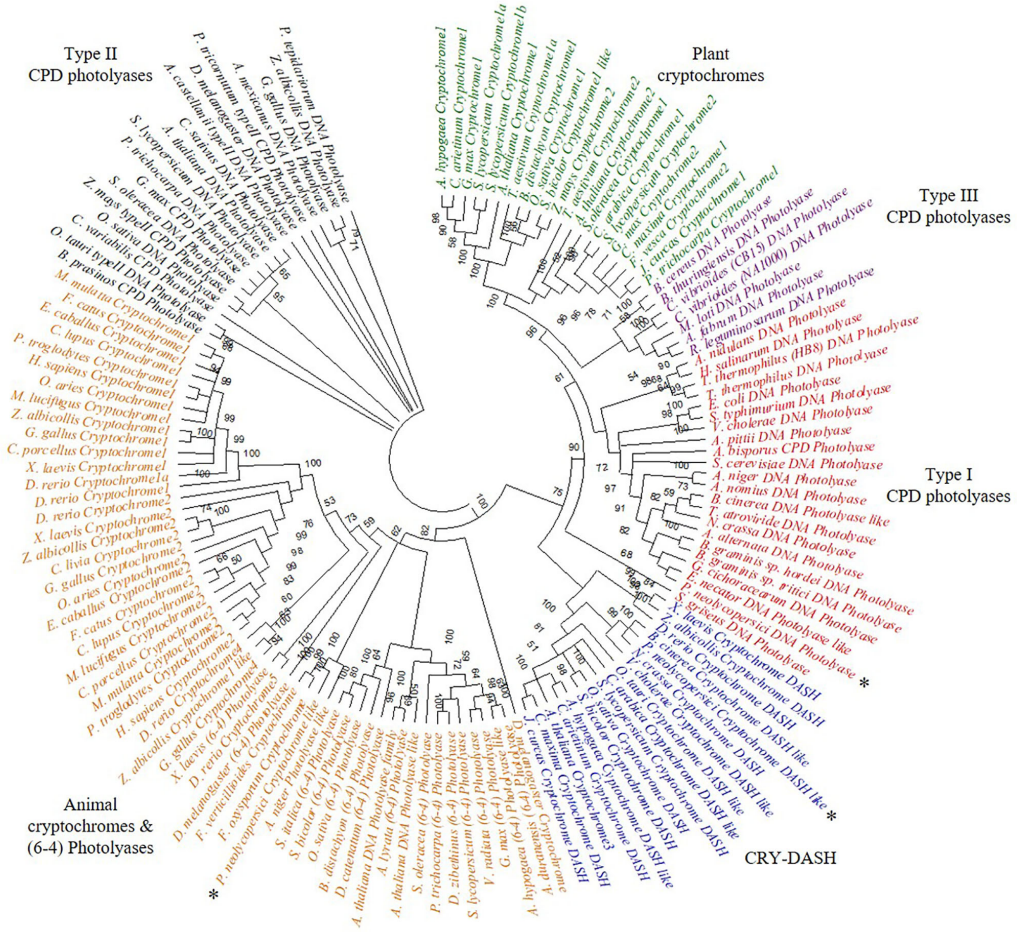

FIGURE 1 | Phylogenetic analysis of cryptochrome/photolyase family (CPF)- like genes, including three CPF- like genes, OINE01015670_T110144 (*P. neolycopersici* cryptochrome like), OINE01000912_T103440 (*P. neolycopersici* photolyase like) and OINE01005061_T102555 (*P. neolycopersici* cryptochrome DASH like), all indicated by asterisk (*). An unrooted phylogenetic tree was constructed using neighbor-joining method. Bootstrap probability of 1000 replicates are expressed in percentage.

were treated with UV-C followed by complete darkness (**Figure 3** and **Supplementary Figure S5**). UV-C treatment, incubation wavelength and UV-C treatment × incubation wavelength, all had significant effect ($P < 0.0001$) on cell survival.

Structural Prediction Model for *P. neolycopersici* Photolyas

The structural prediction model for *P. neolycopersici* photolyase consisted of an N-terminal alpha/beta domain and a C-terminal helical domain with a long connecting loop (**Figure 4A**). Due to the lack of any sequence homology of the 130 amino acids in the N-terminal of the putative photolyase, only a structure model of amino acids 131–634 could be generated with high confidence ($P < 0.0001$). At the surface of the photolyase, two cavities were clearly exhibited, one at the center of the helical domain and the other in the cleft between the two domains (**Figure 4A** and **Supplementary Figure S6**). A 3D structural superimposition of *P. neolycopersici* photolyase with the *E. coli* photolyase (Park et al., 1995) showed perfect alignment of FAD and MTHF binding sites into the cavities without any clashes with neighboring residues (**Supplementary Figure S6**). However, a structural

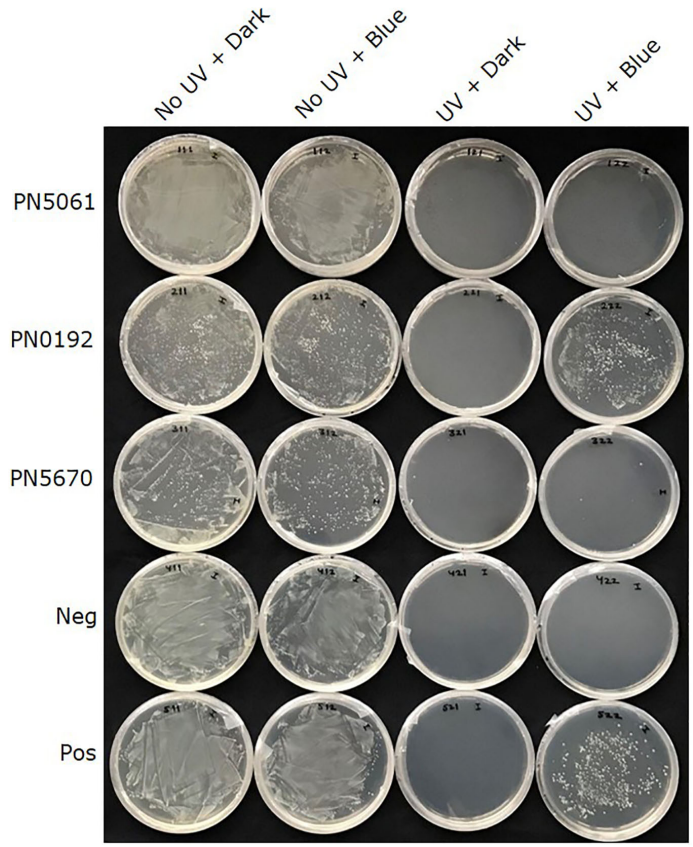

FIGURE 2 | Qualitative survival assay of *Escherichia coli* strains KY1056 (photolyase-proficient, wild type) and KY1225 (photolyase-deficient, mutant) transformed with an empty pQE30-Xa vector served as positive (Pos) and negative (Neg) controls, respectively, and KY1225 transformed with the pQE30-Xa vector harboring codon optimized synthetic genes of PN5670, or PN0912, or PN5061. Actively growing transgenic strains were plated on LB agar (Amp^R, Kan^R) and exposed to either darkness or UV-C (254 nm of 2 ± 0.2 μmol m^{-2} s^{-1}) for 10 s, followed by incubation in either darkness or blue light (454 nm of 25 ± 5 μmol m^{-2} s^{-1}) for 2 h at 25°C and then overnight incubation at 37°C.

superimposition with the 8-HDF-containing photolyase from *A. nidulans* (Tamada et al., 1997) only demonstrated an alignment of the FAD binding site.

Analysis of the amino acid residues involved in the interactions of FAD and MTHF in the photolyase structure showed that all residues involved in FAD binding in *P. neolycopersici* photolyase were completely conserved to FAD binding in *E. coli* (**Figure 4B**) and *A. nidulans* (**Supplementary Figure S7**). The photolyase of *P. neolycopersici* accommodated MTHF in the binding site via His and Glu residues homologous to the photolyase of *E. coli*. However, the N108 (Asn) and K293 (Lys) residues were replaced by D246 (Asp) and M452 (Met) residues, respectively (**Figure 4C** and **Supplementary Figure S7**).

Absorption, Excitation and Emission Spectra of *P. neolycopersici* Photolyase

The absorption spectra showed some absorbance in the measured wavelength range (300–550 nm) with the tendency of strong absorbance around 300 nm (**Figure 5A**).The excitation spectra showed that the maximum fluorescence (measured at 530 nm) was obtained at an excitation wavelength of 410 nm (**Figure 5B**). Upon excitation with 370 nm wavelength, an emission peak at 460 nm was observed (**Figure 5C**).

Action Spectra of *P. neolycopersici* Photolyase

Within the tested incubation wavelength ranges, *E. coli* strain KY1225 harboring pQE30Xa_PN0912 showed a survival rate

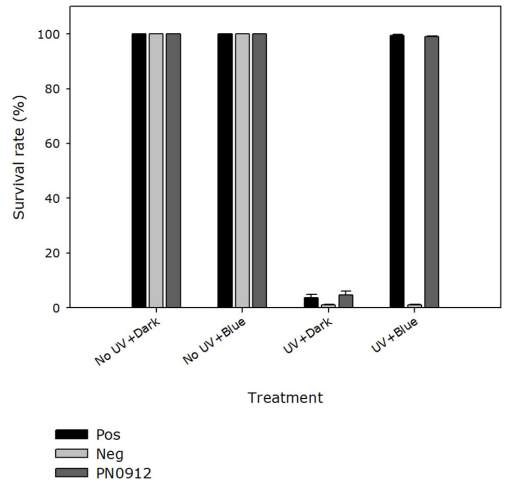

FIGURE 3 | Quantitative survival activity assay of the *Pseudoidium neolycopersici* putative photolyase gene, PN0912. *Escherichia coli* strains KY1056 (photolyase-proficient, wild type) and KY1225 (photolyase-deficient, mutant) transformed with an empty pQE30-Xa expression vector served as positive (Pos) and negative (Neg) controls, respectively. KY1225 transformed with the expression vector containing the gene PN0912. Actively growing transgenic strains were plated on LB agar and exposed to either darkness or UV-C (254 nm of 2 ± 0.2 μmol m^{-2} s^{-1}) for 10 s, followed by incubation in either darkness or blue light (454 nm of 25 ± 5 μmol m^{-2} s^{-1}) for 2 h at 25°C and then overnight incubation at 37°C. The presence of photolyase activity was assessed by the presence of surviving colonies on Petri dishes containing LB agar (Amp^R, Kan^R). Percent survival of *E. coli* strain KY1225_pQE30Xa_PN0912 (PN0912) expressing a putative photolyase gene as well as the positive and negative control was calculated. Plates inoculated with fifty colonies each were exposed to the different treatments, and the number of surviving colonies were recorded. Each value is the mean ± standard error of two experiments with four replicate Petri dishes each (n = 8).

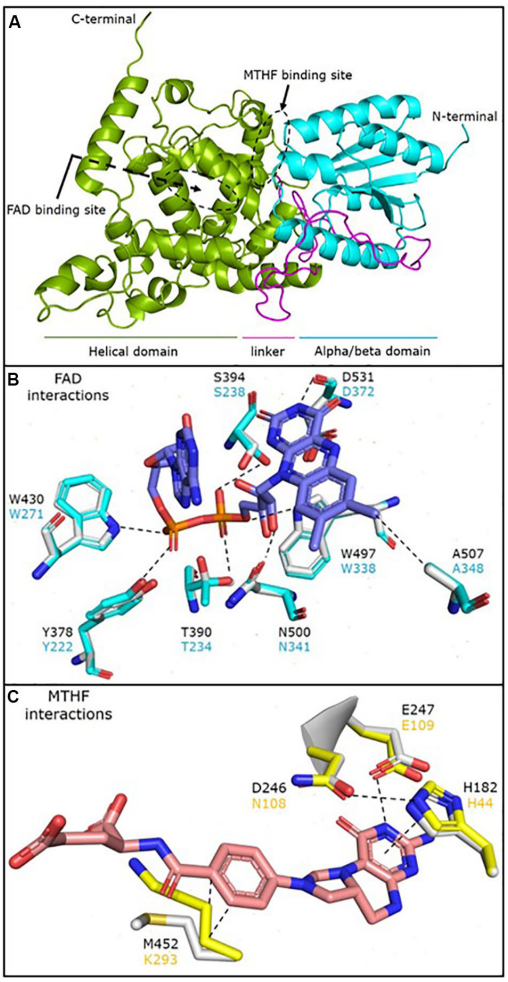

FIGURE 4 | Cartoon representation of the predicted structural model of the *Pseudoidium neolycopersici* photolyase (OINE01000912_T103440), made using the protein structure and function prediction program RaptorX **(A)**. The structure shows an N-terminal alpha/beta domain (cyan) and a C-terminal helical domain (green) connected by a long linker (magenta). The flavin adenine dinucleotide (FAD) and 5, 10-methenyltetrahydrofolate (MTHF) binding sites are also observed on the protein surface (black dashed circles). Molecular interactions of **(B)** FAD and **(C)** MTHF with the neighboring residues in the *Escherichia coli* photolyase (cyan and yellow) superimposed onto the *P. neolycopersici* photolyase (light gray structure and black font). The dashed lines represent a stabilizing interaction between the two moieties. FAD is stabilized via extensive network of H-bonds with neighboring residues with the flavin head and phosphate groups. MTHF is stabilized by a stacking interaction with H182 and H-bond with E247, while the M452 stabilizes the MTHF tail by hydrophobic interactions. A nearly perfect overlay of the interacting residues suggests that the mode of FAD and MTHF binding in *P. neolycopersici* photolyase is similar to *E. coli* photolyase.

of more than 99% when it was incubated with wavelengths of 365, 400, or 454 nm immediately after UV treatment. The survival rate was <1% when it was incubated with 525 nm wavelength or complete darkness immediately after UV treatment. UV-C treatment, incubation wavelength and UV-C treatment × incubation wavelength, all had significant effect (P < 0.0001) on cell survival (**Figure 6A** and **Supplementary Figure S8**). Action spectra for germination recovery in *P. neolycopersici* showed similar results (**Figure 6B**).

Expression of the Photolyase Gene in Conidia of *P. neolycopersici*

Independent of incubation wavelength, expression of the photolyase gene, OINE01000912_T103440, was significantly higher in UV-C treated samples within 30 s. The maximum expression level was reached at 4 h after UV-C treatment. The photolyase gene expression was significantly higher in darkness

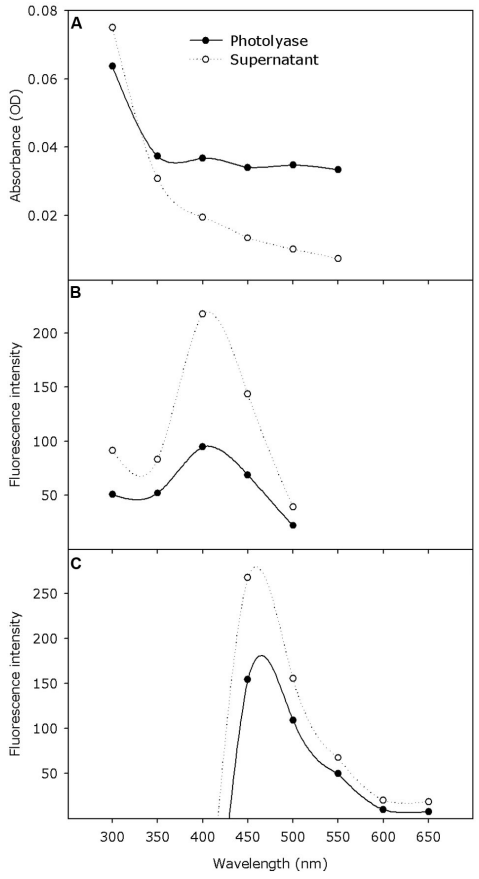

FIGURE 5 | Absorption and fluorescence excitation and emission spectra of purified *Pseudoidium neolycopersici* photolyase protein (solid line) and denatured protein supernatant (dotted line) containing the released chromophore. **(A)** Absorption spectra (scans from 300–550 nm) were recorded at pH 8.0 in storage buffer. **(B)** Excitation spectra (scans from 300–500 nm) were recorded with the emission wavelength adjusted to yield maximum fluorescence at 530 nm. **(C)** Emission spectra (scans from 400–650 nm) were recorded with the excitation wavelength at 370 nm.

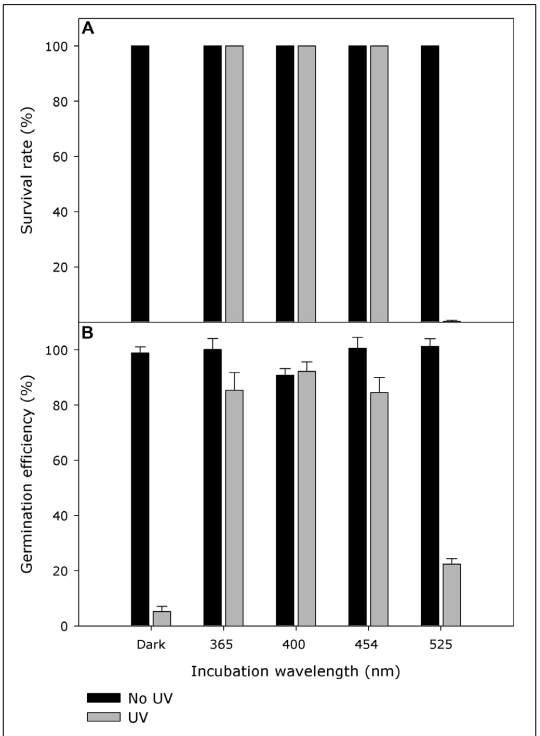

FIGURE 6 | (A) Action spectra of *Pseudoidium neolycopersici* photolyase gene, PN0912. *Escherichia coli* strain KY1225 (photolyase-deficient) transformed with the expression vector pQE30Xa containing *P. neolycopersici* photolyase, PN0912, were used to inoculate LB agar (Amp^R, Kan^R) petri dishes (50 colonies per plate). Plates were exposed for 10 s to either darkness or UV-C (254 nm, 2 ± 0.2 μmol m^{-2} s^{-1}), followed by incubation in either darkness, 365, 400, 454, or 525 nm (all 25 ± 5 μmol m^{-2} s^{-1}) for 2 h at 25°C, and then in darkness overnight at 37°C. Each value is the mean colony survival rate ± standard error of six replicate Petri dishes (n = 6). **(B)** Recovery action spectra of *P. neolycopersici*. Conidia of *P. neolycopersici* were dusted on water agar and exposed to either (i) complete darkness (non-UV) or (ii) UV-C (UV, with a peak of 254 nm, 8 ± 0.2 μmol m^{-2} s^{-1}) for 30 s. All treatments were followed by incubation in darkness (Dark) for 24 h, or irradiation of 365, 400, 454, or 525 nm (all 50 ± 5 μmol m^{-2} s^{-1}) for 16 h followed by 8 h in darkness. Each value is the mean germination efficiency ± standard error of six replicate Petri dishes (n = 6).

and in UV-A/blue light than in red light at all sampling times (30 s, 4 h, and 8 h) after UV-C treatment ($P < 0.0001$), particularly at the latter time points. When incubated in red light, expression in UV-C treated samples dropped to the same level as the non-UV control (**Figure 7**).

DISCUSSION

Among the three tested CPF-like genes identified in the *P. neolycopersici* genome, this study confirmed the presence of one photolyase gene with functional similarity to previously well characterized protein in other life forms. Survival of a photolyase deficient *E. coli* strain transformed with OINE01000912_T103440 under UV-C treatment followed by blue light incubation showed that this candidate gene is a functional photolyase. The non-surviving photolyase deficient *E. coli* strain transformed with the other two candidate genes exposed to the same conditions suggested that those two genes could be the other members of cryptochrome/photolyase family, either cryptochrome or CRY-DASH genes, which do not possess photoreactivation activity (Thompson and Sancar, 2002). Our

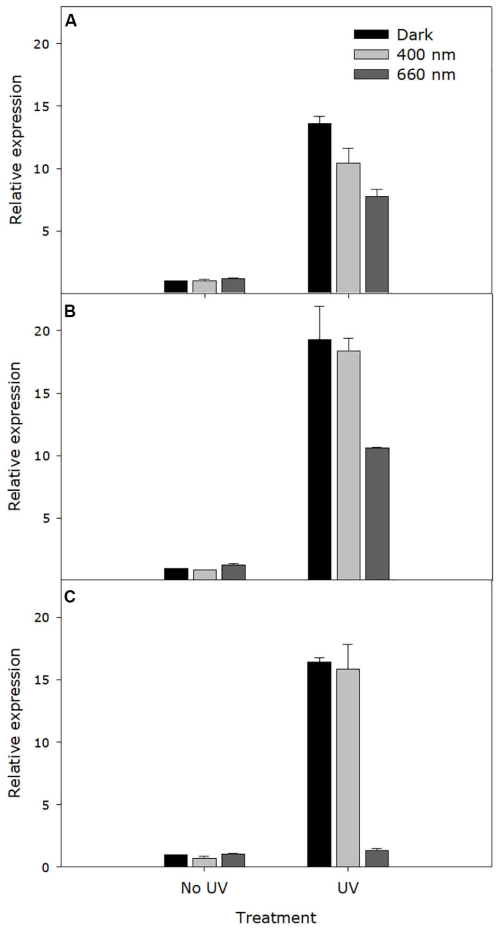

FIGURE 7 | Expression level of the *Pseudoidium neolycopersici* photolyase gene, OINE01000912_T103440. Conidia of *P. neolycopersici* were exposed for 30 s to either complete darkness (control treatment) or UV-C treatment (UV, 254 nm of 8 ± 0.2 μmol m^{-2} s^{-1}), and then immediately incubated either in the dark or under UV-A/blue (peak of 400 nm of 50 ± 5 μmoles m^{-2} s^{-1}) or red light (peak 660 nm of 50 ± 5 μmoles m^{-2} s^{-1}). During incubation, samples were collected at three different time points: **(A)** 30 s, **(B)** 4 h, and **(C)** 8 h. Expression levels were normalized to the corresponding alpha-tubulin gene expression and are shown as fold-change relative to the expression in non-UV-treated (control treatment) samples. Each value is the mean ± standard error of three independent biological replicates (n = 3), each with three technical replicates.

phylogenetic analysis suggests that OINE01015670_T110144 and OINE01005061_T102555 are putative cryptochrome and CRY-DASH, respectively (**Figure 1**). However, further studies are required to confirm their functional characteristics in *P. neolycopersici*. The purified recombinant *P. neolycopersici* photolyase protein showed a molecular mass of about 72 kDa, including a 6× His-tag. This matches the molecular mass of 71.87 kDa, calculated from the deduced amino acid sequence of 634 residues. This is slightly larger than photolyases from other species in both number of amino acid residues and molecular mass (Sancar et al., 1987b; Yajima et al., 1991; Waterworth et al., 2002). The 6× His-tag facilitates single step protein purification without interfering in the folding of protein, thereby its activity (Malhotra, 2009).

The cryptochrome/photolyase superfamily comprises six major subgroups distinguished based on their evolutionary relationship and functions; class I CPD photolyases, class II CPD photolyases, class III CPD photolyases, plant cryptochromes, CRY-DASH proteins and animal cryptochromes which also include (6-4) photolyases (Bayram et al., 2008; Mei and Dvornyk, 2015). Phylogenetic analysis showed that *P. neolycopersici* photolyase classified as a class I CPD photolyase, and this class includes extensively studied *E. coli* CPD photolyase and photolyases from other ascomycetes. Class I CPD photolyases are most prevalent in micro-organisms (Essen and Klar, 2006). All class I photolyases contain an identical catalytic cofactor (FAD) and an additional second cofactor which is either MTHF or 8-HDF, responsible for harvesting light. Depending on the presence of a second chromophore; either 8-HDF or MTHF, class I CPD photolyases are further divided into flavin (8-HDF) and folate (MTHF) types (Sancar, 2003).

Structural prediction model analysis suggested that *P. neolycopersici* photolyase is capable of binding FAD and MTHF as cofactors. This is in accordance with identified cofactors in the majority of photolyases, including in *E. coli* (Park et al., 1995). The photolyase of *E. coli* accommodates MTHF in the binding site via four crucial residues (His44, Asn108, Glu109, and Lys293) (Park et al., 1995). Our results suggest that the photolyase of *P. neolycopersici* binds MTHF via His182, Asp246, Glu247, and Met452. Interestingly, this change in the interacting residues would not affect the bonding pattern, as the Asn108 and Lys293 in *E. coli* stabilizes the MTHF via one oxygen mediated H-bond and hydrophobic interactions, respectively, which would also form with the Asp246 and Met452 in the *P. neolycopersici* photolyase (**Figure 4C**). Glu109, which is involved in MTHF interactions and was conserved here, is proposed to be conserved in all folate classes of photolyases except in the photolyase from *Bacillus firmus* (Park et al., 1995). A limited number of species, including *A. nidulans* and *Thermus thermophilus*, have 8-HDF as second cofactor (Tamada et al., 1997; Klar et al., 2006). Our structural prediction model did not predict the presence of 8-HDF in *P. neolycopersici* photolyase. Crystal structures of photolyases from *E. coli, A. nidulans*, and *T. thermophilus* showed that the structures of all these photolyases are remarkably similar with only about 25% sequence identity, as in the case of *P. neolycopersici* photolyase (Sancar, 2004).

The presence of the FAD cofactor was further corroborated with optical absorption properties of *P. neolycopersici* photolyase. However, we were not able to detect any clear maximum in the absorption spectrum. Absorption properties of the supernatant showed that the cofactor was in a reduced form. Observations in our study were similar to the emission of fully reduced $FADH^{-}$,

which is a catalytically active form that can be reduced by photo- or chemical reduction (Sancar et al., 1987a; Malhotra et al., 1994; Kao et al., 2008). Previous studies reported that an emission peak at 530 nm with an excitation wavelength of 370 nm is an indication of the presence of FAD_{ox} and is characteristic to flavin and MTHF chromophores (Worthington et al., 2003; Teranishi et al., 2008; Tagua et al., 2015). Fluorescence spectra did not show any evidence for the presence of an additional chromophore. Previous studies also showed that FAD could be identified as the only chromophore present when proteins are heterologously expressed (Kleiner et al., 1999). It has been reported that when *E. coli* photolyase was expressed heterologously, approximately 50–70% MTHF was lost during purification (Payne and Sancar, 1990; Sancar, 2003).

This study indicates that the photolyase of *P. neolycopersici* has a broad action spectrum ranging from around 365 to 454 nm. This action spectrum perfectly overlaps with the previously published germination recovery action spectra of *P. neolycopersici* (**Figure 6B**) (Suthaparan et al., 2018). The UV-A/blue range (peak wavelengths of 365 and 400 nm) resulted in larger colonies as compared to pure blue light (peak 454 nm) (**Supplementary Figure S9**). This suggests that UV-A is the most effective wavelength for the functional activity of photolyase in *P. neolycopersici*. All folate (MTHF) classes of photolyases have absorption maxima in the range of 370–440 nm, as reported for *E. coli*, *N. crassa* and *Saccharomyces cerevisiae*, indicating that the folate class has a considerably broader action spectrum (366–450 nm) (Sancar et al., 1987a; Sancar, 1990; Eker et al., 1994). On the contrary, the absorption maximum of the flavin-type (8-HDF) chromophore in *A. nidulans*, *Streptomyces griseus*, and *Methanobacterium thermoautotrophicum* falls between 434 and 443 nm, showing a very narrow range of its action spectrum (Hada et al., 2000; Sancar, 2003). The photolyase action spectrum of *P. neolycopersici* (365–454 nm) and the protein structure model are in agreement with the folate class of photolyases. However, confirmation of the presence of a second chromophore needs further investigation with the native protein isolated from *P. neolycopersici*.

Quantitative PCR results showed that the gene expression of photolyase in *P. neolycopersici* was induced by brief exposure to UV-C. In most fungi, light induces both the expression of genes involved in protection against UV-induced DNA damage and synthesis of protective pigments that can filter out harmful radiation (Braga et al., 2015). Blue light responses are well studied in many fungi, such as *N. crassa*, *Aspergillus nidulans* and *Phycomyces blakesleeanus* (Corrochano, 2011; Fuller et al., 2015). Photoreceptor genes that are involved in blue light perception showed upregulation by blue light, and it was reported that the blue light receptor Wco1 regulates the photolyase gene expression in *Ustilago maydis* (Brych et al., 2016). In *Trichoderma atroviride*, UV-A and blue light induce the *phr1* expression through the white collar complex BLR1/BLR2 (Berrocal-Tito et al., 2007). Our study showed that transcriptional upregulation of *P. neolycopersici* photolyase starts immediately after the brief UV-C exposure, both under subsequent incubation in darkness and in UV-A/blue light, and the upregulated expression is maintained for at least 8 h. Expression was also upregulated under subsequent incubation in red light, but after 8 h it was back to the level of the non-UV treated control. Previously, we have shown that incubation of UV-damaged *P. neolycopersici* conidia in UV-A/blue light can mediate gemination recovery of conidia, while incubation in darkness or red light cannot (Suthaparan et al., 2018). Taken together, our results suggest that (1) photolyase gene expression is induced by the brief UV-C exposure itself and that photolyase gene expression alone is not sufficient for gemination recovery of conidia, (2) UV-A/blue light provides the necessary energy for functional activity of photolyase that mediates germination recovery, (3) the inability of red light to provide necessary energy for functional activity of photolyase may prevent germination recovery, (4) red light dependent downregulation of the photolyase expression, which was induced by UV-C may further enhance this effect. This explains the increased efficacy of UV-C against powdery mildew when used in combination with red light (Suthaparan et al., 2014, 2018). A recent study also showed that UV-C induces the transcription of three putative photolyase genes in *Blumeria graminis*, the causal organism of barley powdery mildew (Zhu et al., 2019).

The study did not provide functional evidence of photolyase directly from the natural host *P. neolycopersici*. Host induced gene silencing (HIGS) employing RNA silencing mechanisms, has been used widely in functional genomics, especially in silencing the targets of invading pathogens including powdery mildews (Pliego et al., 2013; Qi et al., 2019). The follow-up studies will focus on using host induced silencing of *P. neolycopersici* photolyase to provide direct functional evidence in its natural host.

The photoreactivation process plays an important role in UV-based disease control in crops; hence, planning accurate irradiation applications is critical and is highly dependent on lighting conditions. The present findings about the action spectra of photolyase in *P. neolycopersici* will be very helpful in designing efficient UV-mediated disease suppression strategies for greenhouse-grown crops, providing an environmentally friendly alternative for the management of powdery mildew diseases.

DATA AVAILABILITY STATEMENT

The contig and coding sequence data of the *P. neolycopersici* CPF like genes used in this study are deposited in the NCBI database under the accession numbers MT277359, MT277360, MT277361, MT277362, MT277363, and MT277364. The raw data supporting the conclusions of this article will be made available by the authors, without undue reservation, to any qualified researcher.

AUTHOR CONTRIBUTIONS

RP designed and executed the experiments and wrote the manuscript. ASu conceived, designed, executed the experiments, and revised the manuscript. ÅE, ASt, HG, KS, and LC-D contributed in designing of experiments, and critical revision of the manuscript.

FUNDING

This research was partly financed by the Norwegian Research Council under the project VekthusDynamikk (225080) and END-IT (300999). Part of the publication expenses was financed by the NMBU's publishing fund for Open Access Journals.

ACKNOWLEDGMENTS

We thank Prof. Dr. Alfred Batschauer for providing KY1224 and KY1056 *E. coli* strains used in this study. We thank the technical staff at the Centre for Controlled Environment Plant Research (SKP) at Norwegian University of Life Sciences (NMBU) for their excellent support and assistance.

SUPPLEMENTARY MATERIAL

The Supplementary Material for this article can be found online at: https://www.frontiersin.org/articles/10.3389/fmicb.2020.01091/full#supplementary-material

REFERENCES

Bayram, O., Biesemann, C., Krappmann, S., Galland, P., and Braus, G. H. (2008). More than a repair enzyme: *Aspergillus nidulans* photolyase-like CryA is a regulator of sexual development. *Mol. Biol. Cell* 19, 3254–3262. doi: 10.1091/mbc.E08-01-0061

Berrocal-Tito, G. M., Esquivel-Naranjo, E. U., Horwitz, B. A., and Herrera-Estrella, A. (2007). *Trichoderma atroviride* PHR1, a fungal photolyase responsible for DNA repair, autoregulates its own photoinduction. *Eukaryot. Cell* 6, 1682–1692. doi: 10.1128/EC.00208-06

Braga, G. U. L., Rangel, D. E. N., Fernandes, ÉK. K., Flint, S. D., and Roberts, D. W. (2015). Molecular and physiological effects of environmental UV radiation on fungal conidia. *Curr. Genet.* 61, 405–425. doi: 10.1007/s00294-015-0483-0

Braun, U., and Cook, R. (2012). *Taxonomic Manual of the Erysiphales (Powdery Mildews). CBS Biodiversity Series 11*. Utrecht: CBS.

Brych, A., Mascarenhas, J., Jaeger, E., Charkiewicz, E., Pokorny, R., Bölker, M., et al. (2016). White collar 1-induced photolyase expression contributes to UV-tolerance of *Ustilago maydis*. *Microbiologyopen* 5, 224–243. doi: 10.1002/mbo3.322

Corrochano, L. M. (2011). Fungal photobiology: a synopsis. *IMA Fungus* 2, 25–28. doi: 10.5598/imafungus.2011.02.01.04

Eker, A. P. M., Yajima, H., and Yasui, A. (1994). DNA photolyase from the fungus *Neurospora crassa*. Purification, characterization and comparison with other photolyases. *Photochem. Photobiol.* 60, 125–133. doi: 10.1111/j.1751-1097.1994.tb05078.x

Essen, L. O., and Klar, T. (2006). Light-driven DNA repair by photolyases. *Cell. Mol. Life Sci.* 63, 1266–1277.

Fuller, K. K., Loros, J. J., and Dunlap, J. C. (2015). Fungal photobiology: visible light as a signal for stress, space and time. *Curr. Genet.* 61, 275–288. doi: 10.1007/s00294-014-0451-0

Glawe, D. A. (2008). The powdery mildews: a review of the world's most familiar (yet poorly known) plant pathogens. *Annu. Rev. Phytopathol.* 46, 27–51. doi: 10.1146/annurev.phyto.46.081407.104740

Hada, M., Iida, Y., and Takeuchi, Y. (2000). Action spectra of DNA photolyases for photorepair of cyclobutane pyrimidine dimers in sorghum and cucumber. *Plant Cell Physiol.* 41, 644–648. doi: 10.1093/pcp/41.5.644

Janisiewicz, W. J., Takeda, F., Nichols, B., Glenn, D. M., Jurick, Ii, W. M., et al. (2016). Use of low-dose UV-C irradiation to control powdery mildew caused by *Podosphaera aphanis* on strawberry plants. *Can. J. Plant Pathol.* 38, 430–439.

Jankovics, T., Bai, Y., Kovács, G. M., Bardin, M., Nicot, P. C., Toyoda, H., et al. (2008). *Oidium neolycopersici*: intraspecific variability inferred from amplified fragment length polymorphism analysis and relationship with closely related powdery mildew fungi infecting various plant species. *Phytopathology* 98, 529–540. doi: 10.1094/PHYTO-98-5-0529

Källberg, M., Wang, H., Wang, S., Peng, J., Wang, Z., Lu, H., et al. (2012). Template-based protein structure modeling using the RaptorX web server. *Nat. Protoc.* 7, 1511–1522. doi: 10.1038/nprot.2012.085

Kao, Y., Saxena, C., He, T., Guo, L., Wang, L., Sancar, A., et al. (2008). Ultrafast dynamics of flavins in five redox states. *J. Am. Chem. Soc.* 130, 13132–13139. doi: 10.1021/ja8045469

Klar, T., Kaiser, G., Hennecke, U., Carell, T., Batschauer, A., and Essen, L. (2006). Natural and non-natural antenna chromophores in the DNA photolyase from *Thermus thermophilus*. *Chembiochem* 7, 1798–1806. doi: 10.1002/cbic.200600206

Kleiner, O., Butenandt, J., Carell, T., and Batschauer, A. (1999). Class II DNA photolyase from *Arabidopsis thaliana* contains FAD as a cofactor. *Eur. J. Biochem.* 264, 161–167. doi: 10.1046/j.1432-1327.1999.00590.x

Kumar, S., Stecher, G., Li, M., Knyaz, C., and Tamura, K. (2018). MEGA X: molecular evolutionary genetics analysis across computing platforms. *Mol. Biol. Evol.* 35, 1547–1549. doi: 10.1093/molbev/msy096

Li, C., Faino, L., Dong, L., Fan, J., Kiss, L., De Giovanni, C., et al. (2012). Characterization of polygenic resistance to powdery mildew in tomato at cytological, biochemical and gene expression level. *Mol. Plant Pathol.* 13, 148–159. doi: 10.1111/j.1364-3703.2011.00737.x

Livak, K. J., and Schmittgen, T. D. (2001). Analysis of relative gene expression data using real-time quantitative PCR and the 2-ΔΔCT method. *Methods* 25, 402–408. doi: 10.1006/meth.2001.1262

Malhotra, A. (2009). "Tagging for protein expression," in *Methods in Enzymology Guide to Protein Purification*, eds R. R. Burgess and M. P. Deutscher (Amsterdam: Elsevier), 239–258.

Malhotra, K., Kim, S., and Sancar, A. (1994). Characterization of a medium wavelength type DNA photolyase: purification and properties of photolyase from *Bacillus firmus*. *Biochemistry* 33, 8712–8718. doi: 10.1021/bi00195a012

Mei, Q., and Dvornyk, V. (2015). Evolutionary history of the photolyase/cryptochrome superfamily in eukaryotes. *PLoS One* 10:e0135940. doi: 10.1371/journal.pone.0135940

Park, H. W., Kim, S. T., Sancar, A., and Deisenhofer, J. (1995). Crystal structure of DNA photolyase from *Escherichia coli*. *Science* 268, 1866–1872.

Pathak, R., Sundaram, A., Davidson, L. C., Solhaug, K. A., Stensvand, A., Gislerød, H. R., et al. (2017). Sensing of UV and visible light by powdery mildew pathogens. *Phytopathology* 107, 47–48.

Payne, G., and Sancar, A. (1990). Absolute action spectrum of E-FADH2 and E-FADH2-MTHF forms of *Escherichia coli* DNA photolyase. *Biochemistry* 29, 7715–7727. doi: 10.1021/bi00485a021

Pliego, C., Nowara, D., Bonciani, G., Gheorghe, D. M., Xu, R., Surana, P., et al. (2013). Host-induced gene silencing in barley powdery mildew reveals a class of ribonuclease-like effectors. *Mol. Plant Microbe Interact.* 26, 633–642. doi: 10.1094/MPMI-01-13-0005-R

Qi, T., Guo, J., Peng, H., Liu, P., Kang, Z., and Guo, J. (2019). Host-induced gene silencing: a powerful strategy to control diseases of wheat and barley. *Int. J. Mol. Sci.* 20:206. doi: 10.3390/ijms20010206

Sancar, A. (1994). Structure and function of DNA photolyase. *Biochemistry* 33, 2–9.

Sancar, A. (2003). Structure and function of DNA photolyase and cryptochrome blue-light photoreceptors. *Chem. Rev.* 103, 2203–2238. doi: 10.1021/cr0204348

Sancar, A. (2004). Photolyase and cryptochrome blue-light photoreceptors. *Adv. Protein Chem.* 69, 73–100.

Sancar, A. (2008). Structure and function of photolyase and in vivo enzymology: 50th anniversary. *J. Biol. Chem.* 283, 32153–32157. doi: 10.1074/jbc.R800052200

Sancar, G. B. (1990). DNA photolyases: physical properties, action mechanism, and roles in dark repair. *Mutat. Res.* 236, 147–160. doi: 10.1016/0921-8777(90)90002-m

Sancar, G. B., Jorns, M. S., Payne, G., Fluke, D. J., Ruper, C. S., and Sancar, A. (1987a). Action mechanism of *Escherichia coli* DNA photolyase. *J. Biol. Chem.* 262, 492–498.

Sancar, G. B., Smith, F. W., and Heelis, P. F. (1987b). Purification of the yeast PHR1 photolyase from an *Escherichia coli* overproducing strain and characterization of the intrinsic chromophores of the enzyme. *J. Biol. Chem.* 262, 15457–15465.

Sievers, F., Wilm, A., Dineen, D., Gibson, T. J., Karplus, K., Li, W., et al. (2011). Fast, scalable generation of high-quality protein multiple sequence alignments using Clustal Omega. *Mol. Syst. Biol.* 7:539. doi: 10.1038/msb.2011.75

Sinha, R. P., and Häder, D. P. (2002). UV-induced DNA damage and repair: a review. *Photochem. Photobiol. Sci.* 1, 225–236. doi: 10.1039/b201230h

Suthaparan, A., Pathak, R., Solhaug, K. A., and Gislerød, H. R. (2018). Wavelength dependent recovery of UV-mediated damage: tying up the loose ends of optical based powdery mildew management. *J. Photochem. Photobiol. B* 178, 631–640. doi: 10.1016/j.jphotobiol.2017.12.018

Suthaparan, A., Solhaug, K. A., Bjugstad, N., Gislerod, H. R., Gadoury, D. M., and Stensvand, A. (2016a). Suppression of powdery mildews by UV-B: application frequency and timing, dose, reflectance, and automation. *Plant Dis.* 100, 1643–1650. doi: 10.1094/PDIS-12-15-1440-RE

Suthaparan, A., Solhaug, K. A., Stensvand, A., and Gislerød, H. R. (2016b). Determination of UV action spectra affecting the infection process of *Oidium neolycopersici*, the cause of tomato powdery mildew. *J. Photochem. Photobiol. B* 156, 41–49. doi: 10.1016/j.jphotobiol.2016.01.009

Suthaparan, A., Solhaug, K. A., Stensvand, A., and Gislerød, H. R. (2017). Daily light integral and day light quality: potentials and pitfalls of nighttime UV treatments on cucumber powdery mildew. *J. Photochem. Photobiol. B* 175, 141–148. doi: 10.1016/j.jphotobiol.2017.08.041

Suthaparan, A., Stensvand, A., Solhaug, K. A., Torre, S., Mortensen, L. M., Gadoury, D. M., et al. (2012a). Suppression of powdery mildew (*Podosphaera pannosa*) in greenhouse roses by brief exposure to supplemental UV-B radiation. *Plant Dis.* 96, 1653–1660. doi: 10.1094/PDIS-01-12-0094-RE

Suthaparan, A., Stensvand, A., Solhaug, K. A., Torre, S., Telfer, K. H., Ruud, A. K., et al. (2012b). Suppression of cucumber powdery mildew by UV-B is affected by background light quality. *Phytopathology* 102:116.

Suthaparan, A., Stensvand, A., Solhaug, K. A., Torre, S., Telfer, K. H., Ruud, A. K., et al. (2014). Suppression of cucumber powdery mildew by supplemental UV-B radiation in greenhouses can be augmented or reduced by background radiation quality. *Plant Dis.* 98, 1349–1357. doi: 10.1094/PDIS-03-13-0222-RE

Suthaparan, A., Stensvand, A., Torre, S., Herrero, M. L., Pettersen, R. I., Gadoury, D. M., et al. (2010). Continuous lighting reduces conidial production and germinability in the rose powdery mildew pathosystem. *Plant Dis.* 94, 339–344. doi: 10.1094/PDIS-94-3-0339

Tagua, V. G., Pausch, M., Eckel, M., Gutiérrez, G., Miralles-Durán, A., Sanz, C., et al. (2015). Fungal cryptochrome with DNA repair activity reveals an early stage in cryptochrome evolution. *Proc. Natl. Acad. Sci. U.S.A.* 112, 15130–15135. doi: 10.1073/pnas.1514637112

Tamada, T., Kitadokoro, K., Higuchi, Y., Inaka, K., Yasui, A., De Ruiter, P. E., et al. (1997). Crystal structure of DNA photolyase from *Anacystis nidulans*. *Nat. Struct. Biol.* 4, 887–891.

Teranishi, M., Nakamura, K., Morioka, H., Yamamoto, K., and Hidema, J. (2008). The native cyclobutane pyrimidine dimer photolyase of rice is phosphorylated. *Plant Physiol.* 146, 1941–1951. doi: 10.1104/pp.107.110189

Thompson, C. L., and Sancar, A. (2002). Photolyase/cryptochrome blue-light photoreceptors use photon energy to repair DNA and reset the circadian clock. *Oncogene* 21, 9043–9056. doi: 10.1038/sj.onc.1205958

Van Delm, T., Melis, P., Stoffels, K., and Baets, W. (2014). Control of powdery mildew by UV-C treatments in commercial strawberry production. *Acta Hort.* 1049, 679–684.

Waterworth, W. M., Jiang, Q., West, C. E., Nikaido, M., and Bray, C. M. (2002). Characterization of *Arabidopsis* photolyase enzymes and analysis of their role in protection from ultraviolet-B radiation. *J. Exp. Bot.* 53, 1005–1015. doi: 10.1093/jexbot/53.371.1005

Weber, S. (2005). Light-driven enzymatic catalysis of DNA repair: a review of recent biophysical studies on photolyase. *Biochem. Biophys. Acta* 1707, 1–23. doi: 10.1016/j.bbabio.2004.02.010

Worthington, E. N., Kavaklı, I. H., Berrocal-Tito, G., Bondo, B. E., and Sancar, A. (2003). Purification and characterization of three members of the photolyase/cryptochrome family blue-light photoreceptors from *Vibrio cholerae*. *J. Biol. Chem.* 278, 39143–39154. doi: 10.1074/jbc.M305792200

Yajima, H., Inoue, H., Oikawa, A., and Yasui, A. (1991). Cloning and functional characterization of a eucaryotic DNA photolyase gene from *Neurospora crassa*. *Nucleic Acids Res.* 19, 5359–5362. doi: 10.1093/nar/19.19.5359

Zhang, M., Wang, L., and Zhong, D. (2017). Photolyase: dynamics and mechanisms of repair of Sun-Induced DNA damage. *Photochem. Photobiol.* 93, 78–92. doi: 10.1111/php.12695

Zhu, M., Riederer, M., and Hildebrandt, U. (2019). UV-C irradiation compromises conidial germination, formation of appressoria, and induces transcription of three putative photolyase genes in the barley powdery mildew fungus, *Blumeria graminis* f. sp. *hordei*. *Fungal Biol.* 123, 218–230. doi: 10.1016/j.funbio.2018.12.002

Conflict of Interest: The authors declare that the research was conducted in the absence of any commercial or financial relationships that could be construed as a potential conflict of interest.

Paper IV

PhytoFrontiers™
An Open Access Journal from The American Phytopathological Society

Research

Variation in UV-Mediated Damage Recovery Among *Pseudoidium neolycopersici* Isolates: Possible Mechanisms

Ranjana Pathak | Aruppillai Suthaparan † |

Department of Plant Sciences, Faculty of Biosciences, Norwegian University of Life Sciences, 1432 Ås, Norway

† Corresponding author: A. Suthaparan; aruppillai.suthaparan@nmbu.no

Accepted for publication 13 March 2021.

Abstract

The cryptochrome/photolyase family (CPF) consists of a diversified class of flavoproteins that are evolutionarily related. Although their domain architecture is highly conserved, they perform entirely different physiological functions. Previous studies have confirmed the presence of a functional photolyase in *Pseudoidium neolycopersici*, which repairs UV-C-induced DNA damage by using near UV-A/blue light as an energy source. Similar doses of UV-C treatment followed by incubation with dark or blue light was tested on conidia germination of five isolates of *P. neolycopersici* collected from different regions of Norway and the Netherlands. The results showed variations in the effect of UV on germination and germination recovery under blue light incubation after UV treatment. Evolutionary studies confirmed that *P. neolycopersici* photolyase is highly conserved among different isolates of *P. neolycopersici* and among different species. All CPF members have a core domain consisting of an identical cofactor, flavin adenine dinucleotide (FAD), and an additional photoantenna chromophore. An amino acid sequence analysis demonstrated that CPF members have highly conserved C terminals compared with their N terminals, because FAD binds in the C-terminal region. When compared with other CPF members, varying lengths of N and C terminals were noticed in *P. neolycopersici* photolyase and putative cryptochrome, respectively. Further research using comparative genomics targeting pyrimidine base composition, the role of regulatory elements, including promotor architecture, and the characterization of optical properties of native photolyase among isolates may help to explain the differences in the biological responses of conidia germination of *P. neolycopersici* treated with UV.

Keywords: photolyase, polymorphism, powdery mildew, tomato, ultraviolet

Author contributions
Design and execution of experiments by R.P. and A.S., data analysis and manuscript draft by R.P., and manuscript revision by A.S.

Funding
This research was financially supported by the Research Council of Norway, and Norwegian University of Life Sciences Ph.D. grant 1207051033.

e-Xtra: Supplementary materials are available online.

The author(s) declare no conflict of interest.

Powdery mildew caused by *Pseudoidium neolycopersici* is a significant threat to tomato production worldwide (Lebeda et al. 2017). Several strategies, including the application of fungicide and breeding for disease resistance, are currently used in the management of powdery mildews (Jones et al. 2001). However, the rapid emergence of fungicide-resistant pathogen isolates with the potential to quickly overcome the vertical resistance developed in crop varieties, coupled with high research costs, is discouraging investment in the development of fungicides and more resistant varieties. Furthermore, environmental and consumer concerns regarding the use of chemicals in crop production demands alternative strategies which are environmentally conscious. The use of optical radiation (ultraviolet [UV], visible, and infrared) in the management of powdery mildew pathosystems has been reported to be an efficient and environmentally friendly option for a wide range of crops at the experimental greenhouse level (Suthaparan et al. 2012a, b, 2014, 2016a). The efficiency of this strategy is dependent on the selection and combination of effective wavelengths, application time of the day (within a 24-h period), dose (level of irradiance and duration of exposure), and frequency (number of applications within the pathogen development cycle) (Suthaparan et al. 2016a, b, 2017, 2018). Within the optical radiation range tested, a UV range of 250 to 290 nm and a red-light range of 635 to 680 nm have shown a potential to combat powdery mildews (Suthaparan et al. 2016b, 2018). UV has been known to induce damage to DNA, primarily in the form of the formation of dimers between two adjacent pyrimidine nucleotides on the same strand (Sinha and Häder 2002). The existence of this damage inhibits the transcription process of genes and replication process of DNA, which then leads to cell cycle arrest and, ultimately, cell death (Jenkins et al. 2000; Sancar 1994; Tornaletti et al. 1999).

Cryptochromes (CRY) and photolyases (PHR) are evolutionarily related flavoproteins with structural similarity; however, they have distinct physiological roles (Kavakli et al. 2017). The key difference in gene structures between CRY and PHR is that CRY have an extra C-terminal extension, with great variation among different groups of CRY (Chaves et al. 2006; Mei and Dvornyk 2015). All CRY/PHR family (CPF) members contain a core domain, which is highly conserved and subjected to carrying out catalytic activity (Chaves et al. 2006). PHR-mediated DNA damage repair is the most efficient mechanism in relation to other reported mechanisms of recombination repair and nucleotide excision repair (Jans et al. 2005; Manova and Gruszka 2015). PHR are the members of the blue light photoreceptors, which absorb photons in the near-UV/blue regions (300 to 500 nm) as an energy source and repair damage caused by UV in DNA (Sancar 2008; Thompson and Sancar 2002). The enzyme was first functionally characterized in *Escherichia coli*, followed by several other organisms, including fungi, with the exception of placental mammals and a few other species (Mei and Dvornyk 2015; Sancar et al. 1984; Yajima et al. 1991).

As obligate biotrophic phytopathogens with hyaline appearance (except the ascocarp), fungi that cause powdery mildews were assumed to be host dependent for environmental signaling, especially in relation to optical environments. Recent studies have confirmed the presence of genes similar to all major classes of photoreceptors in the range of fungal species that cause powdery mildews in grapevine, tomato, cucumber, and strawberry (Pathak et al. 2017; Suthaparan et al. 2012b). An in-depth sequence analysis of *P. neolycopersici*, *Podosphaera xanthii*, and *P. aphanis* genomes revealed the presence of three putative genes similar to CPF (unpublished data). Further studies on *Pseudoidium neolycopersici* CPF genes with the assistance of an *E. coli* expression system revealed that only one among the three CPF genes is a functional PHR, with the possible presence of flavin adenine dinucleotide (FAD) as a catalytic cofactor and 5,10-methenyltetrahydrofolate (MTHF) as a photoantenna cofactor. The action spectra of *P. neolycopersici* conidia germination recovery and survival of *E. coli* cells both reveal that the action spectra of *P. neolycopersici* PHR falls within the 360- to 460-nm range (Pathak et al. 2020).

However, preliminary studies have shown variation in the efficiency of nighttime UV treatment in the suppression of powdery mildews in cucumber and tomato (unpublished data). In this study, we tested the *P. neolycopersici* isolates collected from different geographical regions for (i) UV tolerance in the conidial germination process, (ii) nucleotide sequence similarity of CPF genes, (iii) phylogenetic classification, and (iv) amino acid sequence conservation of CPF genes in relation to other CPF-like genes available in NCBI.

MATERIALS AND METHODS

Collection and maintenance of *P. neolycopersici* isolates

Four isolates of *P. neolycopersici* collected from different locations in Norway and one isolate from the Netherlands were used in this study. These isolates were named according to their collection locations: Akershus (As), Vestfold (Vf), Finnøy (Fn), and Sandnes (Sn) in Norway, and the Netherlands (Nl).

Powdery mildew-sensitive Espero tomato plants were used to maintain all five isolates of powdery mildew collected from different regions. Tomato plants were propagated by seed and grown in controlled-environment chambers with an air temperature and relative humidity (RH) of 20 ± 2°C and 75 ± 5%, respectively. A daily light cycle of 16 h with an irradiance of 110 ± 10 μmol m^{-2} s^{-1} was provided using high-pressure mercury lamps (Powerstar HQI-BT 400 W/D day light; OSRAM GmbH).

Disease-free Espero tomato leaflets were surface disinfested by soaking in 3% (vol/vol) sodium hypochlorite solution for 3 min, followed by three sequential rinses with sterilized distilled water, and placed in 9-cm Petri dishes containing 1% agar (wt/vol) and 0.03% benzimidazole. To prepare a single-cell isolate from the disease population, a single conidium of each isolate was isolated from the diseased leaves and transferred to the abovementioned surface-disinfested leaflets. All inoculated leaflets in Petri dishes were sealed with parafilm and incubated in a chamber for 10 days with an air temperature of 20 ± 2°C and 16 h of daily light supplied by warm white fluorescent lamps. The level of irradiance at the top of the Petri dish lid was 50 μmol m^{-2} s^{-1}. This process was repeated every 10th day (with visible powdery mildew) for each single-cell isolate in order to multiply them. After a few cycles of repetition of the above process, leaflets with 10-day-old colonies with proficient sporulation were used to prepare conidial suspension using sterilized distilled water containing Tween-20 (20 μl/liter). The concentration of the suspension was adjusted to 4×10^4 conidia/ml. Disease-free Espero tomato plants with five fully developed leaves, propagated in a controlled-environment chamber as described above, were moved to five controlled-environment chambers with similar environmental conditions. The tomato plants were then inoculated by spraying each plant with 20 ml of the conidial suspension as described above, with each suspension prepared with dedicated *P. neolycopersici* isolates. For Petri dish level conidia germination experiments, 8- to 9-day-old

inoculum was used. For conidia germination experiments, 5-cm Petri dishes were used.

UV tolerance and germination recovery of *P. neolycopersici* isolates

To determine the UV tolerance of the conidia germination process among the collected isolates, Petri-dish-level experiments were performed in controlled-environment chambers with an air temperature of 20 ± 2°C and RH of 75 ± 5%. Factorial experiments with four factors (isolates, treatment condition, duration of exposure, and incubation condition) were designed. Conidia were dusted on the surface of a 1% water agar media contained in Petri dishes. Immediately after inoculation, Petri dishes without lids were exposed to (i) complete darkness or (ii) UV-C with an irradiance of 2 ± 0.2 μmol m^{-2} s^{-1}, or (iii) UV-C with an irradiance of 4 ± 0.2 μmol m^{-2} s^{-1}. The durations of exposure were (i) 10 s, (ii) 20 s, or (iii) 30 s. Immediately after UV treatments, the Petri dishes were sealed and transferred to incubation chambers with lighting conditions of (i) complete darkness for 24 h or (ii) blue light with an irradiance of 25 ± 5 μmol m^{-2} s^{-1} for 2 h followed by 22 h of darkness. The conidia were assessed for germination with a light microscope 24 h after inoculation, and 50 conidia were counted for germination using a handheld tally counter. The percent germination was calculated relative to the non-UV control samples. Conidia with germ tubes equal to or longer than the conidial width were counted as successfully germinated while conidia with germ tubes less than the conidial width were considered nongerminated (Suthaparan et al. 2018). The experiment was repeated twice, with three replicated Petri dishes in each experiment.

UV irradiance with a wavelength peak at 254 nm was supplied by 120-W germicidal UV-C fluorescent tubes (Light Tech, U.S.A.). Blue light with a peak at a 454 nm wavelength was provided by a 15-W GreenPower LED module HF blue (Philips, The Netherlands). An Optronic model 756 spectroradiometer (Optronic Laboratories, Orlando, FL, U.S.A.) was used to measure spectral composition and level of irradiances (Supplementary Fig. S1). The temperature and RH of the controlled-environment chambers at Petri dish level were recorded at 5-min intervals using a Priva greenhouse computer (Priva, Zijlweg, The Netherlands) connected to dry and wet bulb thermosensors.

The data analysis was performed using the general linear mixed-effect model, with experimental repeat and replicate as a random effect and isolate type, UV, incubation treatment, and their interactions as fixed effects. Treatment means were separated by way of Tukey's pairwise comparison at $P = 0.05$ (Minitab 18.1; Minitab Corp., State College, PA, U.S.A.). Graphs were plotted using SigmaPlot 10.0 (Systat Software, Inc.).

Comparison of sequence similarity of CPF genes among *P. neolycopersici* isolates

Fungal conidia were harvested from 2-week-old inoculum from diseased tomato plants grown in controlled-environment chambers. Diseased leaves were touched on water agar, and the water agar surfaces were then scraped with a sterile glass slide and conidia were collected in 2-ml Eppendorf tubes. The collected conidia were flash frozen in liquid nitrogen. DNA was extracted using the modified cetyltrimethylammonium bromide method described previously (Robinson et al. 2002), with slight modifications (Supplementary Data S1.1). The quantity and quality of the DNA were measured and checked by a NanoDrop 2000 spectrophotometer (Thermo Fisher Scientific) and agarose gel electrophoresis (Bio-Rad Laboratories), respectively.

The presence of three CPF-like genes and respective coding sequences were identified and characterized with draft genome assembly and transcriptome data of *P. neolycopersici* (isolate As). OINE01015670_T110144, OINE01000912_T103440, and OINE01005061_T102555 were identified in *P. neolycopersici* (NCBI GenBank accession numbers MT277359, MT277360, and MT277361, respectively), hereafter referred to as *PN5670, PN0912*, and *PN5061*, respectively. Known sequences of these genes were divided into 7 to 10 segments with amplicon sizes of 1,006 to 1,135 bp and overlaps of approximately 180 to 200 bp. Primer pairs for each segment were designed (Supplementary Table S1) and three target genes (*PN5670, PN0912*, and *PN5061*) were PCR amplified using genomic DNA extracted from five isolates (As, Vf, Fn, Sn, and Nl) as templates.

The target fragments were PCR amplified using a Phusion Green Hot Start II High-Fidelity PCR Master Mix (Thermo Scientific) with the following PCR program: initial denaturation at 98°C for 30 s; 35 cycles of denaturation at 98°C for 10 s, annealing at 52°C for 30 s, and extension at 72°C for 80 s; followed by a final extension at 72°C for 10 min. PCR amplicons were analyzed using agarose gel (0.8%) electrophoresis (Bio-Rad Laboratories). Amplified fragments were purified using a QIAquick PCR purification kit (Qiagen, Germany). Amplicons were sequenced in both directions (forward and reverse) using the same primers as used in the abovementioned PCR amplification (Supplementary Table S1). Sequencing runs were performed by GATC Biotech, Germany, using an ABI PRISM BigDye Terminator v3.1 Cycle Sequencing Kit on an ABI 3730XL DNA Analyzer (Applied Biosystems).

The raw sequencing reads were trimmed manually using BioEdit v 7.2.5 (Hall 1999) at both ends prior to alignment, then aligned against their respective reference gene sequences (obtained from a draft genome of the As isolate), which were used to design primers. Multiple sequence alignment was carried out by means of MultAlin Interface (Corpet 1988) using default settings (gap penalty at opening and extension) without additional settings. The progressive pairwise alignment of closely related groups of sequences was carried out to achieve a multiple sequence alignment (Corpet 1988). Technical sequencing errors were corrected, and aligned reads were analyzed for the presence of any variations (single-nucleotide variations, insertions, and deletions).

Phylogenetic analysis of CPF-like genes

Amino acid sequences of CPF-like genes from 10 ascomycetes and 17 other representative members (Table 1) (Supplementary Data S1.2) were searched for and obtained from the NCBI (https://www.ncbi.nlm.nih.gov/), in addition to the deduced amino acid sequences of three CPF-like genes from five isolates of *P. neolycopersici.* Because the amino acid sequences of all five isolates were identical, only three CPF-like genes from one isolate were included in the construction of a phylogenetic tree. These selected CPF-like genes are already reported and extensively studied (Kavakli et al. 2017; Ozturk 2017; Tagua et al. 2015; Thompson and Sancar 2002). A multiple sequence alignment of amino acid sequences was carried out using ClustalW with default parameters. A MEGAX (v.10.0.5) software package was used to perform a phylogenetic analysis and an unrooted tree of sequence data was constructed by means of a neighbor-joining algorithm with 1,000 bootstrap replicates (Tamura et al. 2013).

TABLE 1

Amino acid sequence GenBank accession numbers of cryptochrome/photolyase family-like genes used in the phylogenetic analysis[a]

Seq.[b]	Species and taxa	GenBank protein accession number	Designated name
1	***Escherichia coli***	**NP_415236.1**	***E. coli* DNA PHR**
2	*Bacillus cereus*	WP_001179969.1	*B. cereus* PHR like
3	*Bacillus thuringiensis*	WP_001179974.1	*B. thuringiensis* PHR like
4	*Caulobacter vibrioides*	YP_002516868.1	*C. vibrioides* PHR like
5	*Methanobacter thermoautotrophicus*	WP_010876537.1	*M. thermoautotrophicus* DNA PHR
6	*Salmonella typhimurium*	NP_459694.1	*S. enterica* DNA PHR like
7	***Vibrio cholerae***	**NP_231448.1**	***V. cholerae* DNA PHR like**
8	*Agrobacterium tumefaciens*	WP_038490669.1	*A. tumefaciens* DNA PHR like
9	***Anacystis nidulans***	**WP_011377448.1**	***A. nidulans* DNA PHR**
10	*Saccharomyces cerevisiae*	NP_015031.1	*S. cerevisiae* PHR1
11	*Alternaria alternata*	XP_018380931.1	*A. alternata* cryptochrome DASH like
12	*Alternaria alternata*	XP_018388382.1	*A. alternata* cryptochrome2
13	*Aspergillus nidulans*	XP_657991.1	*A. nidulans* PHR like
14	*Aspergillus niger*	XP_001397458.2	*A. nidulans* DNA PHR
15	*Aspergillus niger*	XP_001402217.1	*A. nidulans* DNA PHR like
16	*Blumeria graminis* f. sp. *hordei*	CCU75260.1	*B. graminis* f. sp. *hordei* cryptochrome DASH
17	*Blumeria graminis* f. sp. *hordei*	CCU75653.1	*B. graminis* f. sp. *hordei* cryptochrome like
18	*Blumeria graminis* f. sp. *hordei*	CCU77936.1	*B. graminis* f. sp. *hordei* DNA PHR
19	*Blumeria graminis* f. sp. *tritici*	EPQ63205.1	*B. graminis* f. sp. *tritici* DNA PHR
20	*Blumeria graminis* f. sp. *tritici*	EPQ63708.1	*B. graminis* f. sp. *tritici* DNA PHR
21	*Blumeria graminis* f. sp. *tritici*	EPQ64280.1	*B. graminis* f. sp. *tritici* DNA PHR
22	*Botrytis cinerea*	XP_001548442.2	*B. cinerea* Bccry1
23	*Botrytis cinerea*	XP_024550731.1	*B. cinerea* Bccry2
24	*Erysiphe necator*	KHJ30144.1	*E. necator* DNA PHR like
25	*Erysiphe necator*	KHJ34441.1	*E. necator* DNA PHR like
26	*Erysiphe necator*	KHJ35948.1	*E. necator* cryptochrome DASH like
27	*Fusarium fujikuroi*	XP_023425040.1	*F. fujikuroi* PHR like
28	*Fusarium fujikuroi*	XP_023428189.1	*F. fujikuroi* DNA PHR like
29	*Fusarium fujikuroi*	XP_023431896.1	*F. fujikuroi* DNA PHR like
30	*Fusarium oxysporum*	XP_018235323.1	*F. oxysporum* f. sp. *lycopersici* cryptochrome
31	*Golovinomyces cichoracearum*	RKF54075.1	*G. cichoracearum* DNA PHR
32	*Golovinomyces cichoracearum*	RKF65157.1	*G. cichoracearum* cryptochrome-2
33	*Golovinomyces cichoracearum*	RKF80931.1	*G. cichoracearum* cryptochrome DASH like
34	***Neurospora crassa***	**XP_964834.2**	***N. crassa* DNA PHR**
35	***Neurospora crassa***	**XP_965722.3**	***N. crassa* cryptochrome DASH like**
36	***Pseudoidium neolycopersici***	**QKE45385.1**	***P. neolycopersici* cryptochrome like***
37	***Pseudoidium neolycopersici***	**QKE45387.1**	***P. neolycopersici* DNA PHR***
38	***Pseudoidium neolycopersici***	**QKE45389.1**	***P. neolycopersici* cryptochrome DASH like***
39	*Trichoderma atroviride*	XP_013938084.1	*T. atroviride* DNA PHR*1*
40	*Trichoderma atroviride*	XP_013941790.1	*T. atroviride* PHR like
41	*Trichoderma atroviride*	XP_013942035.1	*T. atroviride* DNA PHR like
42	***Arabidopsis thaliana***	**NP_566520.1**	***A. thaliana* DNA PHR family protein**
43	***Arabidopsis thaliana***	**NP_568461.3**	***A. thaliana* cryptochrome-3**
44	*Arabidopsis thaliana*	NP_171935.1	*A. thaliana* cryptochrome-2
45	*Arabidopsis thaliana*	NP_563906.1	*A. thaliana* DNA PHR II
46	*Arabidopsis thaliana*	NP_567341.1	*A. thaliana* cryptochrome-1
47	*Brassica rapa*	NP_001288891.1	*B. rapa* cryptochrome-1
48	*Brassica rapa*	XP_009110652.1	*B. rapa* DNA PHR
49	*Brassica rapa*	XP_009111106.1	*B. rapa* cryptochrome-2
50	*Brassica rapa*	XP_009111643.1	*B. rapa* cryptochrome DASH like
51	*Brassica rapa*	XP_009115387.1	*B. rapa* (6-4) PHR
52	*Glycine max*	NP_001235220.1	*G. max* cryptochrome-2
53	*Glycine max*	NP_001238710.2	*G. max* CPD PHR
54	*Glycine max*	NP_001242152.1	*G. max* cryptochrome-1 like
55	*Zea mays*	NP_001130580.1	*Z. mays* type II CPD DNA PHR
56	*Zea mays*	XP_008677763.1	*Z. mays* cryptochrome-2
57	***Drosophila melanogaster***	**NP_724274.1**	***D. melanogaster* (6-4) PHR**
58	*Drosophila melanogaster*	NP_523653.2	*D. melanogaster*
59	*Drosophila melanogaster*	NP_732407.1	*D. melanogaster* cryptochrome
60	***Homo sapiens***	**XP_024304612.1**	***H. sapiens* cryptochrome-1**
61	*Homo sapiens*	NP_066940.3	*H. sapiens* cryptochrome-2
62	*Gallus gallus*	NP_989575.1	*G. gallus* cryptochrome-2
63	*Gallus gallus*	NP_989576.1	*G. gallus* cryptochrome-1
64	*Mus musculus*	NP_031797.1	*M. musculus* cryptochrome-1
65	*Mus musculus*	NP_034093.1	*M. musculus* cryptochrome-2

[a] The highlighted (bold) sequences of representative model organisms, including three cryptochrome/photolyase family-like genes (indicated by an asterisk [*]) from *Pseudoidium neolycopersici*, were also used in amino acid alignment analysis. PHR = photolyase; DASH = *Drosophila*, *Arabidopsis*, *Synechocystis*, *Human*; and CPD = cyclobutane pyrimidine dimer.

[b] Sequence number.

Amino acid sequence alignment and analysis

The deduced amino acid sequence for an open reading frame (ORF) of three CPF-like genes (*PN5670, PN0912*, and *PN5061*) of *P. neolycopersici* was compared with amino acid sequences of nine other representative members of CPF (Supplementary Data S1.2). The selected members are extensively studied model organisms. These CPF sequences were also retrieved from NCBI (https://www.ncbi.nlm.nih.gov/) and also included in the phylogenetic analysis. Alignment was performed using Vector NTI Advance 11.5.4 (Invitrogen).

RESULTS

UV tolerance and germination recovery of *P. neolycopersici* isolates

All factors of isolate type, level of UV irradiance, duration of UV exposure, incubation light condition, and isolate–incubation light interaction showed a significant effect on the germination efficiency of conidia ($P < 0.0001$). Independent of isolate type, UV treatments of 2 or 4 μmol m^{-2} s^{-1} followed by dark incubation significantly reduced conidia germination (<30%) compared with the non-UV control (>90%) (Fig. 1A and C). Germination efficiency was found to decrease with increased duration of UV exposure.

The conidial germination efficiency of all isolates was recovered as in the non-UV control, when samples were incubated with blue light after brief UV treatment. The highest germination efficiency was recorded in the isolate from the Netherlands (78 to 89%) followed by the isolate from Finnøy (62 to 77%). All other isolates showed slightly lower germination efficiency of conidia (35 to 66%), independent of UV irradiance level and duration of exposure (Fig. 1B and D).

Nucleotide sequence analysis of CPF genes in *P. neolycopersici* isolates

A nucleotide sequence analysis of three CPF genes (*PN5670, PN0912*, and *PN5061*) showed no polymorphism among the five *P. neolycopersici* isolates collected from different geographical

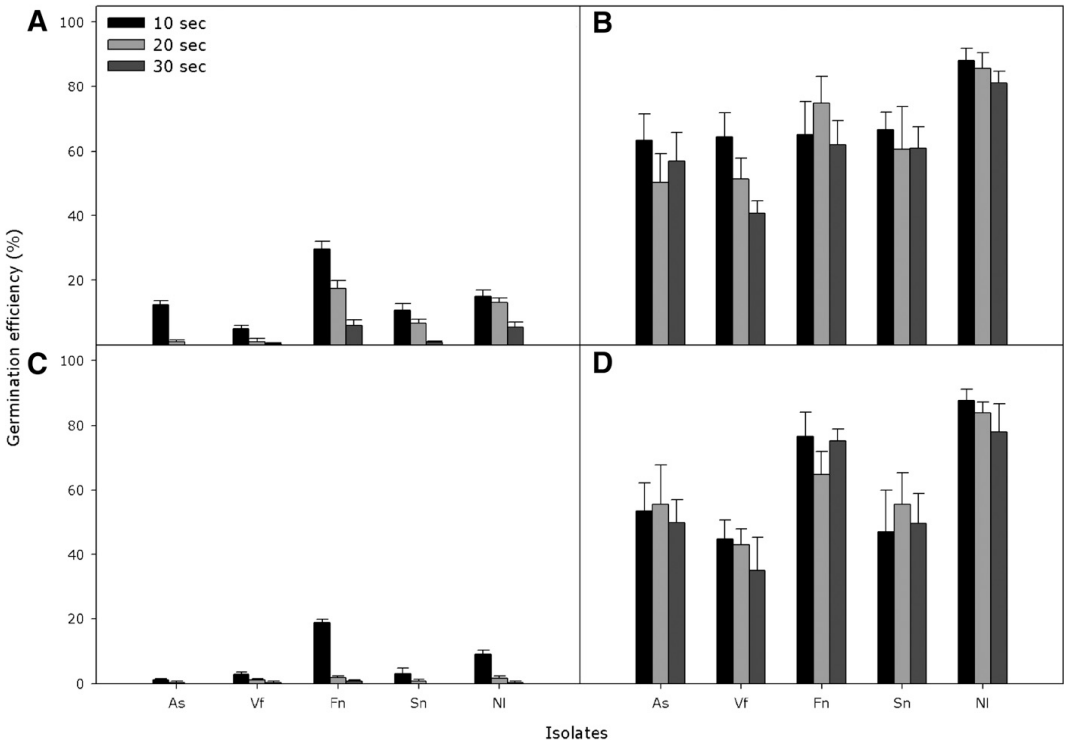

FIGURE 1
Effect of brief UV treatments and subsequent incubation wavelengths on the conidial germination efficiency of five different isolates of *Pseudoidium neolycopersici*. Conidia from 8- to 9-day-old colonies with profound sporulation collected from isolates from Akershus (As), Vestfold (Vf), Finnøy (Fn), Sandnes (Sn), or the Netherlands (Nl) were dusted on a water agar surface in 5-cm Petri dishes, and exposed to brief UV-C (peak of 254 nm) treatments (10, 20, or 30 s) of **A,** 2 ± 0.2 μmol m^{-2} s^{-1} followed by complete darkness; **B,** 2 ± 0.2 μmol m^{-2} s^{-1} followed by 2 h of blue light (454 nm) followed by complete darkness; **C,** 4 ± 0.2 μmol m^{-2} s^{-1} followed by complete darkness; or **D,** 4 ± 0.2 μmol m^{-2} s^{-1} followed by 2 h of blue light (454 nm) followed by complete darkness. Samples were assessed for conidia germination 24 h after inoculation under a light microscope. The percent germination was calculated relative to non-UV-treated control samples. Values are the mean ± standard error of two experiments, each with three replicates ($n = 6$).

regions. The alignments of PCR-amplified and sequenced products for above three genes are presented in Supplementary Figure S2.A, B, and C.

Phylogenetic analysis

Phylogenetic analysis showed that three CPF-like genes (*PN5670, PN0912*, and *PN5061*) from *P. neolycopersici* clustered with CRY, type I cyclobutane pyrimidine dimer (CPD) PHR, and CRY-*Drosophila*, *Arabidopsis*, *Synechocystis*, *Human* (DASH), respectively, together with the other CPF-like genes (Fig. 2).

Amino acid sequence analysis of *P. neolycopersici* CPF-like genes

Amino acid sequences of the ORF for three CPF-like genes identified in *P. neolycopersici* were compared with the ORF of the other representative members of CPF-like proteins, CRY, (6-4) PHR, CPD PHR, and CRY-DASH, which belong to humans, plants, bacteria, fungi, and insects. *PN5670* showed a 34 to 38% sequence homology to human CRY and (6-4) PHR from *Drosophila melanogaster* and *Arabidopsis thaliana*. *PN5061* showed a 48% sequence homology to CRY-DASH from *Neurospora crassa* and 32% homology to CRY-DASH from *A. thaliana* and cry1 from *Vibrio cholera*. *PN0912* showed a 57% sequence homology to CPD PHR from *N. crassa* and 35 to 41% homology to *E. coli* and *Anacystis nidulans* (Fig. 3).

In addition, *PN0912* showed a protruding N-terminal end of 134 amino acid residues similar to *N. crassa* PHR, which was 106 amino acid residues long, and also showed sequence homology in this region. These protruding amino (N) terminal ends were not observed in *E. coli* and *A. nidulans* PHR (Fig. 3).

Amino acid sequence alignment also showed three crucial residues (W277, M345, and N378) as well as a tryptophan triad (W306, W359, and W382), which are highly conserved in CPF members. The alignment showed higher conservation of amino acid residues in the C-terminal ends compared with N-terminal ends. It was also observed that, among all CPF protein members, CRY have considerably longer C-terminal ends compared with PHR, which were observed in *PN5670* and *PN5061* (Figs. 3 and 4).

DISCUSSION

The variation in germination recovery among the tested isolates of *P. neolycopersici* indicates that there is a difference in the efficiency of PHR-mediated UV damage recovery. However, the identical sequences of PHR genes among all tested *P. neolycopersici* isolates (Supplementary Fig. S2) suggests that this biological variation in germination recovery is not due to the sequence variation in the coding regions of PHR genes. PHR are globular proteins having one catalytic cofactor of FAD and an additional cofactor that serves as photoantenna (Vechtomova et al. 2020). Depending on the type and number of additional photoantenna present, the absorption and action spectrum will vary. This can lead to variation in the efficiency of PHR-mediated UV damage recovery. In our previous study, we identified FAD and MTHF as possible cofactors present in *P. neolycopersici* PHR. However, this was based on a structure prediction model and optical properties of heterologous PHR protein expressed in *E. coli* (Pathak et al. 2020). Despite the potential variation in cofactors among the isolates of the same species, an examination of optical properties of native proteins of *P. neolycopersici* PHR may explain the possible reason for underlying biological variation. In addition to optical properties of PHR, the expression level of a PHR gene and its translation efficiency may also affect the efficiency of PHR-mediated UV damage recovery. Detailed studies on the promoter architecture and transcription binding sites may have revealed information beyond the findings of this study. In filamentous fungi, it has been demonstrated that PHR gene upregulation by blue/visible light requires a blue-light-responsive *cis* element in the promotor region of the gene (Kihara et al. 2004). However, little is known about the role and variation of the *cis* element among isolates of the same species. It has been reported that the expression of PHR was induced by white collar 1 in *Ustilago maydis* (Brych et al. 2016). Hence, it is also important to examine the role of regulatory genes involved in the expression of PHR.

The same UV dose showed different effect patterns of UV on the germination of isolates. Two isolates seemed more tolerant, whereas the remaining three isolates were sensitive to the same dosage of UV (Fig. 1). This variation in UV response of fungal isolates may reflect the natural adaptations to their different environmental conditions. The daily optical environment in which organisms thrive, and how they adapt or optimize their genomic and proteomic features to survive in that particular environment, is an important aspect (Zhou et al. 2007). UV radiation has shown great potential in controlling powdery mildew diseases in different crops at the greenhouse level (Suthaparan et al. 2012a, b, 2014, 2016a). Exploring the tolerance or sensitivity to UV of fungal isolates is considered to be an important step in identifying a promising UV dose in UV-mediated powdery mildew disease management. The variation in response to UV among isolates may also be explained by one of the important genomic features, base composition; most importantly, the dinucleotide composition in the genome of a species (Zhou et al. 2007). A major type of UV-induced lesion is CPDs, which are formed between two adjacent pyrimidine nucleotides (Sancar 2008). Therefore, a high pyrimidine content in a genome may lead to the formation of more CPDs that, in turn, leads to a lower repair efficiency or a higher cell death.

All CPF members possess a core domain approximately 500 amino acid residues long but differ significantly in relation to N- and C-terminal extensions (Chaves et al. 2006). The C-terminal ends are highly conserved compared with N-terminal ends as a catalytic cofactor (FAD), which is common to all CPF members, binds in the C-terminal ends (Essen and Klar 2006). The protruding amino terminal ends which were observed in *P. neolycopersici* and *N. crassa* PHR showed a significant similarity in amino acid residues (Figs. 3 and 4). These amino acid residues have homology to a known cleavage site that enables the transport of the mitochondrial leucyl-tRNA synthetase into mitochondria in *N. crassa* (Chow et al. 1989). *Saccharomyces cerevisiae* also possess protruding amino terminal ends which play an important role in transporting PHR into mitochondria, and are capable of repairing pyrimidine dimers in nuclei as well as in mitochondria (Yasui et al. 1992). On the other hand, *S. cerevisiae* expressing an *E. coli* PHR was able to repair a fraction of pyrimidine dimers present in the nucleus but not in mitochondria, likely because *E. coli* PHR lacks a protruding N-terminal signal sequence, which is required for subcellular localization to these organelles (Prakash 1975; Yasui et al. 1992). These protruding amino terminal ends are characteristics only found in fungal PHR, which suggests that they may act as signal sequences with an

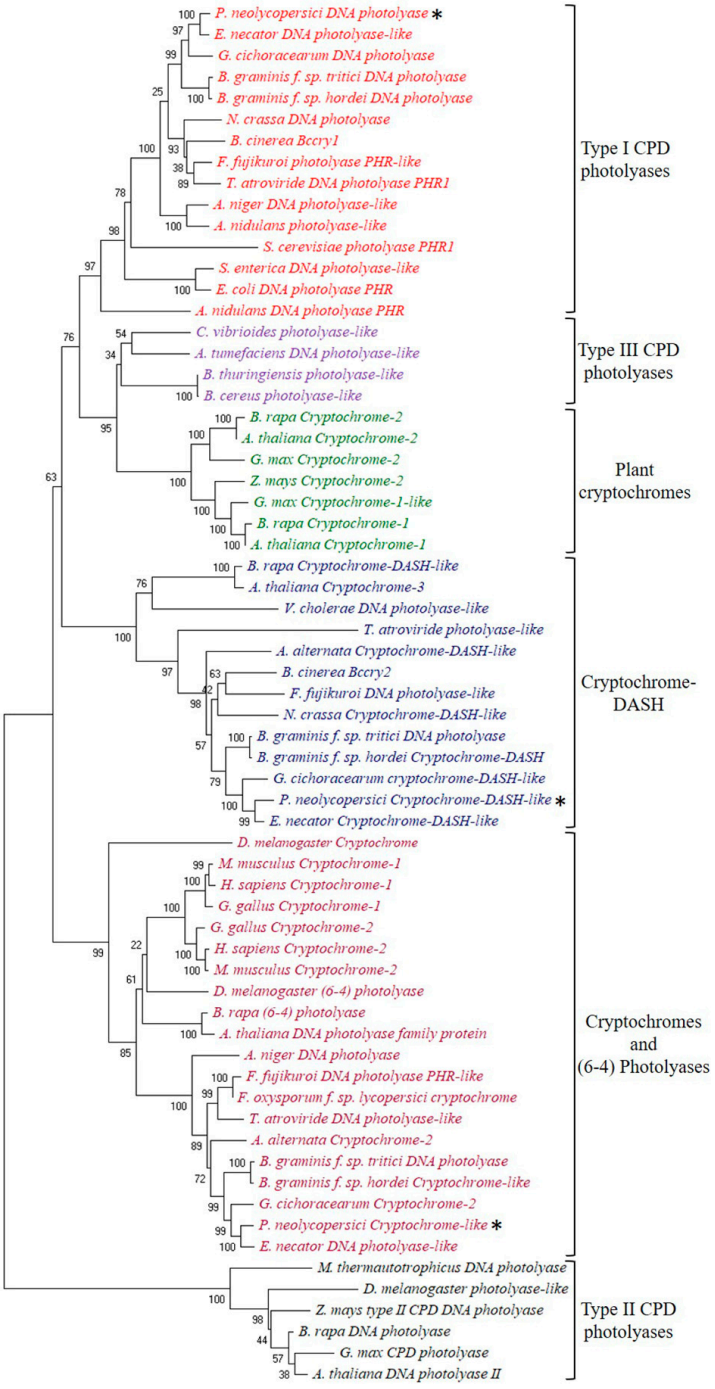

FIGURE 2

Phylogenetic analysis of cryptochrome/photolyase family (CPF)-like genes, including CPF-like genes from *Pseudoidium neolycopersici* (indicated by an asterisk [*]). The neighbor- joining method was used to construct an unrooted phylogenetic tree. The bootstrap probability of 1,000 replicates is expressed in percentages.

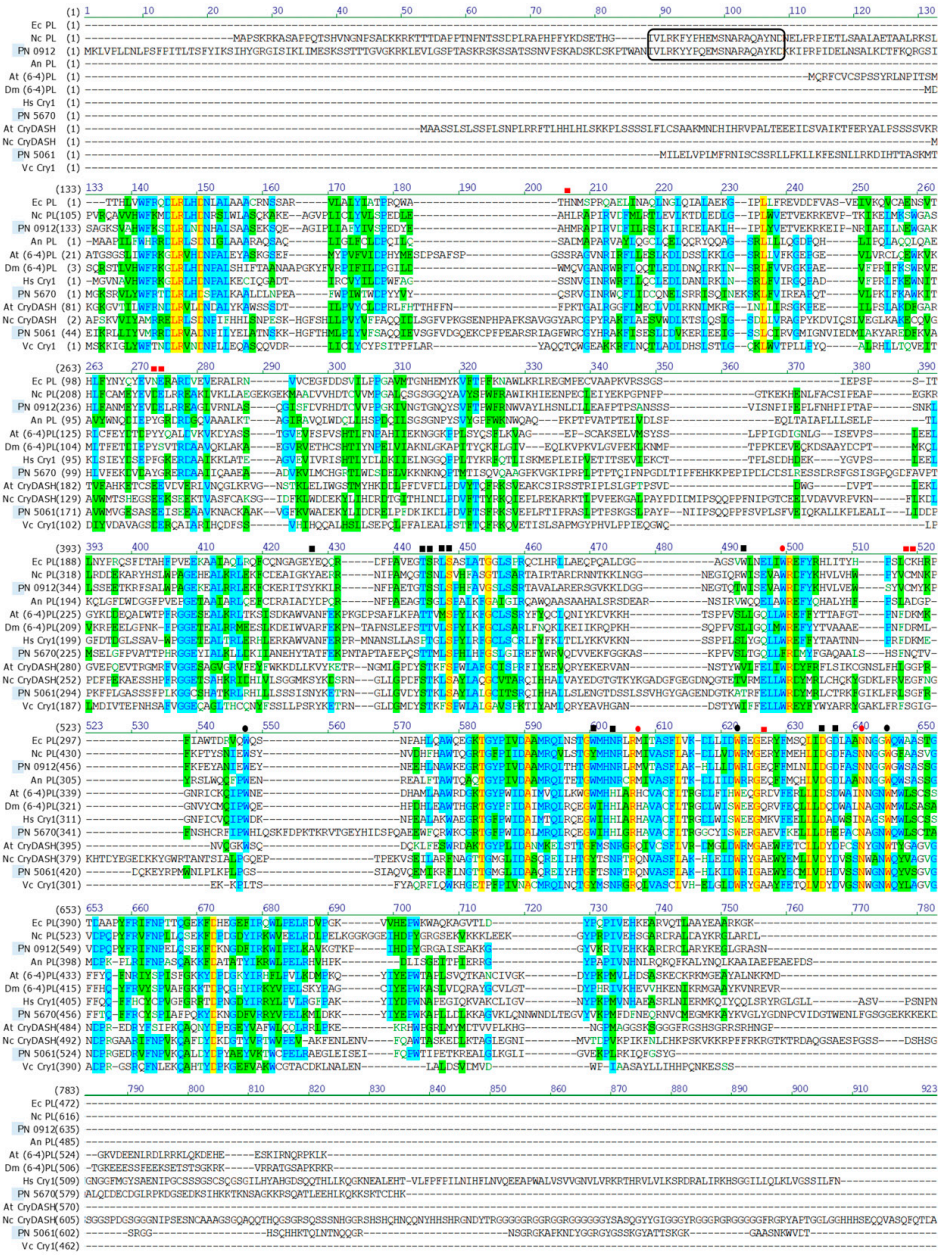

FIGURE 3

Comparative analysis of amino acid sequences of three cryptochrome/photolyase family (CPF)-like genes of *Pseudoidium neolycopersici* (*PN5670*, *PN0912*, and *PN5061*) with other CPF members from *Anacystis nidulans* (An); *Escherichia coli* (Ec); *Neurospora crassa* (Nc); *Arabidopsis thaliana* (At); *Drosophila melanogaster* (Dm); *Homo sapiens* (Hs); and *Vibrio cholerae* (Vc). Alignment was performed using the Vector NTI software program. The black rectangular box showing the homology region, which includes an identical probable signal sequence, RKYYPQ in *P. neolycopersici* to RKFYPH in *N. crassa*. Colors: yellow = identical; green = block conservation; and blue = highly conserved. Symbols: black squares = flavin adenine dinucleotide interactions; red squares = 5,10-methenyltetrahydrofolate interactions; black circles = tryptophan triad (W306, W359, and W382); and red circles = crucial residues (W277, M345, and N378). Abbreviations: PL = cyclobutane pyrimidine dimer photolyase; (6-4) PL = (6-4) photolyase; Cry = cryptochrome; and cry-DASH = cryptochrome-*Drosophila*, *Arabidopsis*, *Synechocystis*, *Human*.

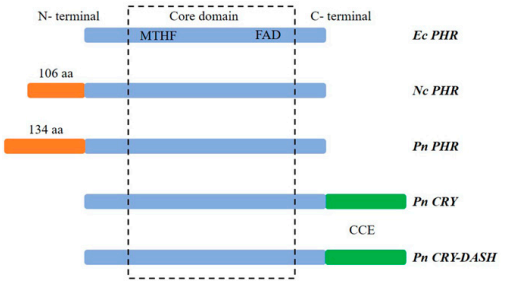

FIGURE 4

Diagrammatic representation of the comparison of cryptochrome (CRY)/photolyase family (CPF)-like genes (*PN5670*, *PN0912*, and *PN5061*) identified in *Pseudoidium neolycopersici* (Pn) with *Escherichia coli* (Ec) and *Neurospora crassa* (Nc) photolyase, showing an N-terminal end, core domain consisting of a flavin adenine dinucleotide (FAD) and 5,10-methenyltetrahydrofolate (MTHF), and a C-terminal end. Fungal photolyases (*phr*) of *N. crassa* and *P. neolycopersici* showed protruding N-terminal ends of 106 and 134 amino acid residues long, respectively. *P. neolycopersici* CRY and CRY-*Drosophila*, *Arabidopsis*, *Synechocystis*, *Human* (CRY-DASH) show Cry C-terminal extensions (CCE).

important role in PHR translocation in *P. neolycopersici* (Fig. 3). Additionally, a tryptophan triad (trp triad) was found to be conserved among PHR, including class I, class II CPD PHR, and (6-4) PHR. Previously, it was reported that this trp triad provides an alternative electron-transfer pathway (W306→W359→W382→$FADH^{\bullet}$) (Fig. 3) (Weber 2005; Zhang et al. 2017). Another three critical residues (W277, M345, and N378) (Fig. 3) are found to be distributed in this superfamily. Residue trp277 (W277) is crucial for substrate binding and plays a role in CPD splitting. Met345 (M345) is restricted to CPD PHR because it discriminates CPD PHR from rest of the superfamily. Asn378 (N378) is highly conserved in the whole superfamily because it stabilizes the neutral FAD radical (Xu and Zhu 2010).

Among different species, CPF members share a highly conserved core domain, which is responsible for their function. It is well acknowledged that the DNA sequences of a gene are highly conserved within the same species and even in distantly related species (Reaume and Sokolowski 2011). Therefore, the fact that the results showed highly conserved nucleotide sequences of all three CPF members of *P. neolycopersici* in all five isolates collected from different regions is justifiable. Nonetheless, the functions of protruding N-terminal ends in PHR and Cry C-terminal extensions in CRY require further investigation in relation to powdery mildews.

ACKNOWLEDGMENTS

We thank Prof. Hans Ragnar Gislerød (collection of pathogen isolates) and K. Svinnset for help in the maintenance of isolates, and other technical staff at the Centre for Controlled Environment Plant Research, Norwegian University of Life Sciences, for their excellent support and assistance.

LITERATURE CITED

Brych, A., Mascarenhas, J., Jaeger, E., Charkiewicz, E., Pokorny, R., Bölker, M., Doehlemann, G., and Batschauer, A. 2016. White collar 1-induced photolyase expression contributes to UV-tolerance of *Ustilago maydis*. MicrobiologyOpen 5:224-243.

Chaves, I., Yagita, K., Barnhoorn, S., Okamura, H., van der Horst, G. T. J., and Tamanini, F. 2006. Functional evolution of the photolyase/cryptochrome protein family: Importance of the C terminus of mammalian CRY1 for circadian core oscillator performance. Mol. Cell. Biol. 26:1743-1753.

Chow, C. M., Metzenberg, R. L., and Rajbhandary, U. L. 1989. Nuclear gene for mitochondrial leucyl-tRNA synthetase of *Neurospora crassa*: Isolation, sequence, chromosomal mapping, and evidence that the leu-5 locus specifies structural information. Mol. Cell. Biol. 9:4631-4644.

Corpet, F. 1988. Multiple sequence alignment with hierarchical clustering. Nucleic Acids Res. 16:10881-10890.

Essen, L. O., and Klar, T. 2006. Light-driven DNA repair by photolyases. Cell. Mol. Life Sci. 63:1266-1277.

Hall, T. A. 1999. BioEdit: A user-friendly biological sequence alignment editor and analysis program for windows 95/98/NT. Nucleic Acids Symp. Ser. 41:95-98.

Jans, J., Schul, W., Sert, Y. G., Rijksen, Y., Rebel, H., Eker, A. P. M., Nakajima, S., van Steeg, H., de Gruijl, F. R., Yasui, A., Hoeijmakers, J. H. J., and van der Horst, G. T. J. 2005. Powerful skin cancer protection by a CPD- photolyase transgene. Curr. Biol. 15:105-115.

Jenkins, G. J. S., Burlinson, B., and Parry, J. M. 2000. The polymerase inhibition assay: A methodology for the identification of DNA-damaging agents. Mol. Carcinog. 27:289-297.

Jones, H., Whipps, J. M., and Gurr, S. J. 2001. The tomato powdery mildew fungus *Oidium neolycopersici*. Mol. Plant Pathol. 2:303-309.

Kavakli, I. H., Baris, I., Tardu, M., Gül, Ş., Öner, H., Çal, S., Bulut, S., Yarparvar, D., Berkel, Ç., Ustaoğlu, P., and Aydın, C. 2017. The photolyase/cryptochrome family of proteins as DNA repair enzymes and transcriptional repressors. Photochem. Photobiol. 93:93-103.

Kihara, J., Moriwaki, A., Matsuo, N., Arase, S., and Honda, Y. 2004. Cloning, functional characterization, and near-ultraviolet radiation-enhanced expression of a photolyase gene (PHR1) from the phytopathogenic fungus *Bipolaris oryzae*. Curr. Genet. 46:37-46.

Lebeda, A., Mieslerová, B., Petřivalský, M., Luhová, L., Špundová, M., Sedlářová, M., Nožková-Hlaváčková, V., and Pink, D. A. C. 2017. Review of tomato powdery mildew–A challenging problem for researchers, breeders and growers. Acta Hortic. 1159:107-116.

Manova, V., and Gruszka, D. 2015. DNA damage and repair in plants–From models to crops. Front. Plant Sci. 6:885.

Mei, Q., and Dvornyk, V. 2015. Evolutionary history of the photolyase/cryptochrome superfamily in eukaryotes. PLoS One 10:e0135940.

Ozturk, N. 2017. Phylogenetic and functional classification of the photolyase/cryptochrome family. Photochem. Photobiol. 93:104-111.

Pathak, R., Ergon, A., Stensvand, A., Gisler˘d, H. R., Solhaug, K. A., Davidson, L. C., and Suthaparan, A. 2020. Functional characterization of *Pseudoidium neolycopersici* photolyase reveals mechanisms behind the efficacy of nighttime UV on powdery mildew suppression. Front. Microbiol. 11:1091.

Pathak, R., Sundaram, A., Davidson, L. C., Solhaug, K. A., Stensvand, A., Gisler˘d, H. R., and Suthaparan, A. 2017. Sensing of UV and visible light by powdery mildew pathogens. Phytopathology 107:47-48.

Prakash, L. 1975. Repair of pyrimidine dimers in nuclear and mitochondrial DNA of yeast irradiated with low doses of ultraviolet light. J. Mol. Biol. 98:781-795.

Reaume, C. J., and Sokolowski, M. B. 2011. Conservation of gene function in behaviour. Philos. Trans. R. Soc. Lond. B Biol. Sci. 366:2100-2110.

Robinson, H. L., Ridout, C. J., Sierotzki, H., Gisi, U., and Brown, J. K. M. 2002. Isogamous, hermaphroditic inheritance of mitochondrion-encoded resistance to Qo inhibitor fungicides in *Blumeria graminis* f. sp. *tritici*. Fungal Genet. Biol. 36:98-106.

Sancar, A. 1994. Structure and function of DNA photolyase. Biochemistry 33:2-9.

Sancar, A. 2008. Structure and function of photolyase and *in vivo* enzymology: 50th anniversary. J. Biol. Chem. 283:32153-32157.

Sancar, A., Smith, F. W., and Sancar, G. B. 1984. Purification of *Escherichia coli* DNA photolyase. J. Biol. Chem. 259:6028-6032.

Sinha, R. P., and Häder, D. P. 2002. UV-induced DNA damage and repair: A review. Photochem. Photobiol. Sci. 1:225-236.

Suthaparan, A., Pathak, R., Solhaug, K. A., and Gisler˘d, H. R. 2018. Wavelength dependent recovery of UV-mediated damage: Tying up the loose ends of optical based powdery mildew management. J. Photochem. Photobiol. B 178:631-640.

Suthaparan, A., Solhaug, K. A., Bjugstad, N., Gisler˘d, H. R., Gadoury, D. M., and Stensvand, A. 2016a. Suppression of powdery mildews by UV-B: Application frequency and timing, dose, reflectance, and automation. Plant Dis. 100:1643-1650.

Suthaparan, A., Solhaug, K. A., Stensvand, A., and Gisler˘d, H. R. 2016b. Determination of UV action spectra affecting the infection process of *Oidium neolycopersici*, the cause of tomato powdery mildew. J. Photochem. Photobiol. B 156:41-49.

Suthaparan, A., Solhaug, K. A., Stensvand, A., and Gisler˘d, H. R. 2017. Daily light integral and day light quality: Potentials and pitfalls of nighttime UV treatments on cucumber powdery mildew. J. Photochem. Photobiol. B 175:141-148.

Suthaparan, A., Stensvand, A., Solhaug, K. A., Torre, S., Mortensen, L. M., Gadoury, D. M., Seem, R. C., and Gisler˘d, H. R. 2012a. Suppression of powdery mildew (*Podosphaera pannosa*) in greenhouse roses by brief exposure to supplemental UV-B radiation. Plant Dis. 96:1653-1660.

Suthaparan, A., Stensvand, A., Solhaug, K. A., Torre, S., Telfer, K. H., Ruud, A. K., Davidson, L. C., Mortensen, L., Gadoury, D. M., Seem, R. C., and Gisler˘d, H. R. 2012b. Suppression of cucumber powdery mildew by UV-B is affected by background light quality. (Abstr.) Phytopathology 102:S4.116.

Suthaparan, A., Stensvand, A., Solhaug, K. A., Torre, S., Telfer, K. H., Ruud, A. K., Mortensen, L. M., Gadoury, D. M., Seem, R. C., and Gisler˘d, H. R. 2014. Suppression of cucumber powdery mildew by supplemental UV-B radiation in greenhouses can be augmented or reduced by background radiation quality. Plant Dis. 98:1349-1357.

Tagua, V. G., Pausch, M., Eckel, M., Gutiérrez, G., Miralles-Durán, A., Sanz, C., Eslava, A. P., Pokorny, R., Corrochano, L. M., and Batschauer, A. 2015. Fungal cryptochrome with DNA repair activity reveals an early stage in cryptochrome evolution. Proc. Natl. Acad. Sci. U.S.A. 112:15130-15135.

Tamura, K., Stecher, G., Peterson, D., Filipski, A., and Kumar, S. 2013. MEGA6: Molecular evolutionary genetics analysis version 6.0. Mol. Biol. Evol. 30:2725-2729.

Thompson, C. L., and Sancar, A. 2002. Photolyase/cryptochrome blue-light photoreceptors use photon energy to repair DNA and reset the circadian clock. Oncogene 21:9043-9056.

Tornaletti, S., Reines, D., and Hanawalt, P. C. 1999. Structural characterization of RNA polymerase II complexes arrested by a cyclobutane pyrimidine dimer in the transcribed strand of template DNA. J. Biol. Chem. 274:24124-24130.

Vechtomova, Y. L., Telegina, T. A., and Kritsky, M. S. 2020. Evolution of proteins of the DNA photolyase/cryptochrome family. Biochemistry (Moscow) 85:131-153.

Weber, S. 2005. Light-driven enzymatic catalysis of DNA repair: A review of recent biophysical studies on photolyase. Biochim. Biophys. Acta Bioenerg. 1707:1-23.

Xu, L., and Zhu, G. 2010. The roles of several residues of *Escherichia coli* DNA photolyase in the highly efficient photo-repair of cyclobutane pyrimidine dimers. J. Nucleic Acids 2010:794782.

Yajima, H., Inoue, H., Oikawa, A., and Yasui, A. 1991. Cloning and functional characterization of a eucaryotic DNA photolyase gene from *Neurospora crassa.* Nucleic Acids Res. 19:5359-5362.

Yasui, A., Yajima, H., Kobayashi, T., Eker, A. P. M., and Oikawa, A. 1992. Mitochondrial DNA repair by photolyase. Mutat. Res. 273:231-236.

Zhang, M., Wang, L., and Zhong, D. 2017. Photolyase: Dynamics and mechanisms of repair of sun-induced DNA damage. Photochem. Photobiol. 93:78-92.

Zhou, P., Wen, J., Oren, A., Chen, M., and Wu, M. 2007. Genomic survey of sequence features for ultraviolet tolerance in Haloarchaea (family Halobacteriaceae). Genomics 90:103-109.

ISBN: 978-82-575-1848-6
ISSN: 1894-6402

Norwegian University
of Life Sciences

Postboks 5003
NO-1432 Ås, Norway
+47 67 23 00 00
www.nmbu.no

112284 / ANDVORDGRAFISK.NO